McKelvey School of Engineering Theses & Dissertations

McKelvey School of Engineering

Spring 5-15-2019

Elucidating the Roles of Astrocyte-derived Factors in Recovery and Regeneration Following Spinal Cord Injury

Russell E. Thompson
Washington University in St. Louis

Follow this and additional works at: https://openscholarship.wustl.edu/eng_etds

Part of the Biomedical Engineering and Bioengineering Commons, and the Neuroscience and Neurobiology Commons

WASHINGTON UNIVERSITY IN ST. LOUIS

Department of Biomedical Engineering

Dissertation Examination Committee:
Dennis Barbour, Chair
Shelly Sakiyama-Elbert, Co-Chair
James Huettner
Robyn Klein
Steven Mennerick
Lori Setton

Elucidating the Roles of Astrocyte-derived Factors in Recovery and Regeneration Following
Spinal Cord Injury

by
Russell Edward Thompson

A dissertation presented to
The Graduate School
of Washington University in
partial fulfillment of the
requirements for the degree
of Doctor of Philosophy

May 2019
St. Louis, Missouri

Table of Contents

List of Figures

List of Tables

__Acknowledgments__

I would like to thank everyone I have had the pleasure of working with both at Washington University in St Louis and at the University of Texas at Austin during my work on this project. First and foremost, I would like to thank Prof. Shelly Sakiyama-Elbert who has been my mentor and has guided me throughout my time in the lab. It was only through her guidance and support that I could complete this work. I hope to one day be as successful a professor as Shelly and I look forward to our continued professional relationship. I would also like to recognize my thesis committee, the members of which have provided invaluable advice throughout this project.

The Sakiyama-Elbert Lab itself has been an outstanding environment to work in. I would like to thank all my labmates: Jennifer Pardieck, Lindsey Crawford, Bill Wang, Nick White, Sara Oswald, Jaewon Lee, Mary Salazar, Thomas Wilems, Nisha Iyer, Hao Xu, Nicholas White, Peter Kenny, and Divya Joshi. I would like to specifically recognize: Jennifer Pardieck who was instrumental in completing the animal studies present here, Peter Kenny and Divya Joshi, both skilled undergraduate researchers, who worked tirelessly on the Aqp4-PAC cell line, Lindsey Crawford who first brought hyaluronic acid hydrogels into the lab, and Sara Oswald who kept the St Louis lab running smoothly.

I would also like to thank administrations of the Washington University in St Louis MSTP and BME programs as well as the University of Texas-Austin BME program for their assistance throughout this project and with moving from St Louis to Austin and back. I would like to recognize my undergraduate research mentor, Elizabeth Orwin, who taught me how to design and pursue my own research project. I would also like to thank our collaborators in this project. Specifically, Prof. Joseph Dougherty and Allison Lake at Washington University in St

Dedicated to my grandfather, Phillip Majerus, who was my inspiration for pursuing a career in medical research

ABSTRACT OF THE DISSERTATION

Elucidating the Roles of Astrocyte-derived Factors in Recovery and Regeneration Following
Spinal Cord Injury

By Russell Edward Thompson

Doctor of Philosophy in Biomedical Engineering

Washington University in St Louis, 2019

Professor Dennis Barbour, Chair

Professor Shelly Sakiyama-Elbert, Co-Chair

Central nervous system (CNS) injury often causes some level of long-term functional deficit, due to the limited regenerative potential of the CNS, that results in a decreased quality of life for patients. CNS regeneration is inhibited partly by the development of a glial scar following insult that is inhibitory to axonal growth. The major cell population responsible for the formation this glial scar are astrocytes, which has led to the belief that astrocytes are primarily inhibitory following injury. Recent work has challenged this conclusion, finding that astrocyte reactivity is heterogeneous and that some astrocytes are pro-regenerative following injury. Astrocyte transplantation studies following spinal cord injury (SCI) have also found that outcomes depend on astrocyte phenotype. Specifically, transplantation of astrocytes with the hallmarks of protoplasmic (grey matter) populations improve behavioral and histological outcomes; whereas, transplantation of astrocytes exhibiting fibrous (white matter) hallmarks worsen outcomes following transplantation. These studies suggest that it could be possible to develop an astrocyte-based CNS injury therapeutic by harnessing regenerative astrocyte populations.

In this work, the ability of mouse embryonic stem cell (mESC)-derived astrocyte populations to provide substrates that improve neuronal growth is explored. In addition, the effect of implantation of mESC-derived astrocyte extracellular matrix (ECM) on SCI outcomes is tested. Methods were developed to derive populations containing predominantly fibrous or protoplasmic astrocytes from mESCs. Since these mESC-derived astrocyte populations contain other cell types as well, CRISPR-Cas9 technology was used to generate a mESC line that expresses puromycin resistance under the control of an astrocyte-specific gene, aquaporin-4. This cell line shows promise as a source of live astrocytes for transplantation in the future; although further experiments will be required to validate it. Growth of mESC-derived motoneurons and V2a interneurons on substrates generated by unselected astrocytes was tested and it was found that both neuronal populations extended significantly longer neurites on protoplasmic substrates than fibrous substrates. Of particular interest, protoplasmic ECM alone was able to support neuronal growth, while fibrous ECM was not. Since ECMs have been successfully used to promote recover in other tissues with poor regeneration, astrocyte ECMs were further characterized with proteomics. Proteomics data revealed that protoplasmic ECMs contained significantly more axon growth permissive proteins, while fibrous ECM contained significantly more axon growth inhibitory proteins. These findings suggest that the mESC-derived protoplasmic astrocyte populations may be able to provide therapeutic value following SCI.

To explore whether astrocyte ECMs provided any recovery benefit after SCI, mESC-derived astrocyte ECMs were mixed with hyaluronic acid (HA) hydrogels. The resulting HA:ECM gels were then injected following SCI and the effects of ECM presence on histological markers of recovery was assessed. These studies found that protoplasmic ECM presence within

the SCI lesion decreased immune cell infiltration, decreased astrocyte reactivity, and increased axonal penetration into the SCI lesion. These benefits were not observed when fibrous ECM was implanted and, in fact, the presence of fibrous ECM caused an increase in the presence of inhibitory molecules within the glial scar compared to HA alone implantation. This suggests that protoplasmic astrocyte ECM has an immunomodulatory effect and alters the phenotype of native astrocytes. Finally, the ability of HA and HA + protoplasmic ECM gels to support cell transplantation was explored by incorporating V2a interneurons into the hydrogels prior to transplantation. HA with and without ECM was found to support the transplantation of the V2a interneurons and the transplanted interneurons were found to migrate into and extend processes within the host spinal cord. Taken together these *in vivo* experiments demonstrate that HA:ECM hydrogels have potential as a SCI treatment and, due to the use of mESCs, this material can be more easily scaled for large-scale material production than would be possible with a primary cell approach.

Chapter 1: Introduction

1.1   Spinal Cord Injury

   Spinal cord Injury (SCI) is characterized as either traumatic or nontraumatic. Traumatic

injuries are defined as sudden damage to spinal cord due to either concussive force or penetration

trauma, and nontraumatic injury are defined as vascular damage, cord stenosis, or resulting from

cancer.(Hatch et al. 2017) Both of these types of insults lead to incomplete or complete lesion of

the spinal cord itself, which severs the connection between the brain and the rest of the body,

often resulting in some level of paralysis. SCI has an annual incidence of 17,000 new cases a

year in the United States with an estimated 243,000 to 347,000 Americans living with chronic

SCI.(Of 2013) About 80% of new SCI occurs in men, most commonly due to automobile

accidents followed by falls. Both of these types of injury tend to cause severe neck motion,

which leads to a cervical cord contusion injury. SCI patients who recover from the initial

traumatic event tend to have shortened life expectancies compared to uninjured peers and have

decreased mental well-being.(Boakye, Leigh, and Skelly 2012) In addition, within the SCI

patient population, life expectancy is shorter when the injury is more rostral.(Of 2013) A big part

of the poor long-term prognosis of patients who suffer from SCI is that human spinal cord has

limited ability to regenerate following injury. This means that SCI patients are not likely to have

significant changes in their level of paralysis following the initial recovery period; therefore, SCI

is a chronic condition that requires lifelong care. Due to the chronic nature of these injuries, there

is a clear clinical need to find ways to improve the long-term prognosis for these patients.

1.1.1 Spinal Cord Injury Biology

A large contributor to the limited regenerative capacity of the human spinal cord is the stereotyped scar environment that forms following injury called the glial scar. In particular, there are two well defined phases of SCI lesion development with the primary injury caused by the original trauma followed by a secondary injury that is caused by the immune and inflammatory response to the injury. The secondary injury causes an increase in the size of the injury area and, in humans, often leads to the formation of a cystic injury cavity. This lesion cavity is filled with inflammatory cells and fibroblasts that have invaded from the periphery, and is surrounded by a fibrotic scar environment that is formed primarily by astrocytes, the main support cell found in the central nervous system (CNS)(Cregg et al. 2014). This scar environment is relatively inhibitory to the growth on new axons due primarily to the presence of both inhibitory chondroitin sulfate proteoglycans (CSPGs) and myelin associated inhibitors (MAIs)(Simonen et al. 2003; Ohtake and Li 2014), and so it is difficult for new neurite growth to occur within the lesion area and so few, if any, new connections to be formed across the scar. This injury progression overall results in a long-term loss of communication between the brain and the rest of the body, which causes paralysis and sensory deficits distal to the injury site.

Both parts of the glial scar, the lesion core and the surrounding scar, limit the ability of axon to extend through the injury. The cavity lacks the normal spinal extracellular environment and contains a high concentration of MAIs(Caroni and Schwab 1988), which accumulate due to the degradation of the myelin sheaths. Myelin sheaths normally surround axons to improve signal transmission, but they degrade into MAIs when the associated axons are damaged or destroyed by the injury. Targeting of MAIs and/or their signaling pathway has been used previous to improve growth of neurons *in vitro*(Caroni and Schwab 1988) and increase neuronal

regeneration following SCI.(Simonen et al. 2003; Wilems and Sakiyama-Elbert 2015) The astrocytic scar that surround the lesion cavity also contains factors that are inhibitory to axon growth. These factors include proteins that are produced by the scar astrocytes such as inhibitory CSPGs(Bradbury et al. 2002), tenascin R(Apostolova, Irintchev, and Schachner 2006), and keratin sulfate proteoglycans.(Chu et al. 2014) Together these proteins represent a significant inhibitory signal to new neurite extension. In addition to this chemical barrier, astrocytes around the lesion expand and undergo significant process hypertrophy. These hypertrophic processes overlap and form a woven physical barrier that prevents access to the lesion area.(Sun et al. 2010) Numerous studies have been performed using different techniques to degrade or block the action of these astrocyte-derived inhibitory molecules in order to improve axon regeneration following SCI.(Bradbury et al. 2002; Wilems et al. 2015; Shinozaki et al. 2016) Due to the production of this large number of inhibitory factors, the prevailing theory in the field has been that astrocytes were predominantly an inhibitory barrier that needed to be removed to allow for improved recovery.

In order to test the idea that astrocytes are inhibitory following SCI, SCI recovery was studied in mice who had been genetically modified to allow for the ablation of the reactive astrocyte population. Astrocyte reactivity was knocked-out in mice prior to SCI with either vimentin and glial fibrillary acidic protein (GFAP) double knock out or conditional knockout of STAT3 (a required factor for astrocyte reactivity) in astrocytes. The result was an increase to the size of the injury area due to worsened secondary injury (increased immune cell infiltration) and further lack of recovery.(Pekny et al. 1999; J. R. Faulkner et al. 2004; Herrmann et al. 2008) These findings indicated that the physical barrier formed by the astrocytes was important to limit the damage caused by inflammation of the injury area.

3

This still left open the possibility that astrocytes were helpful in the acute phase of injury, but detrimental in chronic SCI cases. To test this hypothesis, delayed astrocyte ablation was performed using a GFAP-driven thymidine kinase and ganciclovir injections. These strategies allow for the astrocytes around the SCI lesion to be ablated 2 weeks after injury. This delayed ablation allows the SCI lesion to stabilize in size and the secondary injury to resolve before the astrocytes are removed. However, even in the case of delayed ablation, the lack of astrocytes led to decreased functional recovery and a loss of improvement with transplanted hydrogels.(Anderson et al. 2016; J. R. Faulkner et al. 2004) Together these knockout studies suggest that astrocytes both play a role in the formation of the inhibitory scar, and a role in the creation of an environment that is permissive to axon regeneration. This demonstrates that astrocytes are necessary for recovery following SCI.(Lukovic et al. 2014) Another observation supporting the hypothesis that astrocytes can create axon permissive environment is that axons within an SCI lesion colocalize with "GFAP$^+$ bridge" in both mice(Zukor et al. 2013) and zebrafish.(Yona Goldshmit et al. 2012) Overall these recent studies suggest that astrocytes are an overlooked cell population in terms of their ability to promote recovery following SCI.

To overcome the complexity of the glial scar environment, a multi-faceted treatment approach will be required that addresses the inhibitory aspects of both parts of the glial scar, while also providing a substrate that encourages or, at least, is permissive to the growth of new axons and the formation of new connections within and beyond the scar environment. Furthermore, a treatment scaffold will need to contain the correct growth signals to encourage neurites to extend into the lesion.

1.1.2 Spinal Cord Injury Models

There are many different potential animal models used for SCI research, but rats are the most commonly used species since rats, like humans, form a lesion within the spinal cord following injury. There is a large body of work performed in mice as well due to ready availability of genetically modified mouse strains; however, mice in general do not form a large lesion cavity making mouse SCI less similar to the human pathology.(Byrnes, Fricke, and Faden 2010) Another area of variation in SCI models is the modality of injury used. The most common modalities are contusion, transection/hemisection, and compression. Contusion and compression are the best models for simulating the most common injury modalities in patients and thus are better mimics the neuropathology of human injury. Transection or hemisection, on the other hand, is the superior model to for assessing regeneration since the axons are certain to have been severed when the injury occurred rather than compressed thus ensuring that any growth into the injury region is in fact new growth.(Sharif-Alhoseini et al. 2017)

1.2 Material Transplant in Spinal Cord Injury

One clear option to achieve the goals of generating an improved axon growth environment is to transplant a new material into the lesion cavity. It is important that these materials be biocompatible and minimally immunogenic, a problem for some scaffold systems as breakdown products from the implanted material can cause an immune reaction. To achieve this goal, materials are often composed of natural or synthetic biomaterials. These transplanted biomaterials provide a new substrate within the lesion cavity where the normal extracellular matrix (ECM) substrate has been destroyed. Biomaterials can also be modified to include or release factors that counteract inhibitory signals and/or promote axon growth into the

transplanted substrate. Here SCI treatment materials are divided into two classes: injectable and non-injectable.

1.2.3 Non-injectable Scaffolds

These materials tend to have a relatively defined volume and shape so the scar environment must often be somewhat dissected to create a space that is same size as the scaffold in the case of a subacute implantation. This addition dissection often results in additional damage to the spinal cord at the time of implantation. There are also many studies that perform the implantation acutely and so cut a large enough defect in the spinal cord for the scaffold. A large number of different materials have been used for this including: fibrin, collagen, agarose, chitosan.(M. Kim, Park, and Choi 2014) It is worth noting that both fibrin and collagen can be injectable, in certain formulations, but the formulations discussed here are not injectable. The most commonly used natural materials are fibrin and collagen which are discussed briefly here. An advantage of using these non-injectable scaffolds is that it is easier to control the precise conditions during scaffold formation and so have more precise control of scaffold pore-size and a much wider range of conditions that can be utilized. Furthermore, these scaffolds can be modified prior to implantation to contain fixed growth factor gradients and other specific topographical features that are impossible to form in an injectable scaffold.

1.2.1.1 Fibrin

Fibrin has been used extensively in SCI animal models to promote regeneration due to its flexibility and biocompatibility. There are many drug and cell delivery systems that have been used in fibrin transplantation.(Wilems et al. 2015; D. A. McCreedy et al. 2014; Wilems and Sakiyama-Elbert 2015; Johnson, Parker, and Sakiyama-Elbert 2009; Vadivelu et al. 2015) Fibrin scaffolds are relatively easily produced by mimicking the same enzymatic cross-linking process

that is used during normal clot formation. Unfortunately, fibrin cannot be injected once polymerized which limits the use of these scaffolds in a contusion SCI, since in this type of injury the lesion cannot be accessed without some additional tissue dissection and so injury to the spinal cord. One way to address this issue is to allow the fibrin-thrombin reaction to occur *in situ* and so form a scaffold that fills the lesion and so the polymerization solution can be injected. A drawback to a two-phase approach such as this is that polymerization can difficult to achieve if there is any flow of cerebrospinal fluid (CSF) over the injury site.(Sharp et al. 2012)

A major advantage to fibrin scaffold systems, in addition to its degradability and biocompatibility, is the simple incorporation of growth factors through the use of a heparin binding system.(Sakiyama, Schense, and Hubbell 1999) The heparin system has been use to deliver neurotrophic 3 (NT-3) which has been found to improve SCI outcomes.(Taylor et al. 2006) In addition, fibrin scaffolds have also been used to deliver neural progenitors leading to improved functional outcomes(Johnson et al. 2010), as well as progenitor motoneurons.(D. A. McCreedy et al. 2014) Toward the goal of creating a multi-faceted treatment system, fibrin scaffolds were loaded with NEP1-40 (inhibits MAI signaling) and chondroitinase ABC (degrades CSPGs). This combination treatment was found to decrease CSPG deposition in the scar and increase the axon growth into the SCI lesion(Wilems and Sakiyama-Elbert 2015); however, these benefits were largely lost when progenitor motoneurons were transplant as well.(Wilems et al. 2015)

Fibrin itself has also been functionalized with synthetic peptide ligands that bind to the $\alpha_6\beta_1$ integrin receptor. This modification was found to improve neurite extension from rat dorsal root ganglion *in vitro* and to increase axonal growth cone formation following a complete transection SCI *in vivo*.(J. Silva et al. 2017) There has also been study of different animal fibrins

as potential scaffolds for SCI injury treatment. Human fibrin alone has been found to improve open-field locomotion following subtotal T9 lateral hemisection.(Petter-Puchner et al. 2007) Recently, salmon fibrin scaffolds have been shown to improve locomotor and bladder function recovery following implantation after a T9 dorsal hemisection.(Sharp et al. 2012) Fibrin has also been mixed with other peptides to provide further neuronal growth benefits. In particular, fibrin scaffolds modified with laminin and N-cadherin have been found to enhance axonal regeneration *in vivo*.(Schense et al. 2000) Overall, fibrin has been heavily studied as a scaffold for improving CNS regeneration and has been found to have numerous beneficial effects.

1.2.1.2   Collagen

Collagen is the most abundant extracellular protein in the body and is highly conserved between species. It has a fibrous structure, is inexpensive, easily accessible, and biocompatible. This makes it an appealing biomaterial due to ease of acquisition and low immunogenicity.(M. Kim, Park, and Choi 2014) Collagen has the added advantage of being highly bioactive containing many cell-binding and signaling domains which allows collagen itself to provide cell-signaling. Collagen is also easily modified in the fabrication process to create different fiber diameters with and without alignment. Finally, there are many different crosslinking methods that can be used to modify the mechanical and degradation properties of collagen scaffolds.(Hapach et al. 2015) Due to these factors, collagen-based biomaterials have been widely used in tissue engineering applications and in SCI treatment.(Haggerty, Marlow, and Oudega 2017) Here some more recently documented uses of collagen are mentioned.

Crosslinked, aligned collagen scaffolds placed acutely into a complete spinal cord transections have been found to improve axon regeneration showing the utility of collagen-based materials and alignment on axon growth.(Suzuki et al. 2015) Aligned collagen nano-fibrous

nerve conduits have also been transplanted for SCI treatment and have been found to facilitate cellular infiltrates with limited ED-1 (macrophage) staining visible.(T. Liu et al. 2012) It has also been demonstrated that aligned collagen scaffolds can improve forepaw reaching after a lateral cervical resection injury.(Altinova et al. 2014) Collagen sponges have also been transplanted into complete transections along with synthetic hydrogels to limit pore size with improved axon penetration.(Kaneko, Matsushita, and Sankai 2015) Collagen scaffold with micropatterned porosity have been found to slightly improve locomotion after complete transection.(Snider et al. 2017) A major drawback to the use of collagen as a scaffold material is that the most abundant collagen, collagen I, has been associated with an increase in astrocyte expression of inhibitory genes associated with the glial scar and collagen is not normally a major component of spinal cord ECM.(Hara et al. 2017)

1.2.2 Injectable Scaffolds

Injectable biomaterial scaffolds tend to be hydrogels that can be formed either prior to transplant or *in situ*. These materials will fill the entire lesion area, without requiring any lesion dissection. This avoids one of the major issues with the non-injectable scaffolds, namely the need to match scaffold size to the size of the lesion area. These scaffolding systems tend to be hydrogels which improves their biocompatibility. Unfortunately, the reaction conditions for crosslinking these materials is much more limited due to the requirement that they be shear-thinning or have fast enough reaction kinetics to form *in situ* prior to being overly diluted by CSF flow.

1.2.2.1   Hyaluronic Acid-based Injectable Scaffolding

Hyaluronic acid (HA) is already widely used for clinical applications and the predominant component of the native CNS ECM, making it a popular choice for CNS

injectables.(Pakulska, Ballios, and Shoichet 2012) Unfortunately, HA alone does not form a sufficiently stable gel *in vivo,* so the HA must be mixed with other molecules such as methylcellulose to form an HAMC hydrogel(Gupta, Tator, and Shoichet 2006) or chemically modified to allow a crosslinking reaction to occur. Many chemical modifications have been used to functionalize HA macromolecules so that they will react with a crosslinking molecule and form a stable hydrogel for treatment of SCI. Functionalization of the HA is often achieved by reacting the carboxylic acid group on HA with part of the crosslinking system to be used. Examples of functionalization strategies include: thiol-modified (disulfide bond linkage)(Shu et al. 2002), aldehyde (Diels-Alder linkage)(Nimmo, Owen, and Shoichet 2011), and tetrabutylammonium (TBA) (esterification).(Gaffey et al. 2015)

These systems either can then be injected as a 2-phase system with fast gelation kinetics that will gel *in situ* (disulfide) or will shear-thin following gelation which allows for prefabrication of the gels. Disulfide bond crosslinked HA has been injected as a two phase system acutely following SCI and has been found to be neuroprotective to secondary injury, but did not improve regeneration(Kushchayev et al. 2016; Horn et al. 2007). A major requirement for these multiple phase systems is that they have fast enough gelation kinetics (on the order of seconds to minutes) for the gels to form before the components become too diluted. A way for gels with slower kinetics to still be useable is for the gels to be shear-thinning. This means that the gels can be pre-formed within the barrel of a syringe and then injected into the injury site. Shear thinning HAMC gels have been used intrathecally to improve dural regeneration(Gupta, Tator, and Shoichet 2006) and as a vehicle for cell delivery.(Ballios et al. 2015) HA-aldehyde crosslinked with malemide-PEG-malemide also forms a hydrogel that has been successfully used intrathecal as drug-depo.(Führmann et al. 2015) A major advantage to this crosslinking method

compared to others is that the Diels-Alder reaction used to create the crosslink between HA

molecules does not require the use of a catalyst and the reactants are not toxic. This means that

no clean-up needs to take place after the crosslinking reaction has been completed which greatly

simplifies the use of this system as a treatment.(Nimmo, Owen, and Shoichet 2011) In addition,

Diels-Alder chemistry is stereospecific and highly specific to dienes and dienophiles so other

materials can be incorporated without risking nonspecific reactions. Overall the literature shows

that HA-based materials are very flexible, tolerated biologically making these materials

potentially useful for future treatment modalities. In addition, long HA macromolecules

themselves have been found to improve SCI outcomes.(Khaing et al. 2011)

1.2.2.2　　　Other Injectable Scaffolds for CNS injury

While HA is the most commonly used injectable scaffold used for both acellular and

cellular transplantation in CNS injury, there have been other injectable scaffolds published. One

such scaffold is a hydrogel formed by combining oligomeric gelatin with copper-capillary

alginate. These scaffolds have been shown to support the growth of primary radial glia both *in

vitro* and *in vivo* when transplanted into a hypoxic stroke cavity; however, alginate gels are more

commonly used in other organ systems as a stem cell encapsulation and drug delivery

material(Willenberg et al. 2011). There has also been work exploring *in situ* gelling collagen

hydrogels as a delivery vehicle for GDNF overexpressing mesenchymal stem cells *in vivo*

following stroke and that the collagen hydrogel delivery decreased the reaction of host astrocytes

and immune cells to the transplant.(Hoban et al. 2013) Another injectable hydrogel system that

has been explored is a diblock copolypeptide hydrogel composed on hydrophobic and

hydrophilic segments. This is a synthetic gel system that has tunable material properties and has

been used to successfully support the survival of neural stem cells and to release of hydrophobic

and hydrophilic effector molecules.(Zhang et al. 2014; Zhang et al. 2015) While these injectable

systems show promise, the presence of high levels on HA within the CNS makes HA a appealing

base material for the generation of an astrocyte-derived biomaterial.

1.2.3 Drug Delivery

Many of the materials discussed above have been transplanted without any drugs or other

bioactive molecules being incorporated. Unfortunately, the materials discussed thus far tend to

not have the maximum regenerative benefits without the incorporation of bioactive molecules. In

the case of SCI, the most commonly included molecules are growth factors that are known to

improve neurite extension from host neurons or enzymes that nullify the effects of the inhibitory

molecules present within the glial scar. One approach to load growth factors in fibrin matrices

was to anchor heparin to the fibrin and then rely on the binding affinity between growth factor

and heparin to allow for controlled growth factor delivery.(Sakiyama-Elbert and Hubbell 2000)

Unfortunately, not all bioactive compounds are readily water soluble and/or require enzymatic

activity to be effective which makes this type of delivery strategy more challenging. In the case

of HAMC gels, the incorporation of methylcellulose allows for more direct incorporation of

poorly water-soluble drugs. Altering the methylcellulose concentration can in turn tune the

release of these molecules.(Y. Wang et al. 2009)

Other scaffolds tend to require the incorporation of lipid microtubules, polymer spheres

(such as PLGA microspheres),(Wilems and Sakiyama-Elbert 2015) or have enzymatically

degradable linkages within the scaffold.(Pakulska, Ballios, and Shoichet 2012) A drawback of

having these delivery systems present is that they can generate breakdown products that

negatively impact the regenerative environment. In the case of PLGA microspheres, the

acidification caused by the breakdown of PLGA can cause an increase in the inflammatory

response within the spinal cord.(Wilems et al. 2015) This can mean that combination therapies with many different drug delivery systems can cause unanticipated interactions which can attenuate the positive effects observed when each delivery system was used on its own. Thus, it is appealing to attempt to capture signaling complexity without having to include multiple drug delivery platforms. One method that has been used in other fields to achieve signaling complexity without having to include a large number of different growth factors is to use decellularized extracellular matrix (ECM) materials.

1.2.3.1 Decellularized Extracellular Matrix

The ECM is composed of proteins that are produced by the cells that occupy a given region within the body. The most common ECM proteins are often used as base material for transplantable biomaterials, such the collagen, fibrin, and HA materials discussed above. The ECM also contains several other proteins that are present at lower levels and attach to the base proteins. These proteins all come together to form a complex environment that can bind growth factors, especially since most ECM proteins are quite large and contain multiple functional domains including cell binding and growth binding regions. For example, fibronectin has been found to have a highly promiscuous growth factor binding domain.(Martino and Hubbell 2010) The multifactorial nature of decellularized ECMs makes them an appealing way to deliver a multitude of bioactive molecules at once.

The use of decellularized whole tissue is already used clinically for treatment of peripheral nerve injuries where is defect is longer than a few millimeters. In the case of these injuries, a decellularized nerve graft can be used to enhance regeneration of the damaged nerve(Isaacs 2013). Another approach being used is to pulverize whole tissue and then form a gel out of the resulting powder. This approach has been used in the treatment of myocardial infarctions(Seif-

Naraghi et al. 2013; Singelyn et al. 2012), and for orthopedic tissue engineering.(Benders et al. 2013) In the context of CNS injury, ECM gels made using decellularized brain ECM demonstrated that ECM from the CNS does provide a more growth permissive substrate for neuronal cultures than ECM harvested from other parts of the body *in vitro*.(Crapo et al. 2012) Further work has shown that spinal cord ECM increased neuronal differentiation efficiency of NPCs while brain ECM lead to longer neurite extensions.(Medberry et al. 2013)

The benefit of CNS ECM over other ECMs has largely not extended to *in vivo* treatments. For example, hydrogels made from spinal cord ECM and urinary bladder ECM were found to have no significant differences when transplant acutely following a dorsal hemisection SCI. However, both types of ECM were found to increase neurite growth into the lesion and neovascularization.(Tukmachev et al. 2016) Similar to the case with treatment SCI , urinary bladder ECM implantation into stroke cavities has been shown to increase host cell infiltration into the lesion core and promote the infiltrating macrophages to adopt a more pro-regenerative phenotype(Ghuman et al. 2016a). Taken together, these studies suggest that an ECM-based material could provide significant therapeutic benefits to patients that suffer from a CNS injury.

In additional to their growth benefits, the highly conserved nature of ECMs means that decellularized ECM materials can be xenografted without requiring immune suppression.(Mirmalek-Sani et al. 2013; Hudson et al.) This is especially important since the immune system plays an important role in tissue regeneration as demonstrated by the discovery of M1 and M2 subtypes of macrophages present during the normal repair pathway.(Novak and Koh 2013) In the context on CNS regeneration, microglial have also been found to play an important long term role in the generation of an axon growth promoting environment by clearing cellular debris and secreting factors such as matrix metalloprotease-13 that degrade the fibrotic

scar.(X. Jin and Yamashita 2016) Furthermore, infiltration of T-cells and macrophages from the periphery has been demonstrate to be required for repair following SCI.(Raposo et al. 2014) These observations show that the immune system plays an important role in tissue repair and that it would be desirable to avoid therapy that requires immune suppression, since it could negatively impact recovery in unforeseen ways.

1.3 Cell Transplantation in Spinal Cord Injury

A major issue for acellular spinal implants is the lack of good cell infiltration into the injury site either due to the lack of migration of the native cell populations or a lack of the appropriate migratory signals within the implant. One way to ensure that transplants have cells present within them is to transplant the cells directly into the injury site. Cell transplants have been performed with stem/progenitor cells, neuron populations, peripheral cells and glial cell populations.(Tetzlaff et al. 2011) An issue with cell transplantation is survival of the transplanted cells since they are often being placed into an environment that is full of inflammatory signals.(Medalha et al. 2014) One way that this issue has been addressed is transplantation of the cells in a scaffold that provides them with support to help improve their survival within the spinal cord lesion

1.3.1 Neuronal Population Transplantation

Neurons are the primary cell type responsible for transmitting signals from the brain to the rest of the body via the spinal cord. It is the severing of the axons in an SCI that causes paralysis of the body below the level of the injury. For recovery from SCI to be possible, these connections must be restored. One appealing way to achieve this connectivity is to transplant neurons into the injury area so that they can form a relay circuit or, much more unlikely due to the distances involved, directly reestablish connection. This type of integration has been

successfully achieved in transplants of embryonic medial ganglionic eminence cells. These cells are GABAergic interneurons from the brain that were able to integrate into the host's spinal circuitry and can prevent the development of mechanical hypersensitivity when transplanted prior to peripheral nerve injury.(Etlin et al. 2016) Unfortunately, primary neurons are difficult to isolate and primary cells in general are difficult to translate into the clinic, this makes deriving neurons from tissue culture sources appealing.

One way to acquire neurons in a tissue culture setting is to use an immortalized cell line. A immortalized neuronal cell line, NT2, has been successfully manipulated to allow for transplantation following SCI with the result of reducing allodynia via neurotransmitter production.(Eaton et al. 2007) Another way to acquire neurons is to derive them from embryonic stem cells (ESCs) or another pluripotent population. The major issue with stem cell-derived neurons is that the pluripotent cells remaining within the transplant can form teratomas within the spinal cord.(Johnson et al. 2010) A way to avoid the remaining ESC problem is to create a method by which residual ESCs can be removed. This can be achieved with puromycin selection(D. a. McCreedy et al. 2012) or fluorescence activated cell sorting. Once the ESCs have been removed, the cells can be transplanted without risk of teratoma formation.(D. A. McCreedy et al. 2014; Wilems et al. 2015) One ESC-derived neuronal population that has been used for SCI treatment are progenitor motor neurons derived from human ESCs(Erceg et al. 2010), and mouse ESCs.(Wilems et al. 2015) Although these cells demonstrated relatively mild benefits and this progenitor population also forms astrocytes and oligodendrocytes.(Mccreedy et al. 2014) Overall, there is much work to be done in neuronal transplantation since pure neuronal populations after difficult to acquire from progenitor cells due to their relative fragility in culture. As techniques for acquiring pure neuronal population cultures improve, it will be possible to

explore the effects of different neuronal subpopulation transplants on SCI recovery.(Iyer, Wilems, and Sakiyama-Elbert 2016)

One interesting neuronal population to explore are the spinal interneurons (INs). INs form connections between all the neuronal populations with the spinal cord and have been shown to play important regulatory roles in coordination, rhythmicity, and spinal reflex arcs. It has been shown, in mice, that spontaneous recovery from spatially and temporally separated lateral hemisection SCIs is dependent on neuronal populations present around the level of injury, not sparing of the long tract axons projecting from the brain.(Courtine et al. 2008) This implies that INs are required in order to facilitate the local rewiring that allows spontaneous recovery to occur. Further work based on this study has shown that dl3 INs are necessary for motor function recovery after SCI.(Bui et al. 2016) There has been only limited work demonstrating the effects of transplantation of IN populations into CNS lesion making this an active area of exploration; however, primary GABAergic brain IN precursors have been shown to functionally integrate and limit hypersensitivity in mice following a lumbar spared peripheral nerve injury(Etlin et al. 2016). This study shows the promise of IN transplantation in terms of enabling functional recovery following nerve injury.

A population of spinal INs that has been a particular focus in SCI treatment are V2a INs. V2a INs are a largely glutamatergic, ipsilateral projecting IN population found throughout the spinal cord, but predominantly in the lumber and cervical regions. In the lumbar region, V2a INs are important for left-right alternation in the normal spinal cord, especially at high speeds of locomotion.(Steven A. Crone et al. 2008; S. A. Crone et al. 2009) Further dissection of the roles played by V2a INs in the lumbar spinal cord found that V2a INs tend not to synapse on other V2a INs, but instead tend to project to central pattern generators and ipsilateral motor neuron

pools. Some of V2a INs have also been found to have long ascending or descending branches.(K. J. Dougherty and Kiehn 2010) This suggests that V2a INs play an important rely and coordination role in the lumbar spinal cord, but not a significant role in pattern generation. In contrast, V2a INs in the cervical cord have been linked to central respiratory rhythm based on the loss of respiratory rhythm, and decreased respiratory rate, in V2a knockout mice.(S. A. Crone et al. 2012) The concept of V2a INs as an important population for both relying signals and in the respiratory circuitry is supported by the observation that V2a INs are recruited into phrenic motor circuitry after a high cervical lateral hemisection SCI. This suggest that the V2a population may aid in functional compensation/recovery from cervical SCI.(Zholudeva et al. 2017) Recently methodology to derive V2a INs from mouse ESCs has been developed(Brown et al. 2014) as has a mouse ESC cell line that allows these ESC-derived V2a IN populations to be purified.(Iyer et al. 2016) With the development of these ESC tools it is now possible to transplant V2a INs following SCI. In this work, we perform a pilot study to determine if these mESC-derived V2a INs are able to survive transplantation.

1.3.2 Progenitor Transplantation

Since transplantation of specific neuronal populations has proved difficult, transplantation of proliferative progenitor cells that can differentiate into neurons has been widely attempted. The cells most commonly used in SCI treatment are called neural progenitor cells (NPCs). These cells can become neurons, oligodendrocytes, or astrocytes after further differentiation meaning that, in theory, transplanting these cells can restore all the cell populations normally present within the spinal cord. NPCs are found throughout the CNS in the region surrounding the cerebral spinal fluid system and can be harvested from animals at any age. NPCs can also be acquired by differentiation of induced pluripotent stem cells (iPSCs) or ESCs. Due to the

teratoma formation observed with ESC transplants, any ESC-derived population must be further defined into a specific cell fate prior to transplantation.(Johnson et al. 2010)

NPCs have been transplanted in chronic SCI lesions in rodents and histological improvement has been observed, but it has proven difficult achieve good connectivity between the transplanted cells and the host, limiting functional improvement.(Y Jin et al. 2016) Furthermore, transplantation of primary adult NPCs has been shown to improve functional outcomes when transplanted two weeks after a cervical crush injury.(Wilcox et al. 2014) Unfortunately, it has proved difficult to control the differentiation of NPCs once they are transplanted with most of them differentiating into glial cells (astrocytes or oligodendrocytes).(Pfeifer et al. 2004) This has led to a focus on factors that can be included with the NPCs in order to help better promote differentiation into neurons;(X. Li et al. 2013) however, differentiation of NPCs is also heavily influenced by the local environment within the host.(Ying Jin, Sura, and Fischer 2012) Thus, while there is significant promise to NPC transplantation, the lack of ability to specifically control what these cells differentiate into has led investigators to pursue the use of pre-differentiation prior to transplant to control cellular phenotype. This has proven to be much easier for transplanting glial cell populations than neurons since glial cells are still capable of dividing and so much easier to maintain in *in vitro* cell culture.

1.3.3 Glial Cell Transplantation

Glia are a large population of supporting cells that are found in nervous tissue that primarily serve to support neuronal function. They achieve this by clearing debris following injury, toxic metabolites, maintaining homeostasis, and facilitating signal transmission and propagation. Since these cells are so important for appropriate neuronal function, they are a logical population to use for transplantation following SCI. Comparison of Schwann cells (SCs) , peripheral glial cells,

and olfactory ensheathing cells to fibroblastic populations have shown that these glial

populations are associated with decreased scar formation and improved axon growth into the

lesion demonstrating that glial cells are able to perform CNS specific functions that improve

regeneration.(Toft et al. 2013)

1.3.3.1 Schwann Cell Transplantation

SCs are the primary supportive cell in the peripheral nervous system. These cells have

been studied for an ability to support recovery from spinal cord injury because of the strong

regenerative potential of peripheral nervous system injuries with peripheral axons able to regrow

across small defects. Furthermore, SCs are myelinating so can, in theory, reform the myelin

sheaths that surround axons to allow for faster conduction. Meta-analysis of SC transplantation

studies showed that, regardless of source (primary or stem cell-derived), transplantation of

Schwann cells significantly improved locomotor function after SCI.(Yang et al. 2015) A specific

example of SC transplantation is the use of oligo[poly(ethylene glycol) fumarate] scaffolds as a

vehicle for transplantation. These scaffolds were found to decrease the size of the glial scar and

reduce the presence of inhibitory CSPGs; although, there were signs of increased inflammation

and immune cell infiltration due to the presence of the scaffold.(Hakim et al. 2015) Another use

for SCs is to modify them to overexpress growth factors thus allowing them to serve as both a

permissive cell population and a drug eluting depot. One example of SCs as growth factor

delivery vehicles is the transplantation of fibroblast growth factor-2 (FGF-2) overexpressing

Schwann cells. Transplantation of these SCs were able to improve the growth of motor axons in

the sciatic nerve following injury.(Allodi et al. 2014) Overall SC transplantation has shown great

promise and SCs are currently under investigation in clinical trials for use in humans. One caveat

to the utility of these transplants is that the ability of the Schwann cells to integrate into the host

spinal cord is determined by the phenotype of the host astrocytes and often axons are unable to leave to lesion area in SC transplanted animals.(Bunge 2016)

1.3.3.2   Oligodendrocyte Transplantation

Oligodendrocytes (OLs) are native to the CNS and are primarily responsible for the formation of myelin sheaths. One significant difference between OLs and SCs is that an OL will myelinate many different axons while Schwann cells myelinate only a single axon. Since they are native to the CNS, OL transplantation has been attempted to facilitate myelination of regenerating nerve fibers. Myelination is an important focus of potential regenerative treatments since it is the final step of recovery in the PNS and is critical for appropriate transmission of action potentials and protection of the axons. Native remyelination in the CNS is more difficult to achieve than in the PNS because mature OLs lack the capacity to produce new myelin sheaths.(Keirstead and Blakemore 1997) This means that central remyelination must be carried out by dividing and differentiating oligodendrocyte precursor cells (OPCs), or infiltrating SCs.(Gensert and Goldman 1997; Brook et al. 1998) There has been some work looking to how to activate local remyelination pathways without requiring cell transplantation. One interesting finding is that treatment of the spinal cord with a synthetic TLR4 agonist (E6020) accelerated myelin debris clearance and remyelination following a demyelinating injury with lysolecithin. This data shows that there is a clear role of macrophage activation in remyelination, it is also worth noting that astrocytes express TLR4 so they may play a role as well.(Church et al. 2017)

Unfortunately there are not many native OPCs and their migration distance is limited(Levine, Reynolds, and Fawcett 2001), so transplantation of OPCs and control of their differentiation *in vivo* has been heavily explored. OPCs themselves do not produce myelin, so they must be differentiated into mature, myelinating OLs. Unfortunately, OLs have proven more

difficult to differentiate from stem cells or progenitors than either astrocytes or neurons partially

due to the dependence of OL differentiation on material properties. Materials that are compatible

with OL differentiation have been reviewed by Russell and Lampe.(Russell and Lampe 2016)

Primary OPCs have been transplanted following SCI, after having been cultured and

modified to express ciliary neurotrophic factor, and were found to improved functional recovery

and remyelinated the axons.(Cao et al. 2010) Similarly, it has been found that human induced

pluripotent stem cells can be pre-differentiated into OPCs and that those cells are able to promote

myelination following a thoracic contusion SCI.(Kawabata et al. 2016) Likewise, human

embryonic stem cells (hESCs) pre-differentiated into OPCs have been found to improve

remyelination and functional repair following contusion or complete transection SCI.(J. Faulkner

and Keirstead 2005; Erceg et al. 2010) Extensive study of these hESC-derived OPCs has

indicated that they are safe for clinical trial(Priest et al. 2015), which has led to an ongoing Phase

I/II clinical trial sponsored by Asterias Biotherapeutics that has reported promising initial

efficacy data.(Biotherapeutics 2017) Despite these early successes with this OPC population in

humans, it is worth noting that a review of all SCI treatment studies using rodent-derived

remyelinating populations found that there is significant inconsistencies in recovery findings,

showing that more work is needed on understanding and manipulating myelinating glia

populations.(Myers et al. 2016)

1.3.3.3   Olfactory Ensheathing Cells

Olfactory ensheathing cells (OECs) are a specialized cell found within the nasal mucosa

that facilitates repeated growth of axons from the peripheral nervous system (nasal mucosa) to

the CNS (olfactory bulb).(Tetzlaff et al. 2011) Due to this role, these cells have been heavily

studied as a means to achieve improved regeneration in both the CNS and peripheral nervous

system. In SCI, transplantation of OECs has been shown to improve axon growth and limit immune cell infiltration into the injury leading to overall improved recovery.(Khankan et al. 2016) There is also some evidence that OEC transplantation may improve recovery from autonomic dysreflexia, which can be a fatal complication of SCI. Specifically, rats with a T4 complete transection SCI were found to have reduced automonic dysreflexia with OEC, but not fibroblast, transplantation.(Cloutier et al. 2016) OECs are used as primary cells that can be isolated directly from the patient due to easy access to the olfactory epithelium. Importantly, the exact function of the OECs in transplantation is dependent on where they are isolated from in the body and how they are treated in culture.(Mayeur et al. 2013) Autologous transplantation of OECs has been attempted as a phase I clinical trial and appeared to be safe with 2 of 3 patients showing improvements in their neurological function score with rehabilitation training.(Tabakow et al. 2013) The difficulty with any autologous treatment is donor site morbidity, in the case of OECs there is a risk of anosmia, and the inherent heterogeneity of primary cultures which makes quality control more difficult. These complications have led to a recent decrease in the number of papers published exploring OEC transplantation.

1.4 Astrocyte Roles in CNS Regeneration

Astrocytes are a large heterogeneous population of glia that serve many important functions that support neuronal activity. These support functions include maintenance of the blood-brain barrier, disposal of toxic metabolites by neurons, signal transduction through tripartite synapses, and water homeostasis. Despite this large variety of roles, astrocytes have been relatively poorly studied in terms of their ability to promote regeneration. A significant contribution to lack of astrocyte study was the general belief in the SCI field that astrocytes are largely responsible for creating an inhibitory environment that needs to be circumvented in for

23

recovery to occur. This concept is supported by the fact that astrocytes create a physical barrier

of overlapping processes(Sun et al. 2010; Sun and Jakobs 2012), as well as produce molecules,

such as CSPGs, that are inhibitory to neuronal growth.(Oohira, Matsui, and Katoh-Semba 1991)

1.4.1 Variability in Astrocyte Reactivity

One explanation of the observed duality in astrocytic roles following SCI is that different

astrocyte subpopulations are involved in scar formation versus bridge formation. This hypothesis

is supported by the inherent heterogeneity of astrocytes(Cahoy et al. 2008) and the known

differences in the purpose and functions of different astrocyte subpopulations within certain

brain regions.(Oberheim, Goldman, and Nedergaard 2012) In support of the idea that there is

heterogeneity in astrocyte reactivity, it has been observed that astrocyte gene expression changes

depending on whether the CNS insult was ischemic or inflammatory. Ischemic injury has been

found to lead pro-regenerative reactive astrocytes, while inflammatory insults leads to more

inhibitory reactive astrocytes.(Zamanian et al. 2012) This injury type-dependent reactivity has

led to the concept that astrocytes may have two types of reactive polarization, similar to

macrophages and microglia, which have been termed A1 or A2 reactive astrocytes. A2 (pro-

inflammatory) astrocytes have "harmful" functions, such as synapse destruction, while A1

reactive astrocytes have "helpful" (pro-regenerative) functions. The heterogeneity of astrocyte

reactivity is a newly appreciated concept and has been reviewed by Liddelow and

Barres.(Liddelow and Barres 2017)

In addition to the differences in astrocyte reactivity depending on insult, it has also been

found that different brain regions behave differently in response to injury. While there are many

astrocyte subtypes in the CNS, astrocytes can be broadly defined as either fibrous (found in

white matter) or protoplasmic (found in grey matter). Interestingly, studies looking at the

reactivity of white matter and grey matter astrocytes following CNS injury have found

significant differences in how astrocyte morphology changes in response to injury. Optic nerve

crush and corpus callosum injury studies have shown that fibrous astrocytes initially retract their

processes following insult and then re-extend them leading to a significant increase in the area

covered by each astrocyte. This process re-extension and hypertrophy leads to significant process

overlap, which disrupts the normal lamellar structure of the white matter.(Sun et al. 2010) In

contrast to this, filling studies performed on resting and reactive protoplasmic astrocytes show

that reactive protoplasmic astrocytes exhibit some process hypertrophy, but they do not exhibit

the same increase in process overlap between adjacent astrocytes.(Wilhelmsson et al. 2006)

These observations together suggest that fibrous astrocytes are more involved in the creation of

the physical barrier found in the glial scar environment, and that potentially a subset of

protoplasmic astrocytes may be responsible for the formation of GFAP[+] bridges across lesion

cavities.

1.4.2 Astrocyte Phenotype alters Transplant Outcomes

The inherent functional differences between fibrous and protoplasmic astrocytes has been

observed in SCI transplant studies as well. Glial restricted progenitors (GRPs) are a population

of primary cells that can be isolated from E13.5 embryos and can differentiate into either fibrous

or protoplasmic astrocytes as well as oligodendrocytes, but not neurons.(Rao, Noble, and Mayer-

Pröschel 1998) Pre-differentiation of these cells into astrocytes using basic fibroblast growth

factor (FGF-2), bone morphogenetic protein 4 (BMP-4) and N2 media supplement showed

improved recovery of when compared to the transplantation of undifferentiated GRPs.(J. E.

Davies et al. 2006) These BMP-4 differentiated astrocytes have a phenotype that is most similar

to protoplasmic astrocytes. Interestingly, when GRPs are pre-differentiated into fibrous-like

astrocytes using ciliary neurotrophic factor (CNTF) they have a detrimental effect of recovery leading to decreased axon penetration into the injury site and increasing allodenia.(J. E. Davies et al. 2008; S. J. A. Davies et al. 2011) Similar to other studies using primary cells, there has been heterogeneity of these findings, likely due to variations in the methods used, that affects study outcomes. When the GRPs remain in a more immature state, transplantation of GRP-derived astrocytes has been found to improve axon penetration into the injury site, regardless of phenotype at the time of transplantation.(C. Haas et al. 2012) Further investigation of the CNTF-exposed GRPs and BMP-4-exposed GRPs has demonstrated that one of the factors responsible for the observed functional difference is periostin-1, which is produced by BMP-4 exposed GRPs, but not CNTF-exposed astrocytes.(Shih et al. 2014) Further periostin-1 experiments found that recombinant periostin-1 improved neurite extension *in vitro* and that periostin-1-deficient BMP-4-exposed GRPs did not have the same beneficial effects as wild type BMP-4-exposed GRPs.(Shih et al. 2014)

The major issue with GRP transplantation is that these cells need to isolated from an embryo, making it difficult to acquire human cells for transplantation and study. One way to address this issue is to develop methods to derive these astrocytes from ESCs thereby allowing these astrocytes to be derived entirely *in vitro*. There have been methods developed that allow for astrocytes to be derived from ESCs(Roybon et al. 2013; R. J. Benveniste, Keller, and Germano 2005), but only mixed populations of astrocytes have been produced rather than attempting to specifically derive populations that exhibit more a fibrous-like or protoplasmic-like phenotype. Overall there is significant promise to astrocyte-based therapies, but there is much left to be elucidated in terms of the reactive states of different astrocyte subtypes and how different astrocyte subtypes effect axon growth and regenerative potential.(Chu et al. 2014)

1.4.3 Small Molecule Manipulation of Host Astrocyte Phenotype

Instead of transplanting astrocytes, there have also been studies investigating the use of growth factors and/or small molecules to cause the native astrocytes to adopt a more pro-regenerative phenotype. Metallothionein is one factor that has been shown to induce astrocytes to become more pro-regenerative through both intracellular and extracellular actions (Leung et al. 2009). Furthermore, delivery of metallothionein has been found to improve neuronal regeneration following an optic nerve crush injury (Siddiq et al. 2015). Endogenous glial cells can also be manipulated by FGF-2 exposure. Studies in both mice and zebrafish have shown that FGF-2 signaling facilitates glial bridge formation following SCI.(Yona Goldshmit et al. 2012; Yona Goldshmit et al. 2014) In addition, knockout of spry4, a FGF signaling inhibitor, has been found to reduce inflammatory response and decrease gliosis following SCI.(Y. Goldshmit et al. 2015) FGF-2 within lipid microtubules has been incorporated into collagen-based hydrogels leading to increased astrocyte infiltration into hydrogels *in vitro*.(Macaya et al. 2013)

There is also evidence that astrocytes exhibit plasticity of their reactive phenotype based on the local, extracellular environment. Astrocytes transplanted acutely into an SCI lesion, but not healthy spinal cord, have been shown to adopt an inhibitory phenotype. This phenotypic switch has been shown to be dependent on integrin-binding to collagen I within the scar. Inhibition of collagen I binding with an anti-β1 integrin antibody leads to increase axon penetration into the SCI lesion and improved behavioral recovery following a spinal cord contusion injury in mice.(Hara et al. 2017)

Consistent with the classification of reactive astrocytes using the same system as macrophages, astrocytes express receptors and cytokines that are associated with the immune system. In particular, astrocytes are known to express toll-like receptor 4 (TLR4), suggesting a pathway for activation in response to lipopolysaccharide (LPS).(Bsibsi et al. 2002) Loss-of-

function and gain-of-function studies of TLR4 and triggering receptor expressed on myeloid cells-2 (TERM-2), a negative regulator of TLR signaling, have shown that increased TLR4 activation with LPS increases pro-inflammatory gene expression by astrocytes. In contrast, increased TERM-2 signaling has been found to modulate this response by decreasing NF-κB activation, suggesting that NF-κB signaling could be an important regulator of pro-inflammatory reactive astrocytes.(Rosciszewski et al. 2017)

Astrocytes are also known to upregulate interleukin receptors in response to injury and to express some interleukins. Because of these expression profiles, it stands to reason that interactions with immune cells and their secreted factors may alter astrocyte phenotype. Two interleukins that have been extensively studied in astrocyte phenotype manipulation are IL-6 and IL-10. IL-6 is a pro-inflammatory cytokine that modulates CNS inflammation. IL-6 is produced by astrocytes after injury or infection(E. N. Benveniste et al. 1990), and the presence of IL-6 has been associated with astrocyte proliferation and scar formation, as well as immune cell infiltration in the acute phase following injury.(M. Nakamura et al. 2005) There is also evidence that in the subacute phase of SCI injury, IL-6 expression has pro-regenerative effects, suggesting a duality of roles for this molecule.(Codeluppi et al. 2014) In contrast, IL-10 is an anti-inflammatory cytokine that is important for the resolution of the immune response throughout the body. In the context on CNS injury, IL-10 has been delivered intrathecally and intramuscularly to improve functional recovery.(Jackson et al. 2005) Furthermore, astrocyte-specific production of IL-10 has been shown to increase immune cell infiltration, but also increases motor neuron survival following a facial nerve axotomy.(Villacampa et al. 2015) There
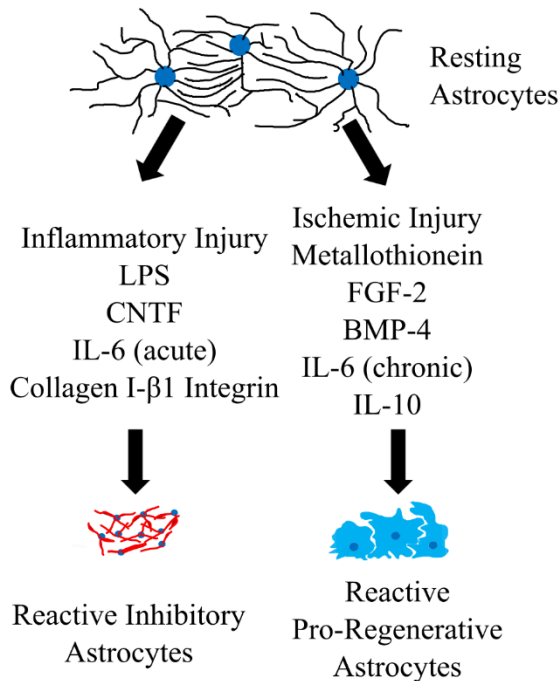
Figure 1.1: Schematic Summary of Factors Known to Affect Astrocyte Reactivity

has been some work using flavopiridol, a cell-cycle inhibitor, as a way to alter the interleukin expression from astrocytes. In particular, flavopiridol delivery from poly(lactic-co-glycolic acid) (PLGA) nanoparticles was found to reduce astrocytic synthesis of pro-inflammatory cytokines, including IL-6, as well as increasing astrocyte-based IL-10 expression.(Ren et al. 2014) These observations of the astrocytic roles in immunomodulation suggest that anti-inflammatory signaling cascades used to alter the immune response in other organ systems may be able to alter reactive astrocyte phenotypes as well. The factors discussed here are summarized in Figure 1.1. Overall the manipulation of astrocyte heterogeneity is still being actively investigated and holds great potential as a means to harness astrocytes as a regenerative population.

1.5   Biomaterial-based Manipulation of Glial Phenotypes

Given the complexities of glial cell response to trauma, with some glia providing a pro-regenerative support and others tending to inhibit regeneration, there is significant potential benefit to use materials to manipulate the phenotypes of both transplanted and native glia. The major approaches used for these manipulations are modifying the mechanical properties, composition, growth factor delivery, and alignment of the materials. Here what is known about

how these biomaterial factors affect the phenotype and differentiation of the major CNS glial populations is discussed.

1.5.1 Material Properties affecting Cell Fate

Matrix stiffness is a powerful tool for the manipulation of cell phenotype and the differentiation of neural progenitor cells (NPCs). NPCs have been shown to differentiate into OLs and neurons on softer matrixes and generally differentiate into astrocytes on stiffer matrices.(Seidlits et al. 2010; Russell and Lampe 2016) In addition to OL differentiation being dependent on matrix stiffness, myelination by either SCs or OLs is affected by matrix elasticity with low elasticity matrices allowing for increased myelin production by OLs. In contrast, high matrix elasticity increases SC myelin production.(Urbanski et al. 2016) These elasticity differences are the result of non-muscle myosin II which has been found to be a positive myelin regulator in the PNS, but a negative myelin regulator in the CNS.(Urbanski et al. 2016; H. Wang et al. 2008) These studies demonstrate that material properties are an important consideration when designing scaffolds for either the CNS or PNS.

Consistent with the observation that material properties affect NPC differentiation, there is also evidence that integrin signaling is important for astrocytic differentiation from neural progenitor populations. In particular, the exposure of NPCs to IKVAV peptide amphiphile (IKVAV-PA) has been shown to increase neuronal differentiation and decrease astrocyte differentiation.(G. A. Silva et al. 2004) IKVAV is an important integrin binding region of laminin, demonstrating the importance of ECM signals in NPC differentiation, and the amphiphile structure used for delivery of the peptides allows for a significant increase in epitope density. Delivery of IKVAV-PA has also been shown to decrease glial scar density, and increase oligodendrocyte infiltration following a compressive SCI in mice.(Tysseling-Mattiace et al.

2008) The observed effect of IKVAV-PA particles on differentiation has been partially attributed to β1-integrin signaling with both ESCs and subventricular zone NPCs demonstrating increased astrocyte differentiation in the presence of IKVAV when β1-integrin is knocked out. The importance of β1-integrin signaling in functional recovery following SCI is further suggested by observed behavioral improvements in mice treated with 2 other β1-integrin binding peptide amphiphiles, RGD-PA or ADEGVFDNFVLK (Tenascin C)-PA.(Pan et al. 2014)

1.5.2 Materials that increase Myelination following CNS Trauma

Since myelination is a critical step in recovery from nervous system trauma, the ability of implanted materials to increase the percent of myelinated fibers could have significant clinical utility. Since remyelination occurs late following SCI and native OLs don't have a high capacity for remyelination, the ability of materials to promote local remyelination *in vivo* has not been extensively studied. A comparative study of different substrates effect on myelination *in vitro* by myelinating cultures composed of primary cells isolated from E15 rat spinal cords found that low molecular weight ε-polycaprolactone (PCL) increased myelination compared to polycarbonate, poly(methyl) methacrylate, polystyrene, poly-L-lactide, polydimethylsiloxane, and high molecular weight PCL. These studies also showed a clear effect on astrocyte phenotype on myelination with media conditioned by astrocytes cultured on PCL decreasing OL myelination, while media conditioned by astrocytes cultured on glass increased OL myelination.(Donoghue et al. 2013) This suggests that astrocyte phenotype should be considered when designing materials to increase remyelination following CNS injury.

There have been some acellular *in vivo* implantation studies that have shown increased myelin production. One strategy is to deliver sonic hedgehog (SHH) and neurotrophin-3 (NT-3). These factors were delivered following a lateral hemisection SCI using lentivirus within a

31

multiple channel bridge composed of PLGA. The inclusion of NT-3 was found to increase myelination by infiltrating SCs, while SHH over-expression significantly increased OL myelination.(Thomas et al. 2014) Another material found to increase myelination is a Chitosan Fragmented Physical Hydrogel suspension (Chitosan-FPHS). This material was found to increase myelination in rats at 4, 8 and 10 weeks after a dorsal over-hemisection SCI from both SCs and OLs. Interestingly, the OL myelination observed in this study was restricted to regions in which astrocytes were able to infiltrate the Chitosan-FPHS.(Chedly et al. 2017)

1.5.3 Materials that Alter Astrocyte Phenotypes

Astrocyte phenotype and penetration is an important consideration for CNS repair materials since astrocytes are known to support neuronal growth and to be required for the survival of certain neuronal populations. It has been found in many biomaterials that neuronal growth into the material is correlated with astrocytes or their processes.(Pawar et al. 2015; Taylor et al. 2006) This makes the astrocytic response to transplanted materials crucial to consider and demonstrates the importance of determining how to push native astrocytes away from a scar phenotype toward a more pro-regenerative state. One material that has been shown to limit inhibitory astrocyte formation is high molecular weight (MW) hyaluronic acid (HA). Acute transplant of high MW HA following dorsal hemisection SCI decreased immune cell infiltration and CSPG deposition.(Khaing et al. 2011) The same is not true of small (40-400 kDa) HA chains, which have been shown to activate NF-κB in astrocytes and so upregulate inhibitory reactive astrocytes.(Pandey et al. 2013) Similar to this observation with HA, implantation of fibrin scaffolds has also be found to slow the accumulation of reactive astrocytes around a SCI lesion.(Johnson, Parker, and Sakiyama-Elbert 2010)

Matrix alignment has been shown to be a powerful tool in glial manipulations with glia cells, and neurons, aligning to a provided matrix. Unfortunately, alignment is extremely difficult to achieve *in vivo,* so much of what is known about alignment effects is based on *in vitro* data. Aligned cell morphology has been shown to result in increased neurite outgrowth in both 2 and 3 dimensions.(Corey et al. 2007; East et al. 2010) Furthermore, when aligned astrocytes enhance neuronal growth in the direction of alignment.(Biran, Noble, and Tresco 2003) In addition, randomly-aligned, electrospun polyamide nanofibers have been found to decrease astrocyte process hypertrophy and GFAP expression *in vitro* compared to poly-L-lysine on either glass or Aclar in response to an inflammatory stimulus (dibutyryladenosine cyclic monophosphate).(Volkan Müjdat Tiryaki et al. 2015; Volkan Mujdat Tiryaki et al. 2012) This suggests that astrocytes may adopt a more quiescent phenotype when on a fibrillar surface *in vitro*, regardless of alignment. Here only the effect of electrospun materials on astrocytes is reviewed, for a complete review of electrospun material in SCI regeneration see Schaub *et al.*(Schaub et al. 2016)

Since electrospinning can be used to generate alignment, the benefit of fibrillar matrices and alignment has been widely used material starting point for astrocyte manipulations *in vitro*. Study of astrocytes cultured on aligned collagen fibers *in vitro* have found that astrocytes in an aligned environment decrease expression of GFAP, a hallmark of astrocyte reactivity, and elongated in the direction of alignment. This in turn led to more organized neurite outgrowth from dorsal root ganglions (DRGs).(T. Liu et al. 2012) Furthermore, these structures could be rolled into 3D conduits that maintain their alignment growth benefits.(T. Liu et al. 2012) Further manipulation of collagen fibers with other matrix proteins can be used to improve astrocyte alignment and decrease the expression of CSPGs. In particular, fibrinogen coating significantly

increased alignment with the collagen fibers, while aggrecan, laminin, and fibrinogen, but not fibronectin decreased CSPG expression of cultured astrocytes.(Hsiao, Tresco, and Hlady 2015)

Astrocytes cultured on aligned PLLA materials have also been found to elongated and upregulate the two major glutamate transporters, glutamate transporter 1 (GLT-1) and glutamate and aspartate transporter 1 (GLAST).(Zuidema et al. 2014) The presence of these transporters is important to the support of excitatory, glutamatergic neurons which are unable to process the glutamate they release leading to excitotoxicity. PLLA scaffolds have also been used to release 6-aminonicotinamide, which is an anti-metabolite, to reduce the metabolic rate of astrocytes cultured on the drug-eluting fibers.(Schaub and Gilbert 2011) In addition to alignment effects, fiber size also impacts astrocyte phenotypes with 400 nm silk fibers inducing longer astrocyte process extension, increasing area per astrocyte, and improving neuronal maturation when compared to 1200 nm fibers.(Qu et al. 2013) Increasing the stiffness of 400 nm cellulose acetate nanofibers from a tensile modulus of around 24 MPa to around 80 MPa resulted in an increase in astrocyte attachment, proliferation, and ECM deposition.(Min et al. 2015) It is important to note that alignment is difficult to achieve in an implantation setting, and so the clinical utility of alignment is currently limited. However, randomly aligned, coated electrospun fibers could have significant potential as a strategy to manipulate glial populations. Electrospun, randomly aligned PCL scaffolds have been seeded with human endometrial stem cells and transplanted following dorsal hemisection in rats. The PCL scaffold implant was found to slightly increase neurite growth into the SCI lesion, demonstrating the potential of electrospun scaffolds as a treatment strategy.(Terraf et al. 2017)

1.6 Summary

Recent work has shown promise for improved treatments for SCI, although there is much work still to done to improve the prognosis for those who suffer from SCI. In this work, methods are developed to derive protoplasmic and fibrous astrocytes from mouse ESCs and the differences in the ability of these populations ability to support the growth of ESC-derived neuronal populations is explored. To further future transplantation and functional studies, a new mESC cell line is developed that could allow for pure ESC-derived astrocyte population acquisition. Finally, the ability of a novel hydrogel, composed of HA and decellularized astrocyte ECM, to improve the expression of histological recovery markers following a thoracic dorsal hemisection SCI was explored as was the ability of these hydrogels to support V2a interneuron transplantation. (R. Thompson and Sakiyama-Elbert 2018)

Chapter 2: Different Mixed Astrocyte Populations Derived from Embryonic Stem Cells have Variable Neuronal Growth Support Capacities

2.1 Abstract

Central nervous system (CNS) injury often leads to functional impairment due, in part, to the formation of an inhibitory glial scar following injury that contributes to poor regeneration. Astrocytes are the major cellular component of the glial scar, which has led to the belief that they are primarily inhibitory following injury. Recent work has challenged this by demonstrating that some astrocytes are required for spinal cord regeneration, and that astrocytic roles in recovery depends on their phenotype. In this work, two mixed populations containing primarily either fibrous or protoplasmic astrocytes were derived from mouse embryonic stem cells (ESCs). Motoneuron and V2a interneuron growth on live cultures, freeze-lysed cultures, or decellularized extracellular matrix (ECM) from astrocytes was assessed. Both neuronal populations were found to extend significantly longer neurites on protoplasmic-derived substrates than fibrous-derived substrates. Interestingly, neurons extended longer neurites on protoplasmic-derived ECM than fibrous-derived ECM. ECM proteins were compared with *in vivo* astrocyte expression profiles, and it was found that the ESC-derived ECMs were enriched for astrocyte-specific proteins. Further characterization revealed that protoplasmic ECM had significantly higher levels of axon growth promoting proteins, while fibrous ECM had significantly higher levels of proteins that inhibit axon growth. Supporting this observation, knockdown of spondin-1 improved neurite growth on fibrous ECM, while laminin α5 and γ1 knockdown decreased neurite growth on

protoplasmic ECM. These methods allow for scalable production of specific astrocyte subtype-containing populations with different neuronal growth support capacities, and can be used for further studies of the functional importance of astrocyte heterogeneity.

2.2 Introduction

Central nervous system (CNS) trauma represents a significant healthcare burden in the United States, in part due to its limited regenerative capacity. Spinal cord injury (SCI) is a good modality for studying CNS regeneration because the cord can be relatively easily accessed, the axonal tracts can be reliably severed by hemisection, and a stereotyped glial scar and lesion cavity forms after injury(Cregg et al. 2014). The lack of regeneration following CNS trauma has historically been partially attributed to the astrocytes present within the glial scar, which represents a physical and chemical barrier to axon growth. This has led to a focus in the field on removing astrocytes to facilitate CNS regeneration.

Astrocyte removal has been achieved in SCI models by using genetic tools to knockout genes required for astrocytes reactivity. In vimentin and glial fibrillary acidic protein (GFAP) double knockout mice, astrocytes do not become appropriately reactive after SCI leading to impaired glial scar formation, and increased bleeding (Pekny et al. 1999). Similarly, conditional knockout of floxed STAT3, an inducer of astrocyte reactivity, using GFAP-Cre has been found to disrupt the formation of the glial scar, increase macrophage infiltration into the spinal cord, and lead to a larger lesion cavity after SCI (Herrmann et al. 2008). Conditional ablation of reactive astrocytes at the time of injury or 5 weeks after SCI using GFAP-thymidine kinase (TK) + ganciclovir has also been shown to lead to worse functional outcomes due to death of dividing GFAP$^+$ cells. These studies demonstrate that astrocytes are required both acutely to control spread of secondary injury and chronically to facilitate functional recovery (Anderson et al. 2016; J. R.

Faulkner et al. 2004). Thus, there is a clear role for astrocytes in CNS regeneration and potential for their contribution to regenerative therapies.

Recent work on astrocytes has shown that there are many more distinct astrocyte populations than previously believed (Cahoy et al. 2008; Oberheim, Goldman, and Nedergaard 2012). Furthermore, the type of insult, inflammatory or ischemic, to the CNS has been shown to affect whether native astrocytes become more pro-regenerative or more inhibitory, supporting the idea that some astrocytes have pro-regenerative roles (Zamanian et al. 2012). The physical barrier represented by the glial scar is primarily due to the woven nature of astrocyte processes adjacent to the lesion (Sun and Jakobs 2012). Structural studies of astrocytes suggest that not all astrocyte populations form such barriers in response to trauma. In particular, fibrous (white matter) astrocytes have been shown to exhibit process hypertrophy and a significant increase in process overlap following injury in optic nerve (Sun et al. 2010); conversely, protoplasmic (grey matter) astrocytes have been demonstrated to exhibit some process hypertrophy after injury, but little to no increase in process overlap (Wilhelmsson et al. 2006). These studies show that fibrous astrocytes adopt a phenotype more consistent with classic glial scar morphology in response to injury, suggesting that these populations may be more involved in glial scar formation. With the lower levels of overlap observed in reactive protoplasmic astrocytes, it is possible that a subset of these astrocytes may be responsible for pro-regenerative effects of astrocytes following CNS injury.

The concept that astrocyte subtypes have variable roles following injury has been explored using primary glial restricted progenitors (GRPs), isolated from rat, mouse and human embryonic spinal cords (Rao, Noble, and Mayer-Pröschel 1998). These cells have been successfully transplanted into rats following a right-sided cervical dorsal column transection SCI

leading to improved recovery (Y Jin et al. 2016; J. E. Davies et al. 2006). Furthermore, GRPs have been pre-differentiated into astrocytes using either ciliary neurotrophic factor (CNTF) or bone morphogenic protein 4 (BMP-4) to generate fibrous-like or protoplasmic-like astrocytes (J. E. Davies et al. 2008). When transplanted following spinal cord injury, GRPs differentiated into fibrous astrocytes were found to have a detrimental effect on axon growth into the lesion and functional outcomes, while protoplasmic transplants improved axon growth and functional outcomes (J. E. Davies et al. 2008; S. J. A. Davies et al. 2011). While isolation of GRPs from humans has been achieved from a fetal brain and spinal cord, these methodologies are not scalable for clinical use. The novel component of our work is the derivation of these astrocyte populations from mouse embryonic stem cells (ESCs). This methodology could be applied to human pluripotent cells, and thus represents a scalable cell source for future pro-regenerative astrocyte-based therapy development. Furthermore, an ESC source of these astrocytes could allow for further elucidation of the mechanisms utilized by pro-regenerative astrocytes that are absent in astrocyte populations inhibitory to axon growth and vice versa.

Previous protocols to derive astrocytes from ESCs have not focused on deriving specific astrocyte subtypes. In this work, glial cell populations containing primarily fibrous or protoplasmic astrocytes are derived from mouse ESCs. These populations are then demonstrated to have different abilities to support the growth of ESC-derived motoneurons and V2a interneurons, with protoplasmic populations allowing neurons to extend significantly longer neurites than observed on fibrous populations. Finally, these neuronal growth support differences are found to be due, in part, to altered extracellular matrix (ECM) composition with fibrous astrocyte populations depositing more axon growth-inhibitory proteins while protoplasmic astrocyte populations deposit more axon growth-permissive proteins.

39

2.3 Materials and Methods

2.3.1 mESC Culture

RW4 (ATCC, SCRC-1018) mESCs were maintained in complete media (10% Fetal Bovine Serum (Invitrogen), 10% Newborn Calf Serum (Invitrogen), 132 µM beta mercaptoethanol (BME) (Sigma, St Louis, MO), 10,000 units/mL mouse leukemia inhibitory factor (Life Technologies, Carlsbad, CA) and passaged when at 60-80% confluency. Cells were passaged using 0.25% trypsin-EDTA (Life Technologies) at 37°C for 5 min to dissociate the cells. The trypsin reaction was quenched and cells were seeded into a new T25 flask coated with 0.1% gelatin (Sigma).

2.3.2 Glial Population Differentiation

$1x10^6$ RW4 ESCs were cultured in suspension on agar-coated 10 cm dishes in 10 mL DFK5 (DMEM/F12 (Life Technologies) plus 5% Knockout Serum Replacement (Life Technologies), 50 µM nonessential amino acids (Life Technologies), 1x Insulin-Transferrin-Selenium (Life Technologies), 100 µM beta-mercaptoethanol (Sigma), 5 µM thymidine, and 15 µM of the following nucleosides: adenosine, cytosine, guanosine, and uridine (Life Technologies) for two days to form embryoid bodies (EBs) followed by 4 days in 10 mL DFK5 plus 2 µM RA and 600nM Smoothened Agonist (SAG) to confer a spinal identity with a media change after 2 days (Roybon et al. 2013). On day 6, the EBs were dissociated and $4x10^6$ cells were seeded onto a gelatin-coated low adherence 10 cm dish (ThermoFisher) in DFK5 media plus 20 ng/mL epithelial growth factor (EGF) (Peprotech), 10 ng/mL fibroblast growth factor 1 (FGF-1) (Peprotech) and 1 µg/mL laminin for 5 days as described in Benvensite *et al.* (R. J. Benveniste, Keller, and Germano 2005). On day 11, the cultures were switched into lineage-specific media for 4 additional days on the same plates. Fibrous media: DMEM/F12 plus 1x G5 supplement

(Invitrogen), 10 µg/mL CNTF (Peprotech); Protoplasmic media: DFK5 plus 10 µg/mL FGF-1,

10 µg/mL BMP4 (Peprotech); Benveniste astrocyte media: DFK5 plus 10 µg/mL FGF-1, 10

µg/mL platelet derived growth factor AA (PDGF-AA) (Peprotech) (R. J. Benveniste, Keller, and

Germano 2005). At day 15 the cells were reseeded onto gelatin-coated plates at a density of

20,000 cells/cm^2 and maintained in lineage specific media for 6 additional days prior to use

(Figure 2.1A).

2.3.3 Immunocytochemistry (ICC)

Cells were fixed in 4% paraformaldehyde (Sigma) for 20 mins and then permeabilized in 0.1%

Triton-X (Sigma) for 15 mins. Cells were then blocked with 5% of an appropriate serum (Goat

(Sigma) or Donkey (Sigma)) in phosphate buffered saline (PBS) for 1 hr. Primary antibodies

were used at the following dilutions: GFAP 1:100 (Immunostar), A2B5 1:25 (DSHB), aquaporin

4 (Aqp4) 1:100 (Santa Cruz Biotechnology), Olig2 1:1000 (Santa Cruz Biotech), CS56 1:250

(Sigma), Spondin-1 1:100 (Abcam), Collagen XIIα1 1:100 (Santa Cruz Biotechnology), Sox2

1:100 (Santa Cruz Biotechnology), HSPG2 1:100 (Fisher), O4 1:100 (Millipore), S100 1:100

(Dako, Santa Clara, CA), SSEA-1 1:25 (DSHB), Oct 3/4 1:200 (Santa Cruz Biotech), β-tubulin

1:1000 (Biolegend), Neurofilament 1:10 (DSHB), Nestin 1:10 (DSHB). Primary antibody

incubation was carried out overnight in 2% of appropriate serum in PBS. Secondary antibodies

(Life Technologies) were all used at a 1:1000 dilution and incubated in 2% of appropriate serum

in PBS for 1 hr at room temperature. 1:1000 Hoechst (Invitrogen) in PBS was incubated with the

cells for 15 min prior to imaging. Nuclear colocalization was determined using Cell Profiler

software (Broad Institute).

2.3.4 Flow Cytometry

Fibrous and protoplasmic populations were removed from the plate surface with 0.25% trypsin-EDTA and fixed using 1% paraformaldehyde for 15 min followed by blocking in 5% goat serum in PBS for 20 min. Primary antibody incubation was performed for 45 min using the same dilutions as ICC. Cells were washed once with PBS and secondary incubation was performed for 45 min prior to washing three times with PBS. Cells were then analyzed using a Guava EasyCyte (Millipore), and the data was quantified using FlowJo. For analysis, a cell gate was drawn based on forward scatter and side scatter. Staining graphs were restricted to events within this cell gate and stain gates were drawn based on secondary only controls to exclude 99% of control events from the gate to minimize the false positive rate. Quadrant gates for double stained samples were drawn based on secondary controls as well as single stained populations.

2.3.5 Quantitative reverse transcriptase PCR (qRT-PCR)

Table 2.1: qPCR primers used to validate astrocyte identity

Target	Primer ID (ThermoFischer)
β-actin	Mm02619580
GFAP	Mm01253033
GLT-1	Mm01275814
GLAST	Mm00600697
GDNF	Mm00599849

Day 21 glial populations were removed from the culture plate via 0.25% trypsin treatment followed by quenching with CM. The resulting cell suspension was then spun down at 300 rcf at 4° C for 5 min, and the RNA was extracted using a Qiagen RNA extraction kit following manufacturer instructions. RNA concentration was determined using an Implen Nanophotomer and 500 ng of RNA from each sample was converted to cDNA using a High-Capacity RNA to cDNA kit (Applied Biosystems). Finally, the mRNA levels of the genes of interest was determined using specific Taqman assays following manufacturer instructions (Life Tech, Table 2.1). β-actin was used as the normalization control in all samples.

42

2.3.6 Viral Knockdown

At day 15 of differentiation, cells were seeded at 10,000 cells/cm^2 in appropriate media. Cells were then infected with mission shRNA lentiviral particles (Sigma, Table 2.2) at a multiplicity of infection of 2.5 on day 16. Infection was allowed to proceed for 1 day and media was then replaced and the cells cultured for an additional day. To ensure only infected cells were present, cultures were selected with 2 µg/mL puromycin for either 1 day for the fibrous cultures or 2 days for the protoplasmic cultures. On day 21, all cells were removed from the plate using trypsin and reseeded onto gelatin-coated 48 well plates. Cells were then cultured for 6 days with media changes every other day to allow for ECM deposition. After ECM deposition, cells were removed by decellularization as described in substrate preparation or stained for ICC.

Table 2.2: shRNA viruses used for ECM knockdown studies

Target	TRC Number
Spondin-1	0000090520
Laminin ɣ1	0000055421
Laminin α5	0000252850
Perlecan	0000256980
Collagen XIIα1 1	0000091115
Collagen XIIα1 2	0000091116
Collagen XIIα1 3	0000335258
Collagen XIIα1 4	0000335319
Collagen XIIα1 5	0000335320
Collagen VIα3 1	0000091854
Collagen VIα3 2	0000091855
Collagen VIα3 3	0000091856
Collagen VIα3 4	0000091857
Laminin β1 1	0000094314
Laminin β1 2	0000094315
Laminin β1 3	0000094316
Laminin β1 4	0000094317
Laminin β1 5	0000094318

2.3.7 Substrate Preparation

Day 21 glial cells were seeded onto gelatin-coated 48-well plates at a density of 20,000 cells/cm^2 and cultured for 6 days in appropriate media to allow for matrix deposition. Following the 6 day culture period, cells were removed via decellularization (using a modified Hudson protocol

(Hudson, Liu, and Schmidt 2004)), lysed via freezing, or left alive. For frozen cells, the plates were sealed with Parafilm (Bemis, Neenah, WI) and placed in the freezer overnight. All plates were washed once with DMEM containing 25mM HEPES (Life Technologies) prior to neuron seeding.

2.3.8 Motoneuron Culture

Motoneurons were derived from Hb9-Puro CAG-TdTomato mESCs that constitutively express TdTomato under the control of the synthetic CAG promoter, as previously described (D. A. McCreedy et al. 2014). To obtain pure motoneuron cultures, EBs were selected with 4 µg/mL puromycin from day 5 to 6 of differentiation prior to dissociation seeding onto the desired substrate at a density of 20,000 cells/cm^2. Motoneurons were cultured in half DFK5 and half Neurobasal media (Life Tech) plus 1x B27. Cultures were then imaged at regular time points over 2 days.

2.3.9 V2a Interneuron Culture

V2a interneurons were generated from Chx10-PAC bact-TdTomato mESCs as previously described (Iyer et al. 2016). After induction, EBs were dissociated with 0.25% trypsin and $2.5x10^7$ cells were seeded onto a poly-L-ornithine/laminin coated T25 flask. Chx10$^+$ cells were then selected in half neural basal-half DFK5 media with 1x GlutaMAX (Life Tech), 1x B27, 2 µg/mL puromycin and 10 ng/mL of the following growth factors for 24 hr: glial-derived neurotrophic factor (GDNF) (Peprotech), neurotrophin-3 (NT-3) (Peprotech), and brain-derived neurotrophic factor (BDNF) (Peprotech). After selection, neurons were lifted from the flasks using Accutase® (Sigma) treatment for 30 min and then reseeded at 50,000 cells/cm^2 onto the desired substrate in half neuro basal-half DFK5 media plus 1x GlutaMAX, 1x B27, and 10

ng/mL of the following growth factors: BDNF, GDNF, NT-3. Neurite extension for both neuronal types was determined using Cell Profiler.

2.3.10 Conditioned Media

After day 15 of differentiation, each population was seeded in its appropriate media for 2 days to condition the media. Conditioned media (CM) was subsequently harvested and spun down at 3000 rcf for 25 min. Motoneurons were seeded at 84,000 cells/cm^2 onto poly-L-ornithine coated 6-well polystyrene dishes in one of three media conditions: 50% unconditioned protoplasmic media and 50% unconditioned fibrous media, 50% protoplasmic CM and 50% unconditioned fibrous media, or 50% unconditioned protoplasmic media and 50% fibrous CM. This 50:50 mixing strategy was used so CM effects could be directly compared without having the growth factors in the astrocyte media affect neuronal growth outcomes. Following the addition of one of the three media solutions to motoneuron cultures, five images of each condition were acquired in a random spatial orientation every 24 hrs for 3 days, and the neurite area per nucleus was quantified with Cell Profiler.

2.3.11 Proteomics and Western Blotting

Day 21 cells were seeded at 20,000 cells/cm^2 onto gelatin-coated plates and allowed to grow for 6 days prior to decellularization. After decellularization, the residual proteins were scraped off the plate into Milli-Q water and lyophilized overnight. The resulting powder was dissolved in 4% sodium dodecyl sulfate (SDS) (Sigma) 100mM Tris-HCl pH 7.6 (ThermoFisher). Protein concentration of this solution was determined using a BCA Assay Kit (ThermoFisher) and then dithiothreitol (DTT) (ThermoFisher) was added to the samples to a final concentration of 100mM. 15 µg of ECM protein was used for proteomics analysis. For western analysis, the samples were run on 4-15% mini-PROTEAN TGX gradient gels (Bio-rad) at 130 V for 1.5 hr.

Western tank transfer was performed at 30 V overnight using 10% methanol (Sigma), 25 mM

Tris Base (ThermoFisher) and 192 mM Glycine (Sigma) transfer buffer to a PVDF membrane

(Millipore). The membrane was then probed with the following antibody dilutions overnight:

Spondin-1 1:150, Collagen XIIα1 1:200, HSGP2 1:100. Licor goat anti-rabbit and goat anti-rat

secondary antibodies were used at a dilution of 1:15000 in PBS and were incubated for 20 min

prior to imaging.

2.3.12 Preparation of peptides for LC-MS

15 µg of ECM proteins solubilized in 30 µL SDT buffer (4%SDS, 100mM Tris-HCl pH 7.6,

100mM DTT) were diluted with 200 µL of 100 mM Tris-HCL buffer, pH 8.5 containing 8M

urea. Detergent was removed by buffer exchange in filter unit with a 30K MWCO (Millipore,

part# MRCF0R030). Iterative centrifugations were performed at 14,000 rcf for 15 min with the

addition of 200 µL of 100mM Tris-HCL buffer pH 8.5 containing 8M urea to the top filter unit.

The proteins were alkylated with 100 µL of 50mM iodoacetamide directly in the top of the filter,

mixing at 25 rcf and incubating at room temperature for 20 min in the dark. The filter was spun

at 14000 rcf for 10 min and the flow through discarded. Unreacted iodoacetamide was washed

through the filter with application of 2 x 200 µL of 100mM Tris-HCL buffer, pH 8.5 containing

8M urea with centrifugation for 10 min after each addition. The urea buffer was exchanged into

100 mM ammonium bicarbonate buffer, pH 8 with two additions of 200 µL each and spinning

after each addition. The filters were transferred to a new collection tube and 100 µL of 0.05

µg/µL trypsin, dissolved in 100mM ammonium bicarbonate buffer, was added to each filter. The

samples were digested overnight at 37°C in a humidity chamber. An additional aliquot of trypsin

(1 µg) was added and digestion was continued for 4 hr. The filter units were spun for 15 min and

the digest was collected in the lower unit. The filter was washed with 50 µL 0.5M sodium

chloride, and the wash was collected with the peptides. Residual detergent was removed by ethyl acetate transfer, followed by acidification to 5% formic acid final concentration in preparation for desalting. The peptides were desalted using micro-tips (C4, BIOMEKNT3C04 and porous graphite carbon, BIOMETNT3CAR) (Glygen) on a Beckman robot (Biomek NX) as previously described (Chen et al. 2012) for analysis using LC-MS.

2.3.13 LC/MS Analysis

LC-ESI/MS/MS analysis was performed using a Q-Exactive™ Plus Hybrid Quadrupole-Orbitrap™ Plus mass spectrometer (ThermoFisher) coupled to an EASY-nanoLC 1000 system (ThermoFisher). The samples were loaded (2 µL) onto a 75 µm i.d. × 25 cm Acclaim® PepMap 100 RP column (ThermoFisher). The peptides were eluted at a flow rate of 300 nL/min with an acetonitrile gradient in aqueous formic acid (0.1%) as mobile phase A. Peptide elution occurred in the following sequence: 0-4% B (buffer B) for 1 min, 4-12% B over 127 min, 12- 22% B over 112 min, 22-30% B over 40 min, 30-70% B over 6 min, hold at 70% B for 6 min, followed by increase in B to 95% B over 1 min and an isocratic wash at 95% B for 6 min. Full-scan mass spectra were acquired using the Orbitrap™ mass analyzer in the mass-to-charge ratio (m/z) of 375 to 1500 and with a mass resolving power set to 70,000. Ten data-dependent high-energy collisional dissociations (HCD) were performed with a mass resolving power set to 35,000, a fixed first m/z 100, an isolation width of 2.0 m/z, and the normalized collision energy (NCE) setting of 27. The maximum injection time was 120 ms for parent-ion analysis and 120 ms for product-ion analysis. Target ions already selected for MS/MS were dynamically excluded for 30 sec. An automatic gain control (AGC) target value of $3x10^6$ ions was used for full MS scans and $5x10^5$ ions for MS/MS scans. Peptide ions with charge states of one or greater than seven were excluded from MS/MS acquisition. The tandem mass spectra were processed using Matrix

47

Science Distiller version 2.5 without charge state deconvolution and deisotoping. The processed

files were used for protein database searches using Mascot (Matrix Science, London, UK;

version 2.5.1). The UniProt Mouse Reference database (downloaded May 3, 2014, 69021

entries) was used. A parent ion tolerance and MS2 fragment tolerance were set to 10 ppm and

0.05 Da, respectively. Carbamidomethyl of cysteine was specified as a fixed modification and

oxidation of methionine was set as a variable modification. Protein identifications were

performed using Scaffold, version 4.4.8 (Proteome Software Inc., Portland, OR) implementing

the Protein and Peptide Prophet algorithms (Keller et al. 2002; Nesvizhskii et al. 2003). Peptide

identifications were accepted with > 90.0% probability. Protein identifications were accepted if

they could be established at greater than 95.0% probability and contained at least 2 peptides with

unique sequences. Protein probabilities were assigned using the Protein Prophet algorithm.

Proteins that contained similar peptides, but could not be differentiated based on identification of

unique peptide sequences, were grouped to satisfy the principles of parsimony**.**

2.3.14 TRAP-Seq analysis

TRAP libraries were sequenced on an Illumina HiSeq 2500, and reads were analyzed as

previously described (Reddy et al. 2016). Differential expression analysis of cortex TRAP vs.

PreIP was performed using the edgeR package. Raw and analyzed RNA-sequencing data are

available at GEO: GSE74456. For the present study, only cortex PreIP and TRAP samples were

used (GSM1920988-1920993). Candidate ECM components were mapped to Ensembl gene IDs

using the biomaRt package, based on gene symbol. Out of the 638 ECM components with ≥99%

protein identification probability, 559 were robustly expressed in the TRAP-seq samples and

thus were used for comparative analysis.

2.3.15 Statistics

Statistical analysis was performed using Minitab software for neurite length measurements (one-way ANOVA with Bonferroni correction). Excel was used for qRT-PCR (pairwise t-test) and colocalization data (Student's t-test). Proteomics data was analyzed using Scaffold4, significance determined with Fisher exact test using the Benjamini-Hochberg false positive correction method.

2.4   Results

2.4.1   Generation of Fibrous Astrocyte or Protoplasmic Astrocyte containing Glial Populations from mESCs

To determine the effect of fibrous and protoplasmic populations on neuron growth, methods were developed to obtain these astrocyte subtypes from mESCs. In particular, this protocol was based on prior ESC-derived astrocyte protocols described in Benveniste *et al.* (R. J. Benveniste, Keller, and Germano 2005) and Roybon *et al.* (Roybon et al. 2013), and the GRP-derived astrocyte protocol described in Davies *et al.* (J. E. Davies et al. 2006). This protocol was designed to generate spinal populations by first caudalizing mESCs with RA treatment (Wichterle et al. 2002) followed by BMP-4 treatment to obtain cultures containing protoplasmic astrocytes, and CNTF treatment to obtain cultures containing fibrous astrocytes (Figure 2.1A, (R. E. Thompson et al. 2017)). To allow for direct comparison of protein expression between the fibrous and protoplasmic populations, a second population containing protoplasmic-like astrocytes was generated using the protocol described in Benvensite *et al.* (R. J. Benveniste, Keller, and Germano 2005). This protocol was not used for future studies because the continued use of PDGF-AA led to significant oligodendrocyte presence within the cultures. To determine the dominant phenotype of the astrocytes within these cultures, the expression of known protoplasmic or fibrous markers was assessed using ICC and qRT-PCR. In particular, A2B5
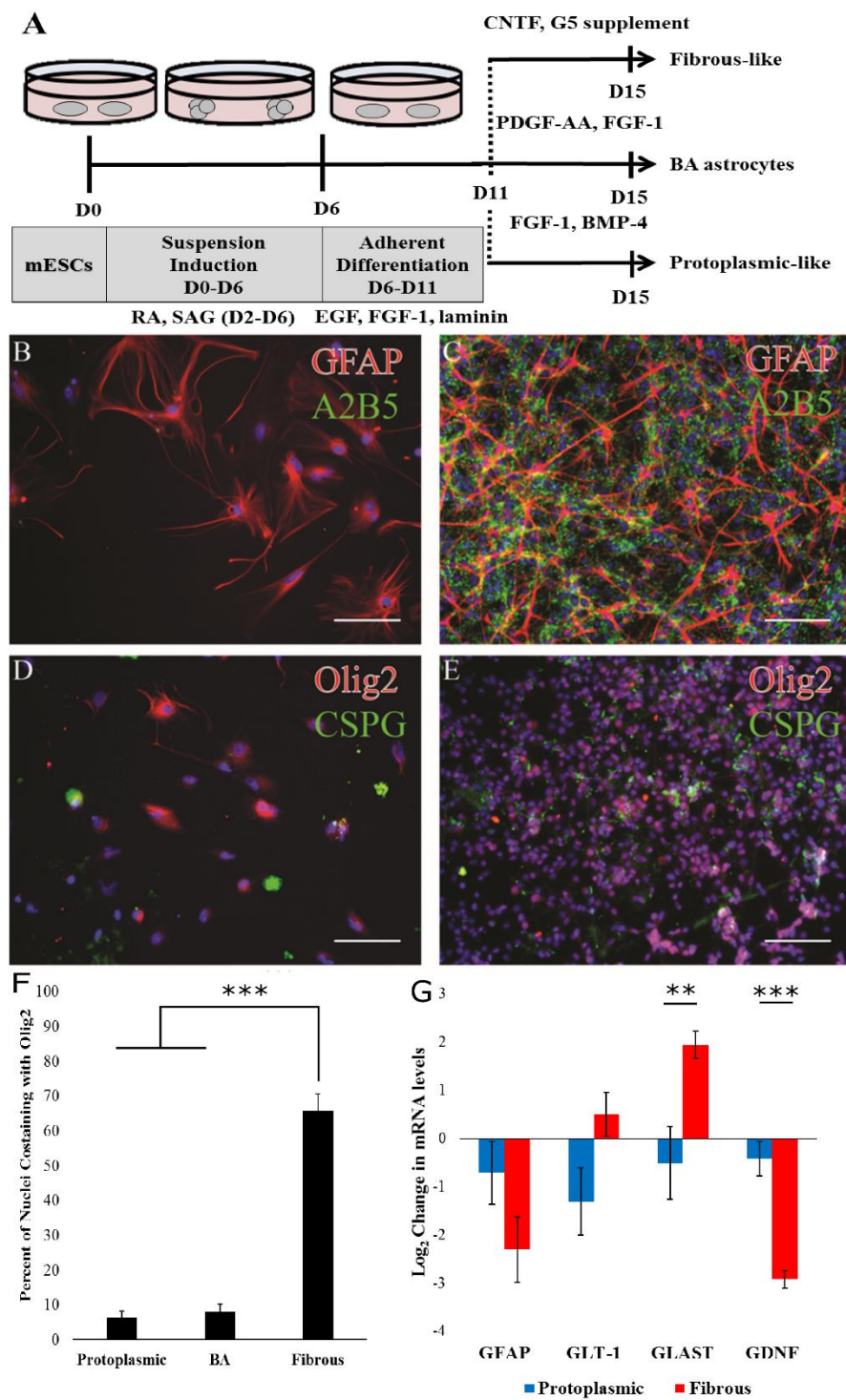
Figure 2.1: mESCs can be selectively differentiated into mixed populations containing either protoplasmic or fibrous astrocytes. **A)** Schematic representation of the astrocyte differentiation protocols used in this work. All astrocytes are subjected to the same initial 11 days after which media factors are changed so that fibrous, protoplasmic or the BA (Benveniste protocol (R. J. Benveniste, Keller, and Germano 2005)) population develops. RA: retinoic acid, SAG: smoothened agonist, EGF: epithelial growth factor, FGF-1: fibroblast growth factor 1, CNTF: ciliary neurotrophic factor, BMP-4: bone morphogenetic protein 4, PDGF-AA: platelet-derived growth factor AA. **B-C)** GFAP (red) and A2B5 (green) staining in protoplasmic (B) or fibrous (C) cultures at the end of differentiation. **D-E)** Olig2 (red) and CSPG (green) staining in protoplasmic (D) or fibrous cultures (E) at end of differentiation. Nuclei stained with Hoechst (blue). Scale bar: 100 µm. **F)** Quantification showing the percent of nuclei that colocalized with Olig2 staining in different cultures.

G) Log_2 expression difference in mRNA levels for fibrous and protoplasmic astrocyte markers compared to BA control population. Error bars represent standard error, n=6. **: $p<0.01$, ***: $p<0.001$

(Holland 2001) and nuclear Olig2 (J. E. Davies et al. 2008) are expected be elevated in fibrous

astrocytes and oligodendrocyte precursors (OPCs). ICC demonstrated that cells exposed to

CNTF and G5 containing media expressed both A2B5 and nuclear Olig2, as expected for fibrous astrocytes (Figure 2.1B-E). Quantification of Olig2$^+$ nuclei in both fibrous and protoplasmic cultures revealed that a significantly higher percentage of nuclei were Olig2$^+$ in fibrous cultures than protoplasmic cultures (Figure 2.1F).

To further confirm the presence of either fibrous or protoplasmic astrocytes within these mixed cultures, qPCR was used to determine mRNA levels of genes known to be differentially expressed between these astrocyte populations, specifically GFAP (general reactive astrocyte marker), glutamate transporter 1 (GLT-1), glutamate and aspartate transporter 1 (GLAST), and glial cell line-derived neurotrophic factor (GDNF). Based on primary cell characterizations and analysis of GRPs in culture, GLT-1 is slightly elevated in fibrous astrocytes (Goursaud et al. 2009), GLAST is significantly elevated in fibrous astrocytes (Goursaud et al. 2009; Vanhoutte et al. 2004), and GDNF is elevated in protoplasmic astrocytes (S. J. A. Davies et al. 2011). Consistent with these observations, the ESC-derived populations showed significant upregulation of GLAST and slight upregulation of GLT-1 in the fibrous population, and significant upregulation of GDNF in the protoplasmic population suggesting that astrocytes within these populations are either protoplasmic or fibrous depending on media exposure (Figure 2.1G).

To determine the percentage of cells in these cultures expressing mature astrocyte markers, flow cytometry was performed for aquaporin-4 (Aqp-4) and A2B5 expression (Cahoy et al. 2008) (Figure 2.2B). Aqp-4 is known to be specifically expressed on the cell membranes of both mature fibrous and mature protoplasmic astrocytes, but not radial glia radial glia *in vivo* (Nagelhus et al. 1998). This makes it an appealing marker to determine the percentage of mature astrocytes in these cultures by flow cytometry. A notable drawback to the use of Aqp-4 is that Aqp-4 is known to have variable expression levels both in cultured astrocytes and *in vivo*. Thus,
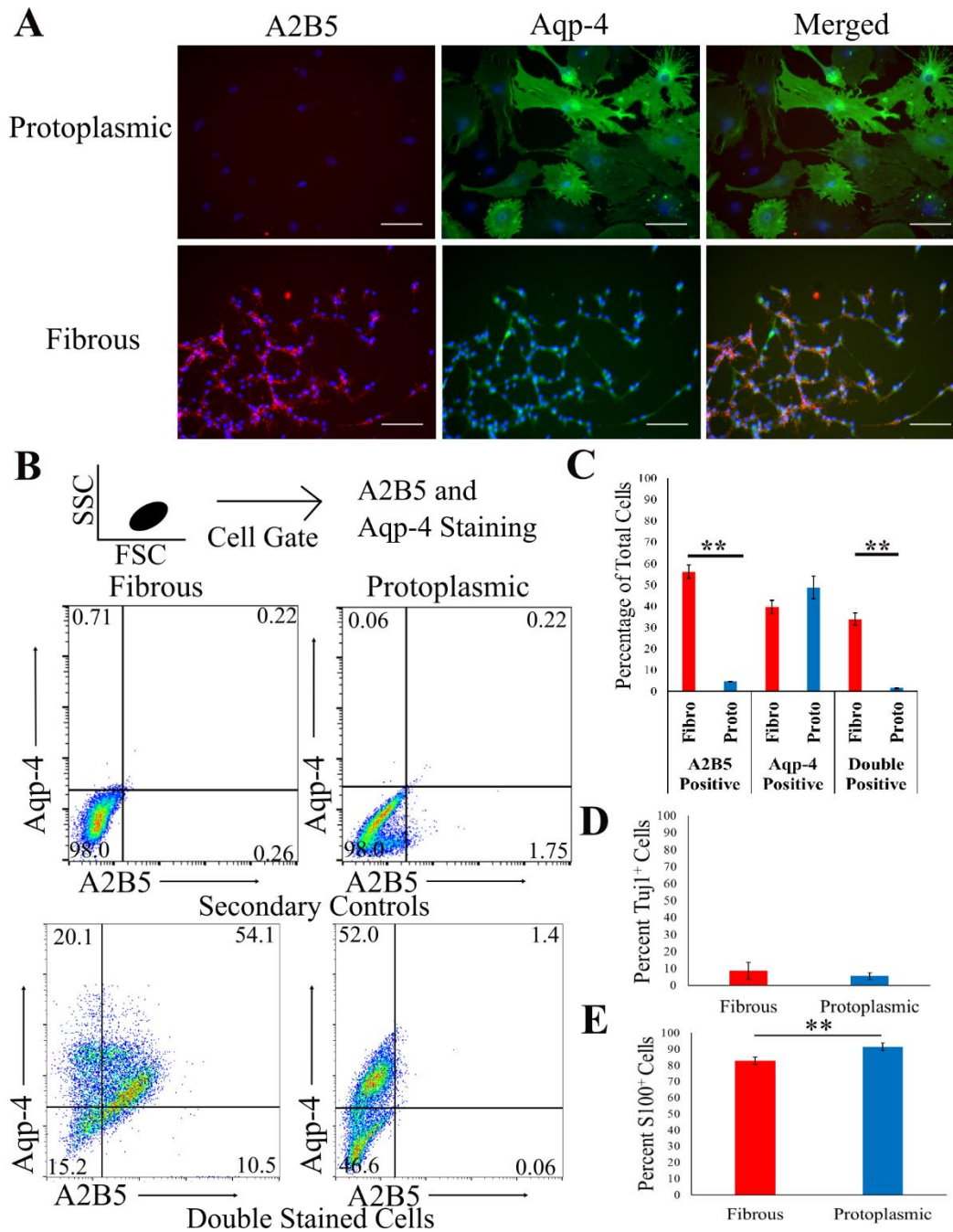
Figure 2.2: Quantification of astrocytes present in mESC cultures. A) Representative images showing A2B5, Aqp-4 and merged staining in protoplasmic and fibrous cultures 6 days after differentiation. Blue represents Hoechst nuclear stain. Scale bar: 100 µm. **B)** Representation flow cytometry graphs of secondary controls and samples stained for Aqp-4 and A2B5 for both fibrous and protoplasmic cultures. Each graph represents 10,000 cells based on a forward scatter (FSC) and side scatter (SSC) gate. Quadrant gates drawn based on single stained samples and secondary controls. Numbers represent the percent of cell events within each quadrant **C)** Average percentage of cells staining for A2B5, Aqp-4, and both markers in Fibrous and Protoplasmic cultures. n=5, error bars: std error, **: p<0.01. **D-E)** Average percent of total cells staining β-tubulin+ (neurons) (**D**) or S100+ (**E**). N=4. error bars: 95% confidence interval. **: p<0.01

Aqp-4 quantification may result in an underestimation of the percent of astrocytes present in the culture (Figure 2.2A) (Kleiderman et al. 2016). Quantification of flow cytometry data demonstrated $48.8\pm0.8\%$ of cells staining Aqp-4$^+$ in protoplasmic cultures and $39.7\pm0.5\%$ of cells staining Aqp-4$^+$ in fibrous cultures with $34.0\pm0.4\%$ of cells in fibrous cultures staining both Aqp-4$^+$ and A2B5$^+$ (Figure 2.2B,C). Overall, fibrous cultures had a significantly higher percentage of A2B5$^+$ cells than protoplasmic cultures and a significantly higher percentage of cells both Aqp-4$^+$ and A2B5$^+$, consistent with the expected fibrous astrocyte phenotype (Figure 2.2).

Since flow cytometry quantification indicated that other cells types may be present, ICC staining was used to determine what non-astrocyte populations were present and to cast a larger net for astrocytes. Cultures were stained for S100, which has been shown to be upregulated in astrocytes as they mature (Raponi et al. 2007), β-tubulin (neurons), O4 (oligodendrocytes), SSEA-1 (mESCs), and Oct 3/4 (mESCs). It is important to note that S100 is also present in some radial glial populations and early oligodendrocyte lineages based on lineage tracing experiments (Hachem et al. 2005), although it is generally used as an astrocyte marker. We found that fibrous populations contained $8.6 \pm 4.9\%$ neurons based on β-tubulin staining and that $82.8 \pm 2.2\%$ of the cells were S100$^+$. Protoplasmic populations were found to have $5.6 \pm 1.9\%$ β-tubulin$^+$ cells and $91.5 \pm 2.3\%$ S100$^+$ cells (Figure 2.2D, E). There was no observable staining of nuclear S100 in either culture, which has been linked to oligodendrocyte differentiation (Deloulme et al. 2004), indicating that, combined with a few to no cells staining O4$^+$, both cultures do not contain significant oligodendrocyte presence (Brunne et al. 2010). There were also few to no cells staining SSEA-1$^+$ or Oct 3/4$^+$, demonstrating limited presence of undifferentiated stem cells.

Taken together, this data suggests that these glial cultures are primarily composed of cells within the astrocyte lineage with some presence of gliogenic radial glia and neurons.

2.4.2 Astrocyte-derived substrates modify neuronal growth

Next, the ability of these two populations to serve as supportive substrates for neuronal growth was assessed and it was observed that live astrocyte substrates exhibiting either phenotype were able support motoneuron neurite outgrowth (Figure 2.3A, D). To determine what aspects of these substrates contributed to neurite outgrowth, modified substrates were
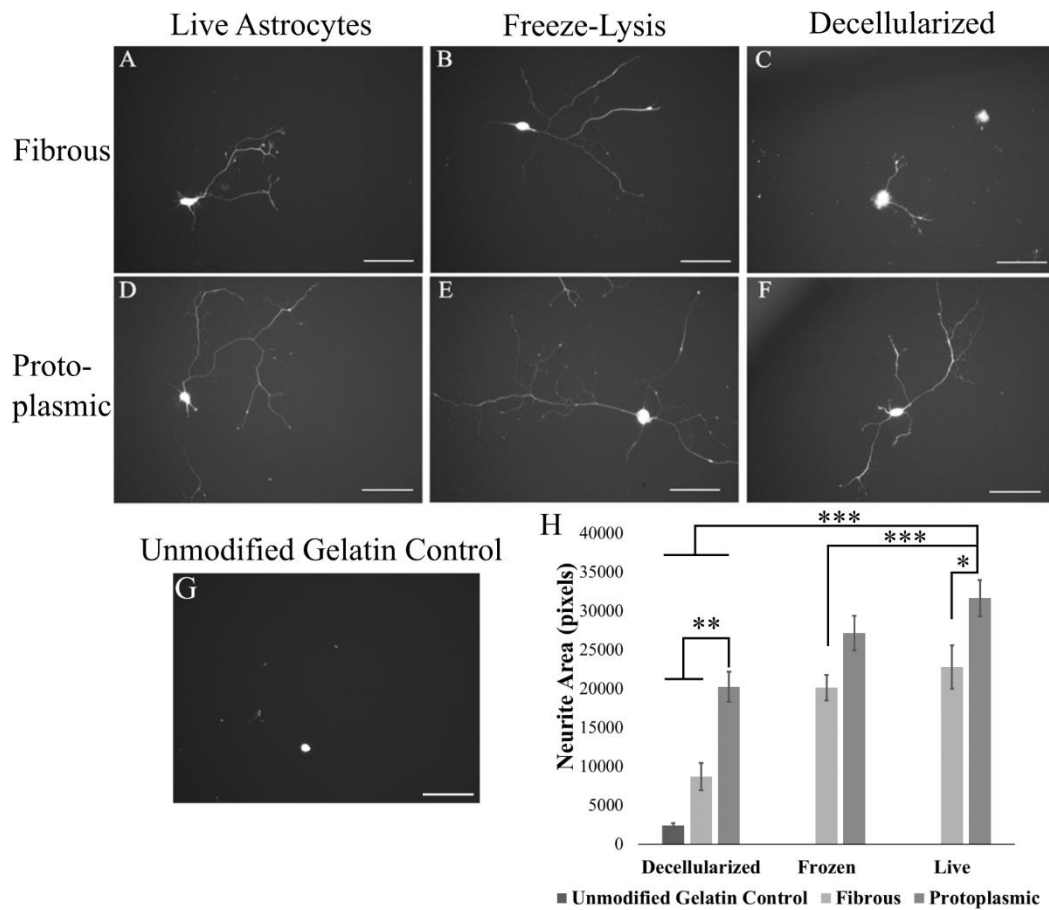
Figure 2.3: Protoplasmic astrocyte-derived substrates are permissive to motoneuron growth and neurite extension. A-G) Representative images of motoneurons on different astrocyte-derived substrates after 48 hours in culture. A-C) Fibrous substrates, D-F) Protoplasmic substrates. A, D) Live astrocyte substrate, B, E) Freeze-Lysed astrocyte substrate, C, F) Decellularized astrocyte substrate. G) Gelatin control shows no clear neurites. Scale bar: 100 µm **H)** Quantification of neurite extension from motoneurons cultured for 48 hours on different astrocyte substrates. Error bars: std error, n: 19-52. * p<0.05, ** p<0.01, *** p<0.001. Dark bars = protoplasmic substrate, light bars = fibrous substrate.

produced using decellularization or freeze lysis. Decellularization leaves only ECM on the plates while freeze lysis leaves behind ECM and cell membranes. The neurite outgrowth area per nucleus from motoneurons was measured on live, decellularized, and frozen substrates to determine the relative contribution of ECM, membrane, and secreted factors. Motoneurons could extend neurites on both live (Figure 2.3A, D) and frozen (Figure 2.3B, E) substrates; however, the motoneurons exhibited only limited neurite extension on decellularized fibrous ECM (Figure 2.3C), while showing robust growth on protoplasmic ECM (Figure 2.3F). Neurite area was also found to be significantly greater on live protoplasmic substrates than decellularized protoplasmic ECM or any fibrous substrate after 2 days of culture (Figure 2.3H). Furthermore, decellularized protoplasmic ECM exhibited significantly greater growth than either unmodified gelatin or decellularized fibrous ECM (Figure 2.3H).

The effect of fibrous and protoplasmic conditioned media (CM) on neurite extension from motoneurons was also tested to determine if there were any growth benefits of the factors secreted by the astrocyte populations. To allow for direct comparison between fibrous and protoplasmic CMs, and control for the effect of the astrocyte growth factors on the neurons, motoneurons were grown in ½ fibrous media and ½ protoplasmic media. These studies found that protoplasmic CM slightly, but significantly, improved neurite extension from motoneurons compared
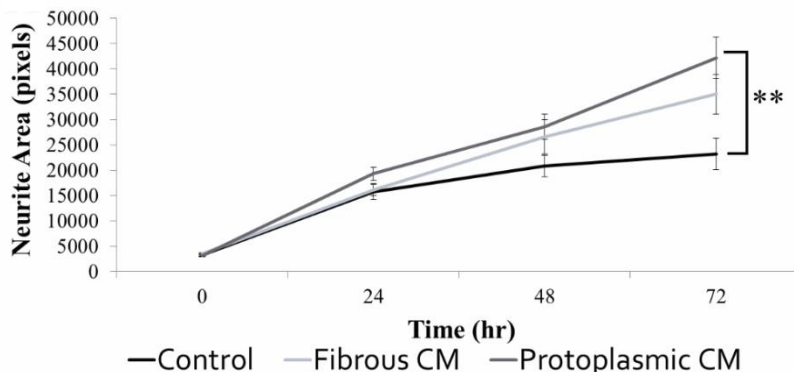
Figure 2.4: Protoplasmic CM significantly improves motoneuron growth. Neurite area per nucleus of motoneurons grown in fibrous and protoplasmic astrocyte CM over 72 hours. Error bars: Std Error, n=14-21, ** p<0.01

55

to unconditioned media after 72 hours (Figure 2.4).

To confirm that these growth differences were not specific to motoneurons, the effect of frozen and decellularized astrocyte substrates on mESC-derived V2a interneuron neurite extension was tested. V2a interneurons were derived from mESCs using a Chx10-PAC cell line with constitutively active TdTomato expression (Iyer et al. 2016). It was found that the interneurons, similar to motoneurons, exhibited significantly longer neurite outgrowth on protoplasmic (Figure 2.5 C-D) versus fibrous substrates (Figure 2.5 A-B); in addition, the magnitude of the ECM effect was found to be greater on the interneuron cultures than the motoneuron cultures (Figure 2.5F).
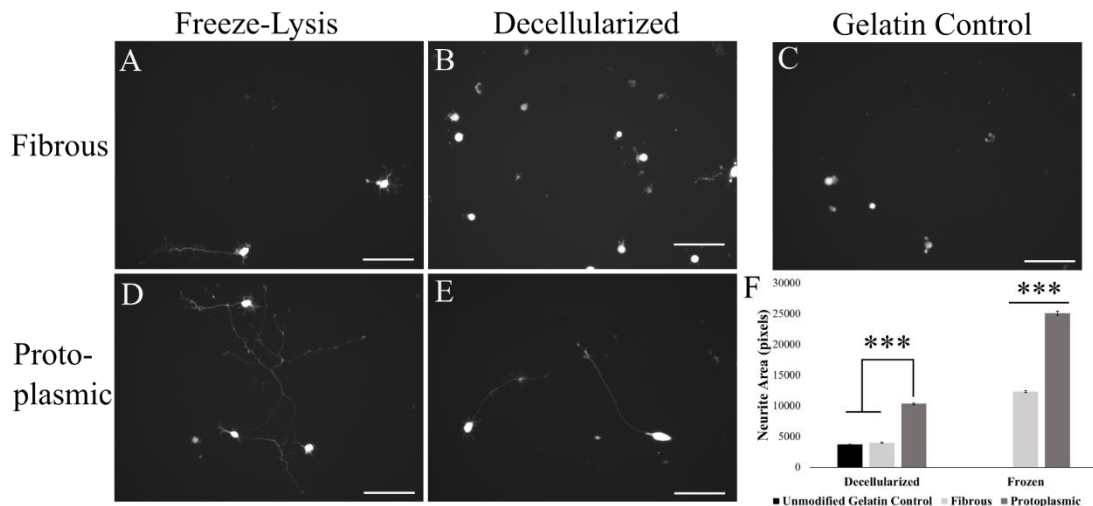
Figure 2.5: Protoplasmic astrocyte-derived substrates are more permissive to V2a interneuron growth than fibrous astrocyte-derived substrates. A-E) Representative images of V2a interneurons after 72 hours in culture on different astrocyte-derived substrates. A,B) Fibrous substrates, D,E) Protoplasmic substrates, A,D) Freeze-Lysed astrocyte substrate, B,E) Decellularized astrocytes substrate. C) Unmodified Gelatin Control. Scale bar: 100 µm **F)** Quantification of neurite extension from V2a interneurons cultured for 3 days on different astrocyte substrates. Error bars: Std. Error, n=40-56, *** p<0.001. Dark bars = protoplasmic substrate, light bars = fibrous substrate.

2.4.3 Fibrous and protoplasmic astrocytes deposit distinct ECMs

Since the ECM deposited by these predominantly glial cultures was sufficient to support neuron growth, label-free LC/MS proteomics was performed to determine what proteins are present in ECMs harvested from both protoplasmic and fibrous populations. Identification of

these proteins will allow for better understanding of the reasons for the observed neuronal growth differences and potentially allow for customized substrate design. ECMs harvested from mESC-derived populations were found to be largely similar with 530 of the 638 proteins identified not being expressed at different levels; however, there were significant expression differences of several key axon growth-related proteins (Figure 2.6A, Table 2.3, Table 2.4). Fibronectin-1 was found to be most abundant protein in both ECMs with significantly more spectral counts detected in the protoplasmic samples (Figure 2.6A). Fibronectin has been described as being expressed by primary astrocytes in culture (Liesi, Kirkwood, and Vaheri
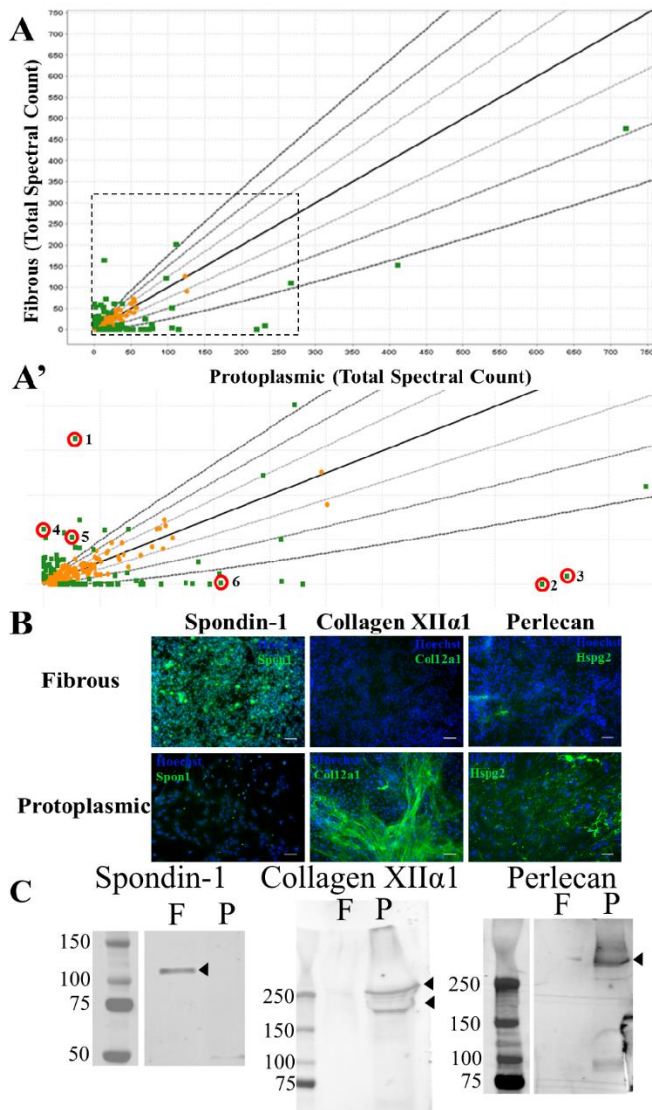
Figure 2.6: Protoplasmic and Fibrous astrocytes have distinct ECM composition. A) Graphical representation of proteomics results. Each point represents the average spectral count of the identified protein from 2 independent runs. Lines denote 1, 2, or 3 standard deviations away from equal spectral count of the specific protein detected. Proteins found to be significantly different between protoplasmic and fibrous ECMs are denoted by green squares, Fisher exact test with Benjamini-Hochberg correction, p < 0.001, n=2. Orange squares denote proteins that did not differ significantly between astrocyte ECMs. **A')** Blow up of indicated area in A. Red circles mark proteins of interest: 1: spondin-1, 2: collagen XIIα1, 3: perlecan, 4: neurocan, 5: versican, 6: laminin α5. **B)** Confirmation of proteomics findings for spondin-1, collagen XIIα1, and perlecan with IHC (target protein in green and nuclei in blue) showing an expression pattern consistent with the proteomics data. Scale bar = 100 µm. **C)** Western blots of ECMs harvested from decellularized plates also shows the expected pattern spondin-1, collagen XIIα1, and perlecan. F: Fibrous ECM, P: Protoplasmic ECM, Arrowhead denotes protein band.

57

1986), is transiently expressed away from the blood vessels during CNS development (Stewart and Pearlman 1987), and has been linked to improved neuron growth in adult white matter (Tom et al. 2004). The proteins with the greatest differential expression between the protoplasmic and fibrous populations, were spondin-1 (spon1), Collagen XIIα1 (col12a1), and perlecan (hspg2). Spondin-1, also known as F-spondin, was expressed at significantly greater levels in fibrous ECM and is known to be involved in axonal pathfinding and turning during development (Burstyn-Cohen et al. 1999) (Figure 2.6A' #1). Col12a1 and perlecan were both found at significantly greater levels in protoplasmic ECM (Figure 2.6A' #2, #3). Perlecan-coated plates have been demonstrated to promote neurite extension *in vitro* (R. Nakamura, Nakamura, and Fukunaga 2015). Also of note is that the chondroitin sulfate proteoglycans (CSPGs) (neurocan and versican), which are known inhibitory molecules(Oohira, Matsui, and Katoh-Semba 1991), were found to be significantly more prevalent in fibrous ECM (Figure 2.6A' #4, #5), while laminins, known to be axon growth promoting, were more prevalent within protoplasmic ECM (Figure 2.6A' #6). To confirm the validity of our proteomics results, ICC was performed on both protoplasmic and fibrous cultures for collagen XIIα1, perlecan, and spondin-1 (Figure 2.6B). To further validate the proteomics, western blotting was performed on ECMs harvested from decellularized astrocyte plates (Figure 2.6C). The expression pattern of these proteins matched the profiles found in the LC/MS data demonstrating the validity of the proteomic results (Figure 2.6B-C).

2.4.4 ECM produced by ESC-derived cultures is consistent with in vivo astrocyte protein expression

The cultures used for this work are not purely astrocytic as there is a clear presence of both neurons and glial progenitors. Thus, it was important to determine if the harvested ECMs were consistent with *in vivo* astrocyte expression profiles to demonstrate if the harvested ECMs

are similar to native astrocyte ECM production. This was achieved by comparing the proteins

found in astrocyte ECMs to a set of genes identified as expressed in astrocytes *in vivo*. *In vivo*

astrocyte expression profiles were determined using a previously described translating ribosome

affinity purification (TRAP) mouse line that targets all *in vivo* astrocyte populations using

ALDH1L1 (Doyle et al. 2008), coupled with RNAseq. This BAC-TRAP methodology compares

the prevalence of mRNA transcripts in the total brain isolate to the prevalence of the same

mRNA transcripts when only the mRNAs attached to astrocyte ribosomes are present. This

approach allows for any transcript that is enriched in the astrocyte (TRAP) fraction to be

considered astrocyte-specific, or at least more highly expressed by astrocytes than other CNS

populations. Genes that are relatively depleted in the TRAP fraction (enriched in the pre-IP

fraction) can be considered more highly expressed by a different population within the CNS or

not expressed by astrocytes. The distinction between enrichment and population-specific

expression was made based on the fold change in expression level of the particular gene between

the TRAP and pre-IP fractions.

The validity of the TRAP-Seq method was confirmed by locating all genes previously

identified as astrocyte- or neuron-specific within the data set (Tien et al. 2012). It was found that

84% of genes previously identified as astrocyte-specific were enriched in the astrocyte fraction,

and 81% of those previously identified as neuron-specific were depleted in the astrocyte fraction,

confirming a successful TRAP (Figure 2.7A). Based on the mean fold change of the neuronal

markers between the astrocyte fraction and whole brain isolate, a threshold was calculated to

allow for genes to be considered astrocyte-specific with 95% confidence. With a threshold

established, the mRNAs that encode for proteins found within the mESC-derived ECMs were

located within the BAC-TRAP RNA-seq samples. Based on this methodology, 183 (33%) of the

ECM proteins identified can be considered to be astrocyte-specific (J. D. Dougherty et al. 2010),

and 159 of these were at least 2-fold enriched in the TRAP fraction (Figure 2.7B). The majority

of these astrocyte-specific ECM proteins were found in both protoplasmic and fibrous ECMs. In

addition to containing astrocyte-specific proteins, ECM components were also found to be more

highly expressed in the TRAP than in the PreIP fraction (Figure 2.7C, paired t-test, $p < 0.0001$).

	ECM candidate	Not ECM candidate	Row total
Expressed in TRAP (95% confident)	183 (32.7%)	2680 (23%)	2863
Not detectable in TRAP	376 (67.3%)	8947 (77%)	9323
Column total	559	11627	*12186*
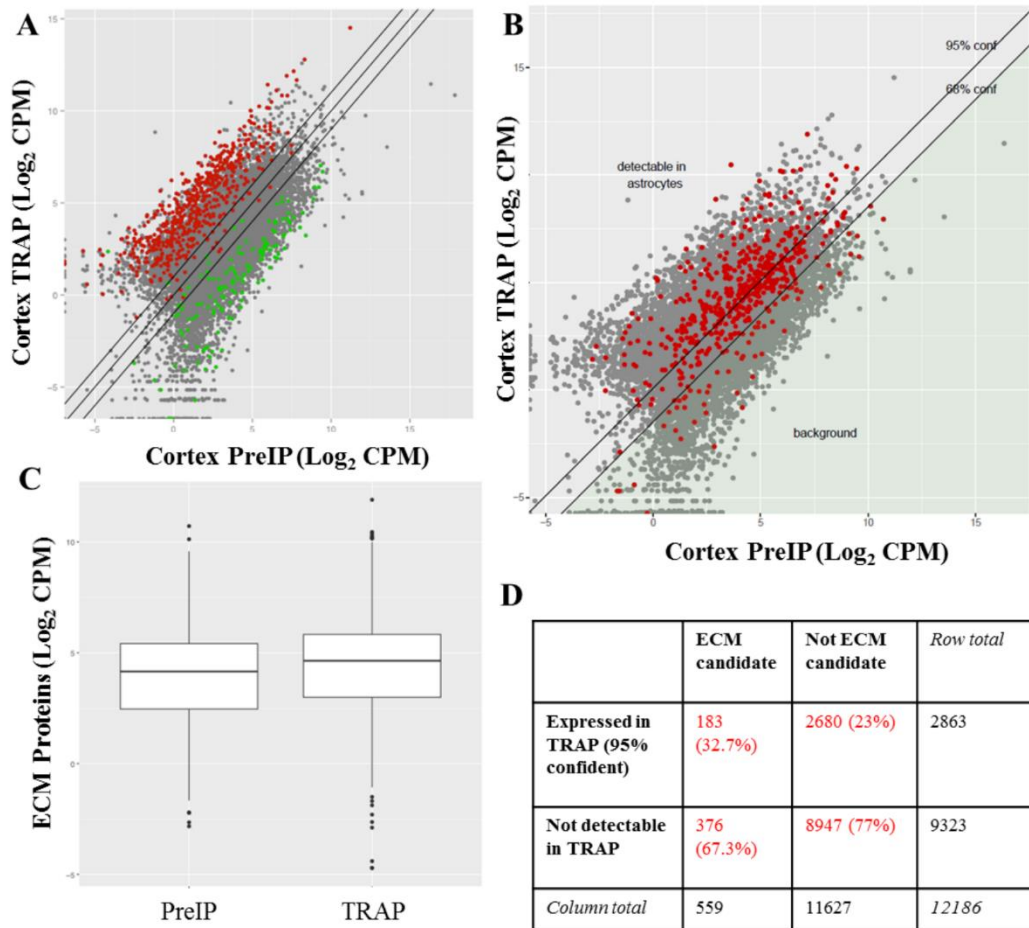
Figure 2.7: ECM components generated by ESC-derived astrocytes are found in cortical astrocytes based on BAC-TRAP. A) Astrocyte-specific genes (red) are enriched in the TRAP fraction while neuronal-specific genes (green) are enriched in the PreIP samples. n=3. **B)** ECM candidate genes are enriched within the TRAP fraction compared to PreIP sample. Lines are 95% and 68% confidence of astrocyte-specific expression. Grey points are all genes detected in the BAC-TRAP data, red points denote genes that code for proteins detected in ECM proteomics data. **C)** ECM proteins are significantly enriched in TRAP fraction as compared to the PreIP fraction. Paired t-test, $p = 5.66 \times 10^{-9}$. **D)** Comparison of identified proteins with the proteomics and BAC-TRAP data. Proteins were considered astrocyte-expressed if there was 95% confidence that the mRNA was enriched within the TRAP fraction compared to the PreIP fraction. The ECM proteins identified in proteomics were enriched for proteins expression in astrocytes based on BAC-TRAP at a significantly higher level than expected by chance. Fisher exact test, $p = 2.x \times 10^{-7}$.

Among those genes detectable in RNA-seq samples, ECM components were more likely than chance to be identified as *expressed* by astrocytes in the BAC-TRAP data (Figure 2.7B,D, Fisher's exact test, $p < 0.001$). Furthermore, ECM components were more likely than chance to be identified as having 2-fold higher expression in astrocytes *in vivo* (Fisher's exact test, $p < 0.05$). This data shows that the proteins found within the ESC-derived ECMs are consistent with *in vivo* astrocyte expression profiles and suggests that the mESC-derived ECMs from both fibrous and protoplasmic populations are consistent with *in vivo* astrocyte ECM.

2.4.5 Motoneuron growth depends on the presence and absence of specific ECM proteins

To test which proteins within the mESC-derived ECMs are important for motoneuron growth, proteins with known roles in neurite growth found to be highly expressed in one ECM, but not the other were targeted with shRNA knockdown. Targets were preferentially chosen from protoplasmic ECM in order to determine growth promoting factors for
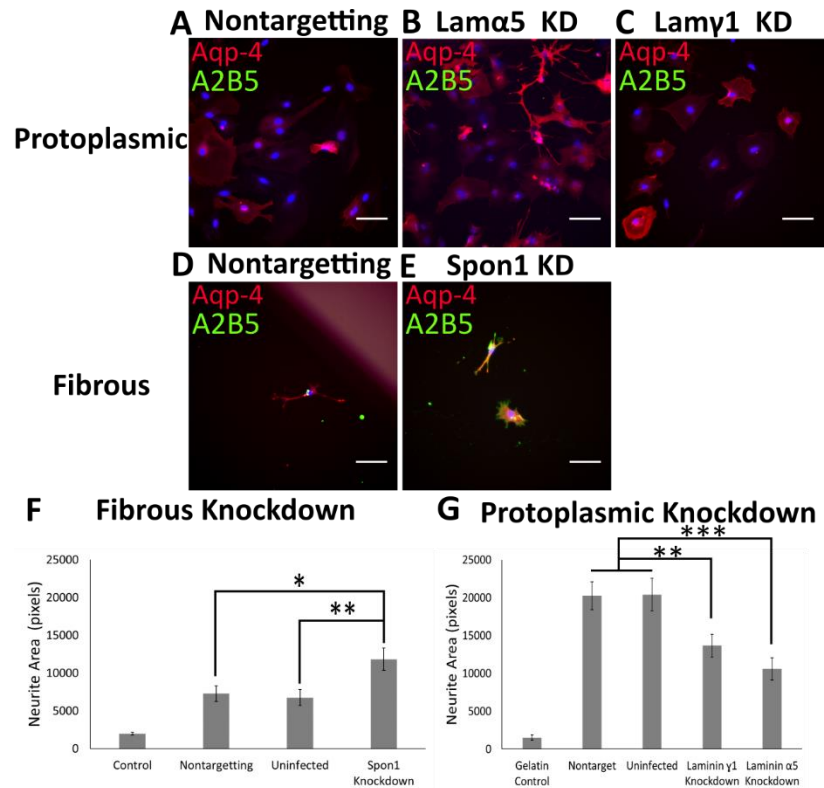
Figure 2.8: Viral knockdown modifies motoneuron growth on astrocyte ECMs. A-E) Aqp-4 (red) and A2B5 (green) staining of infected astrocytes. A-C) Protoplasmic astrocytes infected with nontargeting (A), laminin α5 targeting (B), or laminin γ1 targeting (C) virus. D-E) Fibrous astrocytes infected with nontargeting (D), or spondin-1 targeting (E) virus. Scale bar: 100 μm. **F)** Spondin-1 knockdown in fibrous ECM leads to a significant increase in motoneuron growth. n=39-58 **G)** Laminin α5 or laminin γ1 knockdown decreases motoneuron growth on protoplasmic ECM. n=44-104. Error bars: std error; *: p<0.05; **: p<0.01; ***: p<0.001.

potential future work using a small number of specific proteins. In particular, collagen XIIα1,

collagen VIα3, laminin β1, perlecan, laminin α5, and laminin γ1 were targeted in protoplasmic

ECM, while spondin-1 was targeted in fibrous ECM. Since matrix deposition takes multiple

days, shRNAs were stably expressed using lentiviral transduction. Staining of astrocytes

following infection showed that both fibrous and protoplasmic astrocyte maintained the expected

morphology and phenotype, although cell density was significantly lower than previously

observed (Figure 2.8A-E).
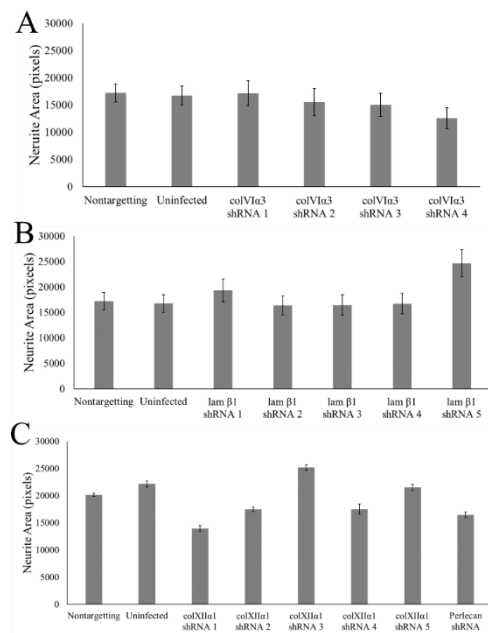
Figure 2.9: Knockdown of collagen VIα3, laminin β1, collagen XIIα1, or Perlecan does not significantly alter motoneuron growth on protoplasmic astrocyte ECM. A) Effect of collagen VIα3 (colVIα3) knockdown on motoneuron neurite length on resulting protoplasmic ECM. N=15-67. 4 separate shRNA constructs were used. **B)** Effect of laminin β1 (lam β1) knockdown on motoneuron neurite length. N=19-67. 5 separate shRNA constructs were used. **C)** Effect of collagen XIIα1 (colXIIα1) and perlecan knockdown on motoneuron neurite length on resulting protoplasmic ECM. N=13-30. 5 separate shRNA constructs were used for collagen XIIα1, 1 previously validated construct was used for perlecan.

Quantification of motoneuron growth on knockdown ECMs found that knockdown of

spondin-1 in fibrous cultures increased neurite extension (Figure 2.8F), while laminin α5 or

laminin γ1 knockdown in protoplasmic astrocytes decreased neurite extension (Figure 2.8G).

There were no significant effects observed for any of the shRNA constructs targeting collagen

XIIα1, collagen VIα3, laminin β1, or perlecan; however, knockdown was not verified in these

cultures due to the lack of effect (Figure 2.9). Using western blotting and qPCR, spon1 shRNA

treatment was found to decrease expression of spondin-1 to 53% of the uninfected control and

decreased mRNA levels to 44% of the non-targeted control (Figure 2.10). The laminin α5 and γ1
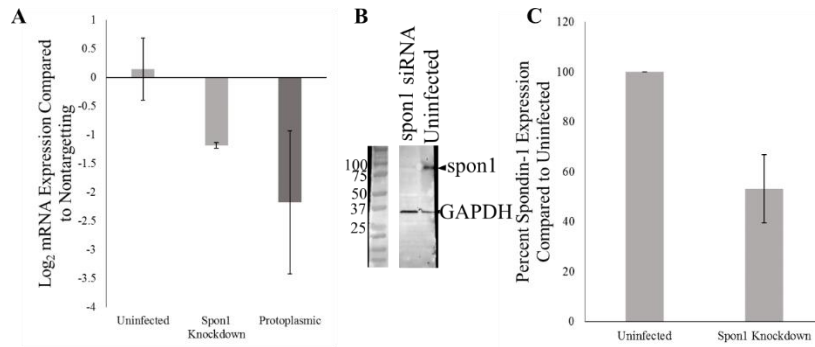
Figure 2.10: Spondin-1 shRNA decreases both mRNA and protein expression. A) mRNA levels decrease in fibrous astrocyte cultures treated with spon1 shRNA when compared to astrocytes infected with nontargeting shRNA. **B)** Western blot quantification using densitometry shows decreased spondin-1 in cultures treated with spon1 shRNA. n=2, Error bars: 95% Confidence Interval.

shRNAs used have been previously validated by Sigma to reduce expression of the target protein by 67% and 95%, respectively, so no further validation was performed on these constructs. Interestingly, the decreases observed in the knockdown ECMs does not fully account for the growth differences observed between protoplasmic and fibrous ECMs suggesting that the neuronal growth effects are multifactorial and due to many different proteins within the ECMs.

2.5 Discussion

CNS injury leads to a significant economic and psychological burden for patients due, in part, to the lack of spontaneous regeneration within the CNS (Boakye, Leigh, and Skelly 2012). Classically, this lack of recovery has been thought to be partially caused by the formation of a glial scar that contains woven astrocyte processes and a large number of proteins that inhibit axon growth (Cregg et al. 2014). Recently, it has been observed that astrocytes are also involved in spontaneous recovery in mice and zebrafish (Yona Goldshmit et al. 2014; Zukor et al. 2013; C. Haas et al. 2012), and that astrocyte transplants can improve recovery following SCI, if they have a pro-regenerative phenotype (J. E. Davies et al. 2008; Chu et al. 2014). Since astrocytes have been successfully used for SCI treatment, a scalable methodology for the derivation of pro-regenerative astrocytes could have a significant clinical impact. This work demonstrates a

scalable method to produce either fibrous or protoplasmic astrocytes from mouse ESCs (Figure 2.1, 2.2), with around 40% astrocytes in fibrous cultures and 49% astrocytes in protoplasmic cultures based on Aqp-4 staining (Figure 2.2). This is likely a conservative estimate, as Aqp-4 staining is known to vary across astrocyte cultures, which is clear in our staining as well (Figure 2.2). Quantification of S100 staining suggests that fibrous cultures contain around 83% astrocytic-lineage cells and protoplasmic cultures contain around 92% astrocytic-lineage cells, even if not all the astrocytes express sufficient Aqp-4 for detection with flow cytometry (Figure 2.2). The significant differences in GLAST, GDNF, and A2B5 expression, coupled with the cell morphology differences, indicate that these methods generate astrocytes that are consistent with *in vivo* fibrous and protoplasmic astrocyte phenotypes, and that fibrous populations contain mostly white matter astrocytes while protoplasmic populations contain mostly grey matter astrocytes (Figure 2.1, 2.2). Astrocyte presence within these cultures was further confirmed with BAC-TRAP demonstrating that ECMs derived from fibrous and protoplasmic cultures were consistent with *in vivo* astrocyte expression profiles during development (Figure 2.7).

Functionally these predominantly astrocytic cultures were found to have differing abilities to support neuronal growth with protoplasmic–derived substrates tending to be more supportive of neuron growth than fibrous substrates. This was especially apparent in the case of decellularized ECMs (Figure 2.3, 2.5). It is important to note that transplanted immature, but not mature, astrocytes have been found to improve outcomes following SCI, while demonstrating further migration from the transplant area and reduction of the glial scar (G. M. Smith and Silver 1988; G. M. Smith and Miller 1991). Due to these observations, and the relatively immature nature of these cultures, it is possible that the functional differences observed in the mESC cultures are applicable to embryonic, but not adult, astrocyte populations. However, this protocol

does provide a readily scalable method to produce populations that can be used to support neuronal growth.

It would be potentially interesting to explore the effects of inflammatory stimulus on the observed neuronal growth support properties of these astrocytes. Recent work has demonstrated that astrocytes exhibit a continuum of reactive phenotypes following injury, with some exhibiting pro-regenerative phenotypes and others exhibiting inhibitory phenotypes (Liddelow and Barres 2017). It has been observed that pro-inflammatory and anti-inflammatory stimuli push reactive astrocyte phenotypes one way or the other on this continuum. In particular, inflammatory injury caused by lipopolysaccharide (LPS) causes a astrocytes to adopt a more

inhibitory phenotype (Zamanian et al. 2012). In addition, interleukin-6 (IL-6), a pro-inflammatory cytokine, leads to an increase in astrocyte proliferation and scar formation *in vivo* (M. Nakamura et al. 2005); while, IL-10, an anti-inflammatory cytokine, has been to shown improve functional recovery following CNS injury when delivered intrathecally or intramuscularly (Jackson et al. 2005). Future experiments could explore the effects of these inflammatory and anti-inflammatory stimuli on the neuronal growth support capacities of these mESC-derived fibrous and protoplasmic populations.

Recent work by Anderson *et al.* showed that astrocytes are required for recovery following SCI in mice (Anderson et al. 2016). As part of this work, they compared axon growth permissive and inhibitory proteins produced by astrocytes and non-astrocytes following injury. The proteomics data set collected in this study was searched for these proteins, and it was found that, if present within the ECMs, permissive proteins tended to be significantly upregulated in protoplasmic.

Table 2.3: Known axon growth modulatory proteins identified in astrocyte ECM proteomics data.

Protein	Significantly upregulated in	Axon Growth Role
Neurocan	Fibrous	Inhibitory
Versican	Fibrous	Inhibitory
Netrin-1	Fibrous	Inhibitory
Semaphorin-3A	Fibrous	Inhibitory
Tenascin C	Fibrous	Permissive
Laminin α1	Protoplasmic	Permissive
Laminin α5	Protoplasmic	Permissive
Laminin β1	Protoplasmic	Permissive
Laminin γ1	Protoplasmic	Permissive
Collagen 4α1	Protoplasmic	Permissive
Fibronectin	Protoplasmic	Permissive
Perlecan	Protoplasmic	Permissive
Matrillin-2	N.S.	Permissive

ECM while inhibitory proteins were upregulated in fibrous ECM (Table 2.3). This suggests that the neuron growth differences observed on the ECMs derived in this study are likely due to both the more inhibitory nature of the fibrous ECM and the more permissive nature of the protoplasmic ECM. This concept is supported by the observed decrease in motoneuron growth on protoplasmic ECM following knockdown of laminin α5 and laminin γ1 and the increase in motoneuron growth on fibrous ECM following spondin-1 knockdown (Figure 2.8). Future work on which proteins are the most important for neuron growth in these ECMs could allow for a small subset of ECM components to be mass produced and delivered to improve recovery following CNS injury. (R. E. Thompson et al. 2017)

Table 2.4: Proteins found to have significantly different expression in mESC-derived astrocyte ECMs. Proteins are listed in decreasing number of average spectra detected. n=2.

Significantly enriched in Fibrous ECM	Average Percent of Total Spectra	Significantly enriched in Protoplasmic ECM	Average Percent of Total Spectra
Cytoplasmic dynein 1 heavy chain 1	0.37	Fibronectin	2.25
Vimentin	0.31	Myosin-9	1.27
Spondin-1	0.30	Basement membrane-specific heparan sulfate proteoglycan core protein	0.74
Tubulin beta-2B chain	0.15	Myosin-10	0.66

Protein	Value	Protein	Value
Latent-transforming growth factor beta-binding protein 1	0.13	Collagen alpha-1(XII) chain	0.59
Combined Horseradish Peroxidase	0.11	Protein Ahnak	0.37
Tenascin	0.11	Protein Col6a3	0.32
Neurocan core protein	0.11	Laminin subunit alpha-5	0.29
Versican core protein	0.10	Plectin	0.21
Glia-derived nexin	0.10	Filamin-A	0.21
Protein Fndc1	0.10	Laminin subunit gamma-1	0.2
Heat shock protein HSP 90-beta	0.07	Fibrillin-1	0.17
Keratin, type I cytoskeletal 14	0.07	Laminin subunit beta-2	0.17
Keratin, type II cytoskeletal 5	0.07	Agrin	0.15
Tissue-type plasminogen activator	0.06	Laminin subunit beta-1	0.13
Desmoplakin	0.05	Protein-glutamine gamma-glutamyltransferase 2	0.12
Peroxidasin homolog	0.05	EMILIN-1	0.10
A disintegrin and metalloproteinase with thrombospondin motifs 4	0.05	Fibrillin-2	0.09
Creatine kinase B-type	0.05	Collagen alpha-1(VI) chain	0.09
Multiple epidermal growth factor-like domains protein 6	0.04	Nidogen-1	0.09
Semaphorin-3A	0.04	Nidogen-2	0.09
T-complex protein 1 subunit delta	0.04	Myosin-11	0.08
Fatty acid synthase	0.04	Laminin subunit alpha-1	0.07
Keratin, type II cytoskeletal 2 epidermal	0.04	Collagen alpha-2(VI) chain	0.07
Unconventional myosin-Va	0.04	Unconventional myosin-Ic	0.06
D-3-phosphoglycerate dehydrogenase	0.04	Periostin	0.06
SPARC-related modular calcium-binding protein 1	0.04	Inter-alpha-trypsin inhibitor heavy chain H5	0.06
Keratin, type I cytoskeletal 10	0.03	Collagen alpha-2(IV) chain	0.05
Splicing factor, proline- and glutamine-rich	0.03	Collagen alpha-1(XVIII) chain	0.05
Transcription activator BRG1	0.03	Collagen alpha-1(IV) chain	0.05

Ubiquitin-like modifier-activating enzyme 1	0.03	Myosin phosphatase Rho-interacting protein	0.04
Alpha-enolase	0.03	Annexin A1	0.04
Phosphoglycerate kinase 1	0.03	Collagen alpha-1(V) chain	0.04
Protein Gm20425	0.03	Tubulointerstitial nephritis antigen-like	0.04
Lamin-B1	0.03	Cytochrome P450 1B1	0.03
Dedicator of cytokinesis protein 1	0.03	Myoferlin	0.03
Junction plakoglobin	0.03	Protein Atp2b4	0.03
Netrin-1	0.03	Sorbin and SH3 domain-containing protein 2	0.03
Mitogen-activated protein kinase kinase kinase kinase 4	0.02	E3 ubiquitin-protein ligase RNF213	0.02
Nuclear pore membrane glycoprotein 210	0.02	Collagen alpha-2(V) chain	0.02
Low-density lipoprotein receptor-related protein 2	0.02	Transforming growth factor-beta-induced protein ig-h3	0.02
Nascent polypeptide-associated complex subunit alpha	0.02	Dysferlin	0.02
WSC domain-containing protein 1	0.02	Thrombospondin type-1 domain-containing protein 4	0.02
Fructose-biphosphate aldolase C	0.02	Collagen alpha-1(XIV) chain	0.01
Plakophilin-1	0.02		
14-3-3 protein theta (Fragment)	0.02		
Interleukin enhancer-binding factor 3	0.01		
Bone morphogenetic protein 1	0.01		
Extracellular sulfatase Sulf-2	0.01		
Nephronectin	0.01		
Heat shock protein HSP 90-alpha	0.01		
Transforming growth factor beta-2	0.01		
Microtubule-associated protein 2	0.01		

Phosphoserine aminotransferase	0.01
Keratin, type I cytoskeletal 16	0.01
Pleiotrophin	0.01
Apolipoprotein E	0.01
Dynactin subunit 1	0.01
Multifunctional protein ADE2	0.01
Fatty acid-binding protein, brain	0.01
T-complex protein 1 subunit theta	0.01

Chapter 3: Generation of Enriched Astrocyte Cultures from a Selectable Mouse Embryonic Stem Cell Line

3.1 Abstract

Central nervous system (CNS) trauma often leads to long term sequalae for patients due to the limited regenerative capacity of the CNS. Part of the reason for the limited recovery following CNS injury is that the native astrocytes form a barrier, called the glial scar, around the injury site that prevents the growth of new axons. The role astrocyte play in the formation of the scar led to the belief that astrocytes were primarily inhibitory following injury; however, recent work on astrocyte knockout mice has found that astrocytes are also necessary for recovery from CNS trauma. Furthermore, primary astrocyte transplantation into spinal cord injuries has been found to lead to improved functional outcomes when protoplasmic (grey matter) astrocytes were transplanted. Since it is difficult to translate primary cells transplantation into the clinic, methods were developed to generate protoplasmic and fibrous (white matter) astrocytes from mouse embryonic stem cell (mESCs). Unfortunately, mESC-derived cell populations need to be purified prior to transplantation to remove the risk of teratoma formation. In this work, a cell line that allows for selection of mESC-derived astrocyte culture is generated by using the *Aqp4* locus to drive the expression of a puromycin resistance gene. Selection of protoplasmic astrocytes derived from this cell line was found to increase the percent of cells positive for Aqp4 and GFAP. These selected astrocyte cultures have the potential to be used for both further *in vitro* characterization of astrocyte functions and *in vivo* transplantation.

3.2 Introduction

Astrocytes have historically been viewed as primarily inhibitory to recovery following CNS trauma. This viewpoint arose because astrocytes are the main cellular component of the glial scar, which represents both a physical and biochemical barrier to axon growth (Cregg et al. 2014). Thus, it seemed logical that mice lacking astrocyte reactivity because of a vimentin and glial fibrillary acidic protein (GFAP) double knockout would have improved recovery from spinal cord injury (SCI). Surprisingly, these double knockout mice were found to have significantly increased bleeding, inflammation, and spread of secondary injury compared to wild-type mice following SCI or stroke (Pekny et al. 1999; Z. Liu et al. 2014). Recent work has also explored the effect of delayed astrocyte knockout using GFAP-thymidine kinase (TK) mice. In these mice, ganciclovir administration causes targeted ablation of dividing GFAP^{+} cells (Bush et al. 1998). Using this model, acute astrocyte ablation was still found to worsen secondary injury following SCI, and to result in a decrease in axonal growth into the lesion area (Anderson et al. 2016; J. R. Faulkner et al. 2004). Delayed astrocyte ablation was also performed 5 weeks after SCI, which resulted in worse functional outcomes than mice with intact astrocytes (Anderson et al. 2016). These genetic strategies demonstrate that astrocytes play some pro-regenerative roles in both the acute and chronic phases of CNS trauma, even though these roles are not as well defined as the known inhibitory effects of scar astrocytes.

The concept of astrocytes as a pro-regenerative population is supported by the observed tendency for the majority of axons within the SCI lesion to be associated with GFAP[+] astrocyte processes in rats (Taylor et al. 2006), mice(Zukor et al. 2013), and zebrafish(Yona Goldshmit et al. 2012). This association between astrocytes and neurons within the lesion led to investigation of the role of transplanted astrocytes in providing a permissive environment for axons in the

71

lesion. Glial restricted progenitors (GRPs) can be isolated from mouse or human embryos and differentiated into both white matter (fibrous) and grey matter (protoplasmic) astrocytes, as well as oligodendrocytes, but not neurons (Rao, Noble, and Mayer-Pröschel 1998; S. J. A. Davies et al. 2011). GRPs pre-differentiated into protoplasmic astrocytes have been shown to improve recovery following right-sided cervical dorsal column transection SCI (J. E. Davies et al. 2006). Interestingly pre-differentiation of GRPs into fibrous astrocytes did not confer these same benefits and instead had a detrimental effect on recovery (S. J. A. Davies et al. 2011; J. E. Davies et al. 2008). Importantly, similar to many primary cell transplantation therapies, there has been some considerable variability in these findings, with another study showing that GRPs pre-differentiated into astrocytes conferred a recovery benefit regardless of the astrocyte phenotype (C. Haas et al. 2012).

Due to the inconsistencies in primary cell cultures, and the difficulty in obtaining sufficient primary cells for transplantation, a pluripotent cell source of astrocytes could be extremely useful. Astrocytes have been derived from human induced pluripotent stem cells (iPSCs) and transplanted following a cervical contusion SCI. These iPSC-derived astrocytes were found to not have significant effects on recovery; however, when modified to expression high levels of glutamate transporter 1 (GLT1), iPSC-derived astrocyte transplantation reduced lesion size and improved diaphragm function (K. Li et al. 2015). These transplantation studies demonstrate that there is potential for astrocyte transplantation following SCI; however, significantly more work it required to determine the best astrocyte populations for transplantation and improve astrocyte-derivation methodology.

A highly purified, renewable source of astrocytes could be extremely valuable for studying astrocyte function *in vitro* and improving *in vivo* outcomes of astrocyte transplantation.

Methods have already been developed to specifically derive protoplasmic or fibrous astrocytes from mESCs (R. E. Thompson et al. 2017); however, ESC-derived cell populations must be purified in some way to remove undifferentiated stem cells. Without removal of the remaining stem cells, there is significantly risk of teratoma formation following transplantation, which can results in worse outcomes that the SCI itself (Führmann et al. 2016; Johnson et al. 2010). One strategy that has been successfully used to remove residual undifferentiated ESCs from cultures is to generate transgenic ESC lines that express puromycin N-acetyltransferase (PAC), which confers resistance to puromycin, under the control of a cell-lineage specific promoter (Mccreedy et al. 2014; Iyer et al. 2016; Xu et al. 2015). In this work, mESCs were modified using CRISPR/Cas9 technology to express PAC under the control of the aquaporin-4 (*Aqp-4*) promoter. Aqp-4 was chosen for this work because it is expressed specially in astrocytes, and all mature astrocyte populations express some level of Aqp-4 (Nagelhus et al. 1998), which should allow this cell line to generate cultures containing predominantly mature astrocytes.

3.3 Materials and Methods

3.3.1 mESC Culture

RW4 (ATCC, SCRC-1018) and Aqp4-PAC mESCs were maintained in complete media (CM) (10% Fetal Bovine Serum (Invitrogen), 10% Newborn Calf Serum (Invitrogen), 132 µM beta mercaptoethanol (BME) (Sigma, St Louis, MO), 10,000 units/mL mouse leukemia inhibitory factor (Life Technologies, Carlsbad, CA) and passaged when at 60-80% confluency. Cells were passaged using 0.25% trypsin-EDTA (Life Technologies) at 37 °C for 5 min to dissociate the cells. The trypsin reaction was quenched with CM and cells were seeded into a new T25 flask coated with 0.1% gelatin (Sigma).

3.3.2 Aqp4-PAC Selection Vector

All cloning steps were carried out in DH5α *E. coli*. The targeting cassette was constructed in a Gateway-compatible plasmid (pStart-K; Addgene #20346, Cambridge, MA) using a 718 bp SalI-AscI fragment of the 3' end of the 2nd intron of the *Aqp4* gene and a piece the 5' untranslated region of the 3rd exon of *Aqp4* (5' arm) and a 618 bp AscI-NotI fragment containing the genomic sequence of the 3' end of the 3rd exon of *aqp4* (3' arm).

Figure 3.2: Plasmid map of the aqp4-PAC targeting cassette in a pStartK backbone.

This site was chosen of PAC insertion so that homologous recombination would result in the *Aqp-4* start codon being removed and replaced with the *PAC* sequence. Between these 2 homology arms a *PAC/Pgk-neo* dual resistance gene was inserted. This dual resistance cassette contains, from 5′ to 3′: an Asc1 site, Kozak sequence, the coding region of PAC with bGH polyA signal (PKO-Select Puro; Agilent Genomics, Santa Clara, CA), floxed phosphoglycerate kinase I (Pgk) promoter driving the neomycin phosphotransferase gene (Neo) with bGH polyA signal, and another AscI site. Gateway recombination with the LR Clonase II Kit (Life Technologies #11791) was used to insert the entire region between the attL1 and attL2 sites into a pWS-TK3 vector, which contains the thymidine kinase gene to allow for negative selection of the electroporated ESCs (Wu et al. 2008) (Figure 3.1).

3.3.3 RW4 Electroporation and Clonal Analysis

Electroporation and clonal analysis was performed as previously described (Iyer et al. 2016). To facilitate a higher efficiency of homologous recombination in electroporated ESCs, a CRISPR/Cas9 system was used. Guide RNAs (gRNAs), inserted into a derivative of Addgene plasmid #43860, and Cas9 expression vectors (Addgene plasmid #43945) were generated by the

74

Genome Engineering Core at Washington University in St Louis. For both gRNAs, there were no

common polymorphisms within the gRNA sequence and there was at least a 3 bp mismatch with

the 20 nucleotide targeting sequence and any other sites in the mouse genome (Table 3.1). By

meeting these two criteria, the probability of an off-target cuts is greatly decreased (Veres et al. 2014). 1×10^7 RW4 ESCs were suspended in

Table 3.2: Guide RNA (gRNA) and Junction PCR (jPCR) Primer Sequences

Name	Sequence
Aqp4 gRNA 1	GTGACAGAGCTGCGGCAAG
Aqp4 gRNA 2	ACAGAGCTGCGGCAAGGCGG
jPCR Forward	ACCCCGATGCCAAGTGGCTG
jPCR Reverse	GCGCCAGGAGGCCTTCCATCTGTTGCT

electroporation buffer (20 mM HEPES pH 7.5, 137 mM NaCl, 5 mM KCl, 0.7 mM Na_2HPO_4,

and 6 mM dextrose) with 8 µg Aqp4-PAC vector, 1 µg Cas9 expression vector and 1 µg of one

of the 2 gRNA vectors. Electroporation was performed in a 0.4 cm cuvette (Bio-Rad, Hercules,

CA) at 0.23 kV and 960 µF. Following electroporation cells were seeded in CM on a gelatin

coated 10 cm dish overnight to recover followed by 10 days of CM with 150 nM fialuridine

(FIAU, Moravek #M251, Brea, CA) and 40 µg/mL geneticin (G418, Life Technologies #10131),

replaced every 2 days.

After selection, 48 colonies were picked from each gRNA plate and the clones screened

by junction PCR (jPCR) with the primers in Table 1. jPCR positive clones were expanded until

they could be frozen in liquid nitrogen and analyzed for PAC and Glyceraldehyde 3-phosphate

dehydrogenase (GAPDH) copy number with quantitative real-time PCR (qPCR) using a

customized TaqMan Copy Number Assay according to manufacturer instructions. For these copy

number assays, mouse telomerase reverse transcriptase (Tert) was used as the endogenous

75

control, RW4s were used as the negative control, and a previously validated PAC line, Hb9-PAC, was used as the positive control (Mccreedy et al. 2014).

3.3.4 Derivation and Selection of Astrocyte Populations

Astrocyte were derived from Aqp4-PAC positive clones as previously described (R. E. Thompson et al. 2017). Briefly: $1x10^6$ ESCs were cultured in suspension on agar-coated 10 cm dishes in 10 mL DFK5 (DMEM/F12 (Life Technologies) plus 5% Knockout Serum Replacement (Life Technologies), 50 µM nonessential amino acids (Life Technologies), 1x Insulin-Transferrin-Selenium (Life Technologies), 100 µM beta-mercaptoethanol (Sigma), 5 µM thymidine, and 15 µM of the following nucleosides: adenosine, cytosine, guanosine, and uridine (Life Technologies) for two days to form embryoid bodies (EBs) followed by 4 days in 10 mL DFK5 plus 2 µM retinoic acid and 600nM Smoothened Agonist (SAG). On day 6, the EBs were dissociated and $4x10^6$ cells were seeded onto a gelatin-coated tissue culture treated 10 cm dish (ThermoFisher) in DFK5 media plus 20 ng/mL epithelial growth factor (EGF) (Peprotech), 10 ng/mL fibroblast growth factor 1 (FGF-1) (Peprotech) and 1 µg/mL laminin for 5 days. On day 11, the cultures were switched into lineage-specific media for 4 additional days on the same plates. Fibrous media: DMEM/F12 plus 1x G5 supplement (Invitrogen), 10 µg/mL ciliary neurotrophic factor (CNTF) (Peprotech); Protoplasmic media: DFK5 plus 10 µg/mL FGF-1, 10 µg/mL bone morphogenic protein 4 (BMP4) (Peprotech). On day 15, the cells were reseeded onto gelatin-coated plates at a density of 20,000 or 100,000 cells/cm^2 and maintained in lineage specific media for 2 additional days prior to selection in appropriate lineage specific media from D17 to D18 at different concentrations of 0, 2, 4, or 8 µg/mL puromycin (Sigma).

3.3.5 qPCR

RNA was harvested at various time points throughout the astrocyte differentiation protocol by removing the cells from the culture plate with 0.25% trypsin treatment. Cells were then spun down at 300 rcf for 5 minutes and the RNA extracted using a Qiagen RNeasy extraction kit according to manufacturer instructions. For qPCR, 500 ng of RNA from each sample was converted into cDNA using a High-Capacity RNA to cDNA kit (Applied Biosystems). Finally, the mRNA levels of the genes of interest was determined using specific Taqman assays following manufacturer instructions. β-actin was used as the normalization control in all samples.

3.3.6 Immunocytochemistry

Cells were fixed in 4% paraformaldehyde (Sigma) for 20 mins and then permeabilized in 0.1% Triton-X (Sigma) for 15 mins. Cells were then blocked with 5% of an appropriate serum (Goat or Donkey (both from Sigma)) in phosphate buffered saline (PBS) for 1 hr. Primary antibodies were used at the following dilutions: GFAP 1:100 (Immunostar), Aqp4 1:100 (Santa Cruz Biotechnology), β-tubulin 1:1000 (Biolegend). Primary antibody incubation was carried out overnight in 2% of appropriate serum in PBS. Secondary antibodies were all used at a 1:1000 dilution and incubated in 2% of appropriate serum in PBS for 1 hr. 1:1000 Hoechst (Invitrogen) in PBS was incubated with the cells for 15 min prior to imaging. Percent of cells positive for each marker in the cultures was determined by counting the number of nuclei visible per image, and then the number of cells staining positive for the given marker. For each well, a minimum of 3 images taken at different locations were counted, and the average of those percentages used as the percent positive for the given biological replicate.

3.3.7 Statistics

Percent positive cells at different concentrations of puromycin were compared using a paired t-test in Excel at a 95% confidence interval. When appropriate, a Bonferroni correction was used to account for multiple comparisons.

3.4 Results and Discussion

3.4.1 Aqp4-PAC ESC-derived Protoplasmic, but not Fibrous, Astrocytes Express PAC mRNA

Clustered regularly interspaced short palindromic repeats combined with Cas9 endonuclease (CRISPR-Cas9) technology allows for high-efficiency, specific double strand break creation based on the sequence 20 nucleotide guide RNA (gRNA) (Cong et al. 2013). Double strand breaks are generally repaired by non-homologous end joining, but rarely, in the presence of a donor DNA strand, homologous recombination repair occurs. The specificity of the CRISPR-Cas9 double strand break allows for significantly shorter homology arms to be used in the donor strand than previous required and the efficiency of the double strand break at the targeted location enhances the need for repair. Here CRISPR-Cas9 was used to insert a PAC gene into one of the two *aqp4* alleles in the RW4 mESCs genome through a homology-directed repair mechanism. PAC insertion designed to occur at the location of the normal aqp4 start codon in the third exon of the gene (Figure 3.2A). After electroporation, mESC colonies were selected with both neomycin (positive selection) and ganciclovir (negative selection). Surviving colonies were then screened using junction PCR (jPCR) to confirm that PAC was inserted into a *aqp4* locus. jPCR revealed that 2 of the 48 picked clones for one of the gRNAs contained PAC in the desired location (Figure 3.2B). Since insertion of PAC into both *aqp4* loci and/or randomly into the genome is theoretically possible, qPCR was used to determine the total number of copies of PAC gene within the genome of the jPCR positive clones. Both jPCR positive clones were

78
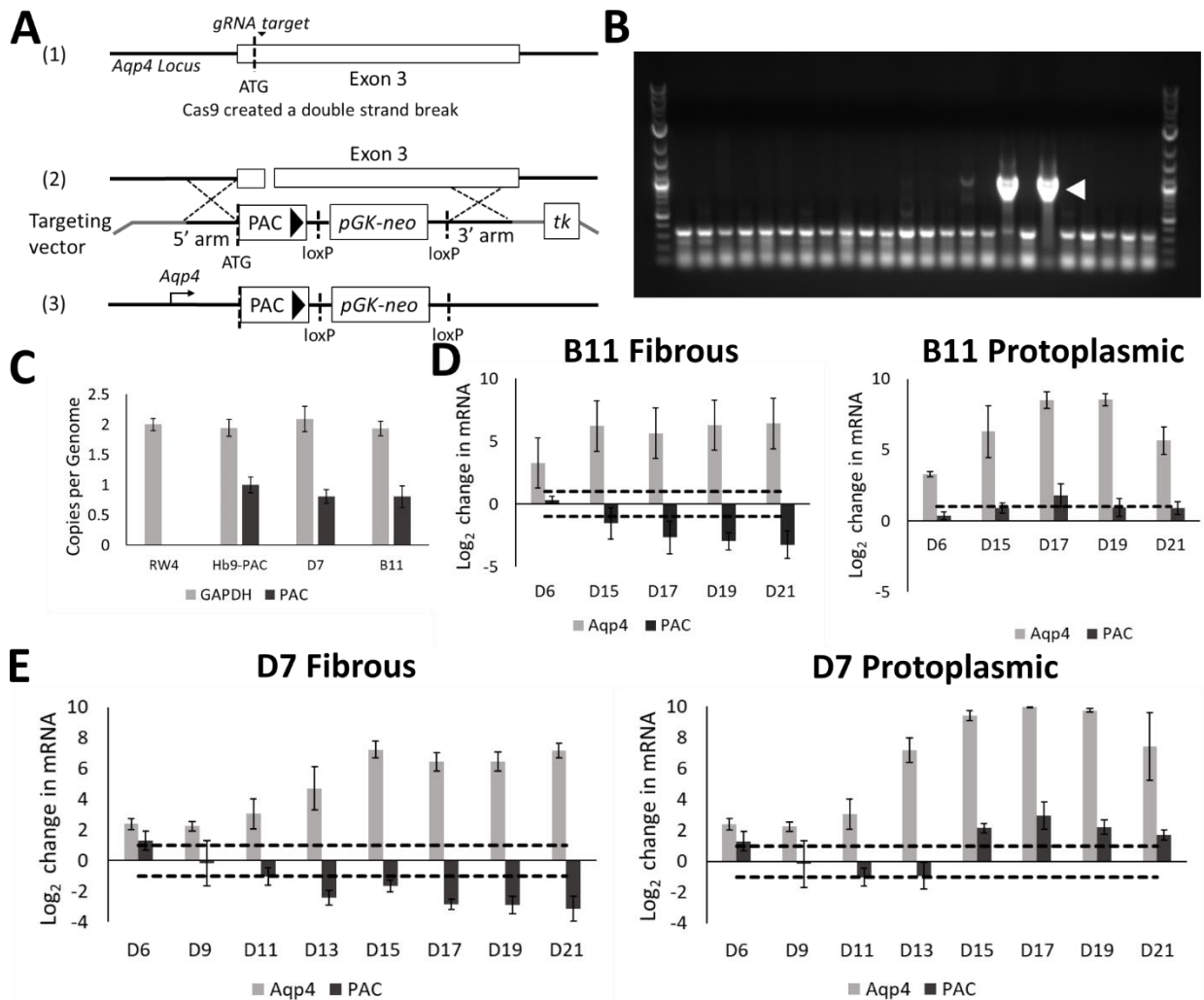
Figure 3.2: PAC was successfully inserted into 1 copy of the *aqp4* gene and is expressed in protoplasmic astrocyte cultures. A) Schematic representation of the CRISPR-Cas9 mediated strategy used to insert a copy of the PAC gene into one of the two *aqp4* alleles. **B)** Junction PCR demonstrating successful PAC insertion into the targeted *aqp4* locus (arrowhead). **C)** Copy number assay comparing GAPDH and PAC copies detected in unmodified RW4 ESCs, previous described and validated selectable ESC line (Hb9-PAC), and 2 Aqp4-PAC clones (D7 and B11). N=4, error bars: std err. **D)** qPCR data showing mRNA levels of aqp4 and PAC in astrocytes cultures derived from D7 aqp4-PAC ESCs at different time points of either fibrous (left) or protoplasmic (right) astrocyte differentiation. N=3-5; Error bars: std err; dashed lines: 2-fold change (either up or down regulated), compared to undifferentiated ESCs **E)** qPCR data showing mRNA levels of aqp4 and PAC in astrocytes cultures derived from D7 aqp4-PAC ESCs at different time points of either fibrous (left) or protoplasmic (right) astrocyte differentiation. N=2-5; Error bars: std err; dashed lines: 2-fold change, either increase or decrease, compared to undifferentiated ESCs.

found to have a single copy of PAC, based on comparison to a previously validated PAC

containing cell line, Hb9-PAC (Mccreedy et al. 2014) (Figure 3.2C).

With both clones validated to contain only a single PAC at the expected location in the genome, expression of both Aqp-4 and PAC throughout either fibrous or protoplasmic astrocyte differentiation was determined with qPCR. qPCR revealed that neither B11 or D7 derived fibrous astrocyte cultures exhibited a significant increase of PAC mRNA levels compared to mESCs over the tested time course (Figure 3.2D, E, left panels). This lack of PAC upregulation indicates that these Aqp4-PAC cell lines are not useable for selection of fibrous astrocyte cultures. One potential option for future studies to pursue to obtain a selected fibrous astrocyte culture would be to use a previously developed Olig2-PAC cell line (D. a. McCreedy et al. 2012). This cell line has been used to acquire progenitor motor neurons, which can form astrocytes, oligodendrocytes and neurons, and has been transplanted following dorsal hemisection SCI (D. A. McCreedy et al. 2014; Wilems et al. 2015). Fibrous astrocytes are known to maintain Olig2 expression, while protoplasmic astrocytes translocate Olig2 to the cytoplasmic and then stop expression (Cassiani-Ingoni et al. 2006; J. E. Davies et al. 2008). This effect has been observed to occur at around D15-17 in the mESC-derived astrocyte cultures, and so this Olig2-PAC mESC line could be used to select for specifically fibrous astrocytes at a later time point in the differentiation protocol. Delayed selection should also remove any motoneurons, which express olig2 early in their differentiation, from the cultures as well.

In contrast to the observations in fibrous differentiation, both B11 and D7 demonstrated a clear upregulation of PAC mRNA levels compared to mESCs during protoplasmic astrocyte differentiation. This peak was found to occur at around D17 of the protoplasmic astrocyte differentiation protocol and coincides with the peak of Aqp-4 expression in both clones. Also, it appears that PAC mRNA levels in general track with Aqp-4 mRNA levels, an indication that PAC and Aqp-4 are driven by similar regulator mechanisms (Figure 3.2D, E, right panels). Since

the D7 clone exhibited slightly higher levels of PAC mRNA than B11, puromycin selection experiments were carried out using this cell line.

Previous experiments have shown that neurons extend longer neurites on protoplasmic than fibrous substrates (R. E. Thompson et al. 2017), and that protoplasmic astrocytes improve *in vivo* outcome when transplanted (S. J. A. Davies et al. 2011; J. E. Davies et al. 2008). These observations suggest that a selected protoplasmic population is worth pursuing, even if the same cell line cannot be used to generate selected fibrous populations. A potential explanation of the lack of significant upregulation in PAC in the fibrous cultures is that fibrous differentiation does not drive a large enough change in Aqp-4 levels over the mESCs to surpass the low levels of expression of the PAC in ESCs. This is somewhat supported by the lower level of the Aqp-4 mRNA peak in the fibrous cultures than the protoplasmic cultures (Figure 3.2D, E). A potential reason for the apparent low levels of aqp4-PAC expression is that the PAC-containing transcript is not as well controlled by the posttranscriptional mechanisms that are known to be important for normal *Aqp-4* gene regulation (Moe et al. 2008).

3.4.2 Puromycin Selection of Aqp4-PAC Protoplasmic Astrocytes Increases the Percent of Aqp4$^+$ Cells

Since PAC mRNA was found to be upregulated in protoplasmic astrocytes at D17 of differentiation, selection of astrocyte cultures derived from clone D7 Aqp4-PAC ESCs was performed to determine if the PAC was functional, and if post-selection cultures were enriched for astrocytes. Cells were selected for 24 hours at 2 different seeding densities (20,000 cells/cm^2 and 100,000 cells/cm^2) and exposed to 3 different concentrations of puromycin (0 µg/mL, 2 µg/mL, and 4 µg/mL). Post-selection cells were stained of Aqp-4 and GFAP to determine the astrocyte percentage within the cultures (Figure 3.3A). Quantification of the percent of cells

expressing these markers revealed that selection with 4 µg/mL puromycin significantly increased the percent of aqp4 positive cells from $38 \pm 5\%$ to $62 \pm 14\%$ in plates seeded with 100,000 cells/cm^2 (Figure 3.3B). There was also a significant increase from $44 \pm 8\%$ to $80 \pm 12\%$ GFAP$^+$ cells on plates seeded with 20,000 cells/cm^2 following selection with 4 µg/mL puromycin (Figure 3.3C).
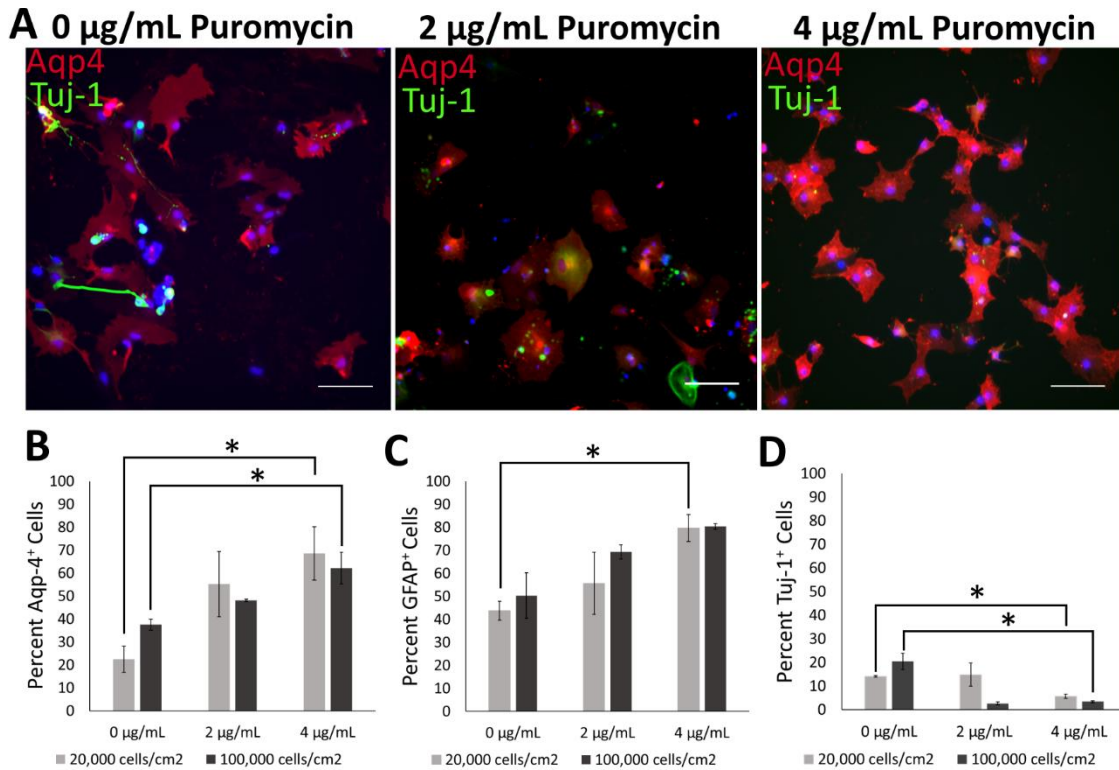
Figure 3.3: Puromycin selection increases astrocyte percentage is aqp4-PAC ESC-derived protoplasmic astrocyte cultures. A) Representative images of selected and unselected protoplasmic astrocyte cultures derived from Aqp4-PAC ESCs stained for Aqp-4 (red) and Tuj-1 (green). Scale bar: 100 µm, blue: nuclei. **B)** Quantification of the percent of cells expressing aqp-4 at different concentration of puromycin and cell densities. Error bars: Std. err. n=3-4. **C)** Quantification of the percent of cells expressing GFAP at different concentrations of puromycin and cell densities. Error bars: Std. err. n=2-3. **D)** Quantification of the percent of cells expressing β -tubulin III at different concentrations of puromycin and cell densities. Error bars: Std. err. n=2-3. *:p<0.05.

These plates were also stained for β-tubulin III (Tuj-1) since neurons have previously been shown to be the primary non-astrocytic population in these ESC-derived cultures (R. E. Thompson et al. 2017). β-tubulin III staining demonstrated a clear presence of neurons in unstained plates, and an apparent loss of these cells in plates that had been exposed to puromycin

(Figure 3.3A). Quantification of β-tubulin III staining revealed a significant decrease in neurons following selection of both 100,000 and 20,000 cells/cm^2 cultures. In 100,000 cells/cm^2 cultures the percentage β-tubulin III$^+$ decreased from $20 \pm 7\%$ to $3 \pm 1\%$ (Figure 3.3D). These preliminary findings indicate that selection of the Aqp4-PAC cultures increases the percentage of astrocytes present with the culture and removes most of the main contaminating cell type, neurons. Further experiments are required to validate these findings, explore potential alterations to selection to improve purity, determine if any ESCs are remaining within the cultures, and establish if there is functional maturation of these astrocytes.

It would be potentially interesting to perform calcium imaging on these post-selection astrocyte cultures to determine the level of functional maturation. Calcium signaling in astrocytes has recently been shown to be a major component of normal glial and neuronal interactions, so any ESC-derived astrocyte population should exhibit appropriate calcium signaling. In particular, astrocytes have been shown to propagate calcium waves in response to neurotransmitters, adenosine triphosphate (ATP), and mechanical stimulus through 2 distinct mechanisms: gap junctions and extracellular ATP release and subsequent signaling via P2Y purinoceptors (Oberheim, Goldman, and Nedergaard 2012). It has been found that fibrous astrocytes rely on the purinoceptors, P2Y$_1$ and P2X$_7$, to propagate calcium waves (Hamilton et al. 2008). In contrast, protoplasmic astrocytes are reliant on gap junctions between neighboring cells for calcium wave propagation. Although protoplasmic astrocytes do expressing P2Y$_1$, and so are responsive to exogenous ATP signaling (Fam, Gallagher, and Salter 2000; B. Haas et al. 2005). Together these observations of *in vivo* astrocytic calcium wave dynamics offer an appealing approach to functionally confirm the fibrous or protoplasmic identity of the ESC-derived astrocyte cultures following selection. This can be achieved by observing calcium wave

propagation in these cultures in the presence of purinoceptor or gap junction antagonist in response to ATP addition or a mechanical stimulus.

Chapter 4: Effect of Hyaluronic Acid Hydrogels Containing Astrocyte-Derived Extracellular Matrix and/or V2a Interneurons on Spinal Cord Injury Recovery

4.1 Abstract

Spinal cord injury (SCI) represents a substantial financial and psychological burden for patients, due to the limited capacity of the central nervous system (CNS) for spontaneous recovery. One reason for the lack of regeneration, and poor clinical outcomes, is the formation of an astrocyte-derived glial scar that inhibits new axon growth. Astrocytes have also been shown to be important for spontaneous SCI recovery in rodents, suggesting some astrocyte populations are pro-regenerative, while others are inhibitory following injury. In this work, the effect of implanting hyaluronic acid (HA) hydrogels containing extracellular matrix (ECM) harvested from mouse embryonic stem cell (mESC)-derived astrocytes on SCI recovery in rats was explored. In addition, the ability of HA hydrogels with and without ECM to support the transplantation of mESC-derived V2a interneurons was tested. The incorporation of ECM harvested from protoplasmic (grey matter) astrocytes, but not ECM harvested from fibrous (white matter) astrocytes, into hydrogels was found to reduce the size of the glial scar, increase axon penetration into the lesion, and reduce macrophage/microglia staining two weeks after implantation. HA hydrogels were also found to support transplantation of V2a interneurons and the presence of these cells caused an increase in neuronal processes both within the lesion and in the 500 µm surrounding the lesion. Overall, protoplasmic mESC-derived astrocyte ECM showed

potential for future development to treat CNS injury. In addition, ECM:HA hydrogels represent a novel scaffold with potentially beneficial effects on SCI recovery both with and without cells.

4.2 Introduction

Every year 17,000 Americans experience a spinal cord injury (SCI) and, due to the chronic nature of SCI, there are an estimated 243,000 to 347,000 Americans living with some level of disability due to SCI (Of 2013). The high number of chronic SCI patients is due to the lack of native regenerative capacity of the spinal cord, which means that SCI patients often experience some degree of lifelong paralysis. This paralysis results in a decrease in both life expectancy and quality of life for people living with SCI (Boakye, Leigh, and Skelly 2012). Due to the high healthcare burden for SCI patients, there is significant interest in developing materials and treatments that can be used to improve SCI outcomes. To facilitate treatment development, it is important to understand the native repair pathways and the factors that inhibit these pathways.

One of the major inhibitors of spinal cord regeneration is the glial scar that develops around the spinal cord lesion (Cregg et al. 2014). This scar has a stereotyped morphology with astrocytes forming a scar penumbra that represents both a physical barrier, due the woven morphology of astrocyte processes, and a biochemical barrier to new axon growth. One major class of axon growth inhibitors present within the glial scar is chondroitin sulfate proteoglycan (CSPG) (Oohira, Matsui, and Katoh-Semba 1991). Degradation of CSPGs with the enzyme chondroitinase ABC has been show to improve SCI outcomes in rodents, indicating the importance of CSPGs in axon growth inhibition (Bradbury et al. 2002; Wilems and Sakiyama-Elbert 2015). These observations, coupled with the role astrocytes play in the formation of a physical barrier in the glial scar, led to the belief that astrocytes are primarily inhibitory following SCI.

Recent studies have challenged the conclusion that astrocytes are solely inhibitory following SCI, with astrocyte knockout studies demonstrating that astrocytes are required for recovery following SCI as well. In particular, glial fibrillary acid protein (GFAP)-thymidine kinase (TK) mice, which allows ganciclovir administration to be used to ablate all dividing GFAP$^+$ cells, have been used to study the conditional ablation of astrocytes either at the time of injury or 5 weeks after injury. These studies have found that the lack of astrocytes around the SCI lesion acutely results in larger lesion area and decreased axonal growth into the lesion (J. R. Faulkner et al. 2004; Anderson et al. 2016). Delivery of ganciclovir 5 weeks after injury caused delayed scar ablation, but did not result in increased axonal growth. Furthermore, it was found that hydrogel-based delivery of neurotrophin-3 (NT-3) and brain-derived neurotrophic factor (BDNF) improved axon penetration into the lesion only when the glial scar was intact (Anderson et al. 2016). These data suggest that some astrocytes can be pro-regenerative following SCI, and that they are required for recovery.

These knockout observations are supported by recent astrocyte reactivity studies, which found that reactive astrocytes exist on a phenotypic spectrum from pro-regenerative to inhibitory for axon growth. (Liddelow and Barres 2017). One illustration of this reactivity spectrum is the changes in astrocyte phenotype depending on insult. In particular, an inflammatory insult from lipopolysaccharide has been found to lead to inhibitory reactive astrocytes, while an ischemic insult leads to pro-regenerative reactive astrocytes (Zamanian et al. 2012). In addition, cytokines have also been found to manipulate reactive astrocyte phenotype as well, with acute IL-6 exposure promoting inhibitory, scar astrocytes (E. N. Benveniste et al. 1990; Codeluppi et al. 2014) and IL-10 promoting pro-regenerative astrocytes (Jackson et al. 2005). These

observations suggest that there is a role of the immune response in regulating the regenerative potential of astrocytes.

Astrocyte populations from different regions of the central nervous system (CNS) have also been found to have different responses to injury. Injury to fibrous (white matter) astrocytes has been found to cause process hypertrophy and overlap reminiscent of the glial scar (Sun et al. 2010), while protoplasmic (grey matter) astrocytes exhibit minimal process overlap following injury (Wilhelmsson et al. 2006). Functional differences between protoplasmic and fibrous astrocyte populations have also been observed in transplantation following right-side cervical dorsal column transection SCI. In particular, transplantation of human or mouse glial restricted progenitor-derived astrocytes exhibiting a protoplasmic phenotype led to improved outcomes, both histologically and behaviorally, compared to transplantation of astrocytes exhibiting a fibrous phenotype (J. E. Davies et al. 2008; S. J. A. Davies et al. 2011). Recently, methods were developed to specifically derive these astrocyte populations from mouse embryonic stem cells (mESCs). Studies of *in vitro* neuron growth on substrates derived from these astrocytes revealed that neurons extended significantly longer neurites on protoplasmic-derived substrates than fibrous-derived substrates, particularly when only decellularized extracellular matrix (ECM) from each type of astrocyte was tested (R. E. Thompson et al. 2017).

The ability of astrocyte-derived ECM alone to support neurite extension is particularly appealing because ECMs often contain many bioactive molecules that can promote regeneration (Badylak, Freytes, and Gilbert 2009). The capacity for ECM to promote regeneration has been harnessed to improve recovery from bone and cartilage injury (Benders et al. 2013), peripheral nerve injury (Moore et al. 2011) and myocardial infarction (Singelyn et al. 2012). Importantly for implantation into patients, ECM xenografts have been successfully used without any

indication of immune rejection from the host (Seif-Naraghi et al. 2013; Mirmalek-Sani et al. 2013; Hudson et al.). Given both their bioactivity and low immunogenicity, compared to cell transplantation, ECM-based materials have significant appeal for promoting tissue regeneration; however, many ECM-derived materials require animal sacrifice for tissue harvest. One way to avoid the animal harvest requirement is to derive ECMs from *in vitro* sources, such as ESC-derived or induced pluripotent stem cells (iPSCs)-derived cell populations. One drawback to *in vitro* harvested ECM is that they do not form a hydrogel without additional crosslinking. This means that the *in vitro* ECM needs to be incorporated into a gelation system or crosslinked to be useable as a scaffold.

Hyaluronic acid (HA) plays the major structural role in the native CNS ECM and naturally binds to other CNS ECM components making HA a logical choice as a base scaffold for SCI treatment (Bignami, Hosley, and Dahl 1993). HA needs to be crosslinked to have sufficient stability for implantation, and a gentle, specific crosslinking reaction is required to avoid modifying incorporated ECM proteins (Pakulska, Ballios, and Shoichet 2012). A previously developed HA gelation system uses a Diels-Alder reaction between HA-furan and polyethylene glycol (PEG)-dimaleimide that meets these requirements and forms an injectable, biocompatible HA hydrogel (Nimmo, Owen, and Shoichet 2011; Führmann et al. 2015). Injectability of the hydrogel is a desirable trait since it allows the entire, irregular lesion cavity to be filled without requiring significant dissection of the glial scar to create space (Matthews et al. 2016).

Interneurons (INs) are the main neuronal population that facilitates local connectivity between spinal cord neurons. This role makes INs key for coordination, left-right alteration, reflex circuits, and central pattern generation. Interestingly, rodents have been found to

demonstrate recovery from spatially and temporally separated left and right lateral transections, but not just spatially separated left and right lateral transections. This suggests that local rewiring, which is likely due to local IN populations, is important for spontaneous recovery from SCI (Courtine et al. 2008). One IN population that has known involvement in spontaneous SCI recovery is V2a INs. These cells have been implicated as required for normal left-right alternation in the lumbar spinal cord, especially at high speeds of locomotion, as well as respiratory recovery following cervical SCI (Steven A. Crone et al. 2008; S. A. Crone et al. 2009; Zholudeva et al. 2017). Recently, a mESC line has been developed that allows for highly enriched populations of V2a INs to be derived *in vitro*, making transplantation of this specific IN population possible (Iyer et al. 2016; Brown et al. 2014).

This work examines the effect of HA hydrogels containing ECM derived from different mESC-derived astrocyte populations on motoneuron growth *in vitro* and the effects of these astrocyte ECMs on recovery of rats from a thoracic dorsal hemisection SCI. The ability of HA hydrogels with and without ECM to support transplantation of mESC-derived V2a INs into a SCI lesion is also explored. This work represents the first implantation of a mESC-derived ECM for the treatment of SCI, and, to the authors' knowledge, is the first implantation study using an *in vitro* derived ECM. The utility of the implanted ECM was found to depend on the phenotype of the astrocyte-containing population that produced it. Fibrous ECM (F-ECM) was found to confer no benefit and in some cases detrimental effects histological outcomes, while protoplasmic ECM (P-ECM) was found to decrease the size of the glial scar, decrease macrophage/microglia infiltration, and increase axonal ingrowth. mESC-derived V2a INs were found to survive in HA hydrogels both with and without incorporation of P-ECM, and the presence of V2a INs was found to increase the presence of neuronal processes within and around

the SCI lesion. These data demonstrate a novel material platform that shows significant promise as a material for development of future CNS injury treatments.

4.3 Materials and Methods

4.3.1 mESC Culture

RW4 (ATCC, SCRC-1018), Hb9-PAC CAG-TdTomato and Chx10-PAC bact-TdTomato mESCs were maintained in complete media (CM) (10% Fetal Bovine Serum (Invitrogen, Carlsbad, CA), 10% Newborn Calf Serum (Invitrogen), 132 µM beta mercaptoethanol (BME) (Sigma, St Louis, MO), 10,000 units/mL mouse leukemia inhibitory factor (Life Technologies, Carlsbad, CA) and passaged every 2 to 3 days (60-80% confluency). 0.25% Trypsin-EDTA (Life Technologies) incubation at 37°C for 5 min was used to dissociate mESCs from the culture flask. This reaction was then quenched with fresh CM and cells were seeded into a new T25 flask coated with 0.1% gelatin (Sigma).

4.3.2 Astrocyte ECM production

Fibrous and protoplasmic populations were derived from RW4 ESCs as previously described (Figure 4. 1A) (R. E. Thompson et al. 2017). Briefly, $1x10^6$ RW4 ESCs were cultured in suspension on agar-coated 10 cm dishes in 10 mL DFK5 (DMEM/F12 (Life Technologies) plus 5% Knockout Serum Replacement (Life Technologies), 50 µM nonessential amino acids (Life Technologies), 1x Insulin-Transferrin-Selenium (Life Technologies), 100 µM beta-mercaptoethanol (Sigma), 5 µM thymidine, and 15 µM of the following nucleosides: adenosine, cytosine, guanosine, and uridine (Life Technologies) for two days to form embryoid bodies (EBs) followed by 4 days in 10 mL DFK5 plus 2 µM RA and 600nM Smoothened Agonist (SAG) (Roybon et al. 2013). On day 6, EBs were dissociated and $4x10^6$ cells were seeded onto a gelatin-coated low adherence 10 cm dish (ThermoFisher) in DFK5 media plus 20 ng/mL

91
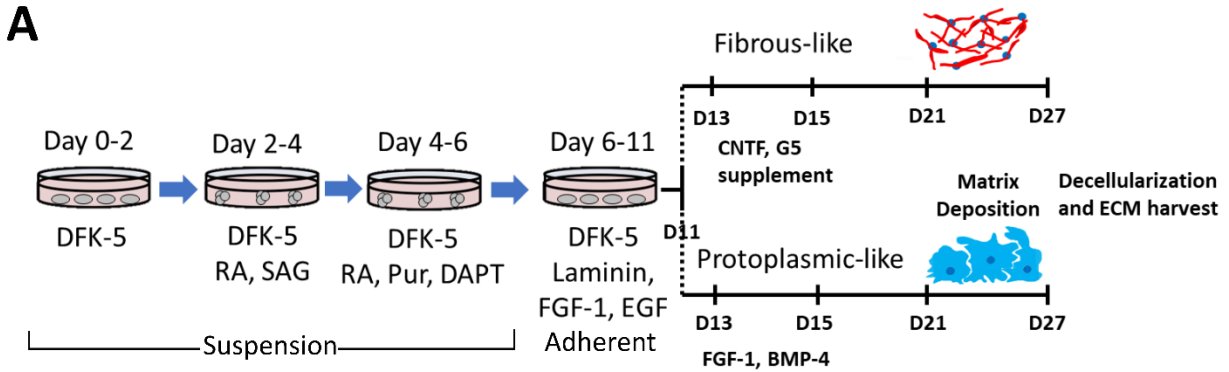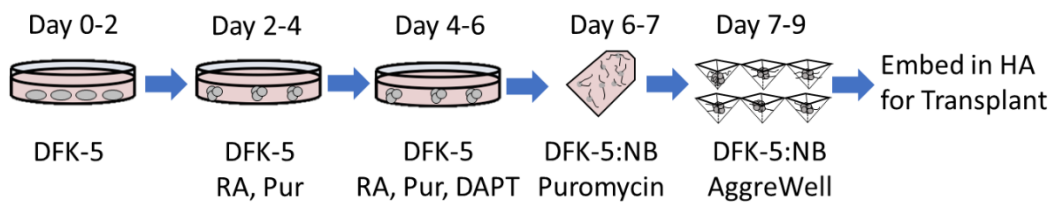
Figure 4.1: Schematic representation of astrocyte ECM production and V2a derivation. A) Protoplasmic-like and fibrous-like astrocytes were derived from mouse embryonic stem cells (mESCs) using a 15-day protocol. Following the 15 days of induction, astrocytes were allowed to mature in appropriate media for 6 days (D15-D21) prior to being seeded for matrix deposition (D21-27). After deposition, plates were decellularized, and the ECM scraped off the plates and lyophilized in 50 mM trehalose solution. **B)** V2a interneurons were derived from a mESC line that expresses puromycin resistance under the control of the Chx10 promoter and has constitutively active TdTomato expression. Following selection, interneurons were seeded onto aggrewell plates for 2 days to allow neuroaggregates to form prior to embedding them into HA hydrogels.

epithelial growth factor (EGF) (Peprotech, Rocky Hill, NJ), 10 ng/mL fibroblast growth factor 1 (FGF-1) (Peprotech) and 1 µg/mL laminin (Fisher Scientific) for 5 days. On day 11, the cultures were switched into lineage-specific media for 10 additional days. Fibrous media: DMEM/F12 plus 1x G5 supplement (Invitrogen), 10 µg/mL ciliary neurotrophic factor (CNTF) (Peprotech); Protoplasmic media: DFK5 plus 10 µg/mL FGF-1, 10 µg/mL bone morphogenetic protein 4 (BMP4) (Peprotech).

At D21, astrocytes were seeded onto gelatin-coated TC treated 10 cm dishes (ThermoFisher) at a density of 20,000 cells/cm^2 and culture in appropriate lineage media for 6

days to allow for matrix deposition. After matrix deposition, cells were removed from the culture

plates using a modified Hudson decellularization protocol (Hudson, Liu, and Schmidt 2004).

Following decellularization, 1 mL of 50 mM trehalose was added to each plate and the proteins

on the plate were scraped from the plate surface with a cell scraper. The resulting suspension of

ECM proteins was then lyophilized overnight and stored at -20 °C until use in hydrogels.

4.3.3 Preparation of V2a Interneuron Neuroaggregates

V2a INs were generated from Chx10-PAC bact-TdTomato mESCs as previously

described (Iyer et al. 2016). After induction, EBs were dissociated with 0.25% trypsin and

$2.5x10^7$ cells were seeded onto a poly-L-ornithine/laminin coated T25 flask. Chx10$^+$ cells were

then selected in half neural basal (Life Technologies)-half DFK5 media with 1x GlutaMAX (Life

Tech), 1x B27, 2 µg/mL puromycin and 10 ng/mL of the following growth factors for 24 hr:

glial-derived neurotrophic factor (GDNF) (Peprotech), NT-3 (Peprotech), and BDNF

(Peprotech). After selection, neurons were lifted from the flasks using Accutase® (Sigma)

treatment for 30 min and then 500,000 cells/well were placed into an AggreWell 400 plate with

1,200 small aggregation wells (Stemcell Technologies, Vancouver, BC). V2a INs were

maintained in V2a neuronal media (half neurobasal–half DFK5 media plus 1x GlutaMAX, 1x

B27, and 10 ng/mL of the following growth factors: BDNF, GDNF, NT-3) on the AggreWell™

plate for 2 days to allow for neuroaggregate (NA) formation (Figure 4.1B). After aggregate

formation, NAs were washed from the AggreWell plates with 100 µL of V2a neuronal media.

4.3.4 Preparation of HA Hydrogels

30% conjugated HA-furan and 39% conjugated HA-methylfuran were synthesized as

previously described from 250 MDa MW HA (Creative PEGWorks, Chapel Hill, NC) (Nimmo,

Owen, and Shoichet 2011). Percent conjugation signifies the percentage of carboxylic acid

groups within the HA macromolecules that have been reacted to add the furan functional group. For ECM incorporation, lyophilized ECMs were dissolved in 50 µL water and the protein concentration determined using a Pierce 660 nm assay (ThermoFisher) according to manufacturer instructions. All hydrogels had a final HA concentration of 1 mg/mL and a 3.5:3.0 molar ratio of the PEG-dimaleimide (Creative PEGWorks) crosslinking molecule to furan groups added. For *in vitro* motoneuron assays, ECM was added to 2 mg/mL HA-furan at different weight ratios prior to PEG addition, and then sterile phosphate-buffered saline, pH 7.4 (PBS) was added until HA concentration was 1 mg/mL. To form thin HA gels, 50 µL of gel was added to each well of a 48 well plate, and the plates were incubated overnight at 37 °C prior to motoneuron seeding.

For acellular implantation studies: 2 mg/mL HA-furan was dissolved in water, or 50 mM trehalose for HA alone implantation, followed by addition of the reconstituted astrocyte ECM at a 1:100 weight ratio of ECM to HA, and finally the solution was diluted with sterile PBS. PEG-dimaleimide was then added and 50 µL of gel solution was loaded into a Hamilton syringe and the syringe placed at 37 °C overnight to allow gelation to occur prior to implantation. For V2a IN transplantation: HA-methylfuran was dissolved in V2a neuronal media at a concentration of 4 mg/mL, and then astrocyte ECM was added at a 1:100 weight ratio of ECM to HA followed by addition of sufficient NA suspension to obtain a final concentration of approximately 6 NAs/µL. The final solution was then diluted with V2a neuronal media to 1 mg/mL HA. The NA number used results in roughly 60 NAs, or 25,000 cells, being transplanted per animal. Once the gel solution was prepared, 50 µL of gel was loaded into a Hamilton syringe, and the syringe placed at 37 C for 2 hours to allow gelation to occur prior to transplantation.

4.3.5 Motoneuron Culture on Thin HA Hydrogels

Motoneurons were derived from Hb9-Puro CAG-TdTomato mESCs that constitutively express TdTomato under the control of the synthetic CAG promoter, as previously described (D. A. McCreedy et al. 2014). To obtain pure motoneuron cultures, EBs were selected with 4 μg/mL puromycin from day 5 to 6 prior to dissociation and seeding onto the prepared HA hydrogels at a density of 20,000 cells/cm^2. Motoneurons were then cultured in half DFK5 and half Neurobasal media plus 1x B27 and imaged daily over the next 2 days.

4.3.6 Dorsal Hemisection Surgery

All animal procedures used in this work were approved by the Institutional Animal Care and Use Committee at the University of Texas at Austin, followed the NIH Guide for the Care and Use of Laboratory Animals, and were supported by the Animal Resources Center at the University of Texas at Austin. Animals (female Long-Evans rats, 225-275 g, Envigo, Indianapolis, IN) were anesthetized with 1.5-5% isoflurane and subcutaneous (SQ) injection of 5 mg/kg xylazine, surgery was performed on a heated pad. A single incision was made through the skin on the back from approximately T4 to T12, then blunt dissection was used to expose the muscular layer. Parallel cuts were made on either side of the spinal cord from T7 to T10 and the muscles along the spinal cord were retracted. To expose the spinal cord, a T8 dorsal laminectomy was performed using fine tipped rongeurs and the dura mater was removed with fine-tipped tweezers and microscissors.

To ensure a consistent injury, the spinal column was stabilized with spinal clamps attached to a stereotactic frame (Narishige, Tokyo, JP) and vitrectomy scissors, attached a micromanipulator, were lowered 1.5 mm into the spinal cord. To ensure a consistent dorsal hemisection, three cuts were administered at three separate locations moving from left to right

across the entire spinal cord. Following hemisection, the muscular layer was closed with degradable suture and the skin stapled closed. Post-op animals were given cefazolin (25 mg/kg SQ) to limit infection and cefazolin injections were continued 2x/day for 5 days. For pain management, animals were given buprenorphine (0.04 mg/kg SQ) 2x/day for the first 2 days post-op followed by 0.01 mg/kg SQ buprenorphine injections 2x/day for an additional 3 days. Bladders were expressed manually 2x/day until spontaneous bladder emptying resumed.

4.3.7 Hydrogel Transplantation Surgery

Two weeks after the dorsal hemisection procedure was performed, injured spinal cords were re-exposed via the same approach used in the injury surgery. Once the spinal cord was exposed, a small hole was made in the scar tissue to allow access into the SCI lesion cavity for a blunt-tipped Hamilton syringe. HA hydrogels were prepared as described above and 10 µL of gel was injected into each lesion cavity, which is sufficient gel to slightly overfill the cavities. For sham implants, the lesion cavity was exposed as in the HA implantation animals and 10 µL sterile 50 mM trehalose was injected. For the acellular implantation study animals were divided into 4 groups: sham implant, HA alone, HA + Fibrous ECM (F-ECM), HA + Protoplasmic ECM (P-ECM) (Table 4.1). In the V2a IN transplantation study animals were divided into 5 groups: sham implant, HA-mF alone, HA + P-ECM, HA + Cells (V2a IN NAs), HA + P-ECM + Cells

Table 4.1: Study design of acellular implantation study to compare astrocyte ECM effects on SCI recovery.

T8 Dorsal hemisection Injury	→ 2 weeks →	Implantation (Treatment) Surgery	→ 2 weeks →	Immunohistochemistry
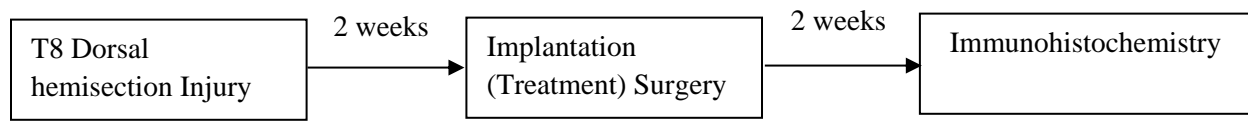
Treatment Group	N
Sham Implant (Injury Only)	8
HA alone Implant	8
HA + Fibrous Astrocyte ECM (F-ECM)	7
HA + Protoplasmic Astrocyte ECM (P-ECM)	8

(V2a IN NAs) (Table 4.2). Post-op care was performed as in the injury surgeries, all animals in the V2a IN transplantation study were immune suppressed with daily SQ injections of cyclosporine-A (10 mg/kg, Novartis, Basel, CH) starting on the day of transplantation and continuing for the duration of the study.

Two weeks after the transplantation surgery animals were euthanized via overdose of FatalPlus (pentobarbital) and transcardial perfusion was performed with 4% paraformaldehyde (PFA) (Fisher Scientific) in phosphate buffered saline (PBS). After dissection, spinal cords were post-fixed in 4% PFA for 4 hours at 4 °C and washed overnight with phosphate buffer at 4 °C prior to being cryoprotected in 30% sucrose in water for 3 days at 4 °C. Cryoprotected cords were embedded in Tissue-Tek OCT compound, frozen and cut into 20 µm sagittal sections on a Leica CM1950 cryostat.

Table 4.2: Study design of V2a IN transplantation study to confirm benefits of P-ECM incorporation in a different HA hydrogel and explore the ability of HA hydrogels to support cell transplantation.

T8 Dorsal hemisection Injury	2 weeks →	Implantation (Treatment) Surgery	2 weeks →	Immunohistochemistry

Treatment Group	N
Sham Implant (Injury Only)	7
HA alone Implant	7
HA + Protoplasmic Astrocyte ECM (P-ECM)	7
HA + V2a Interneuron Aggregates (Cells)	8
HA + P-ECM + Cells	8
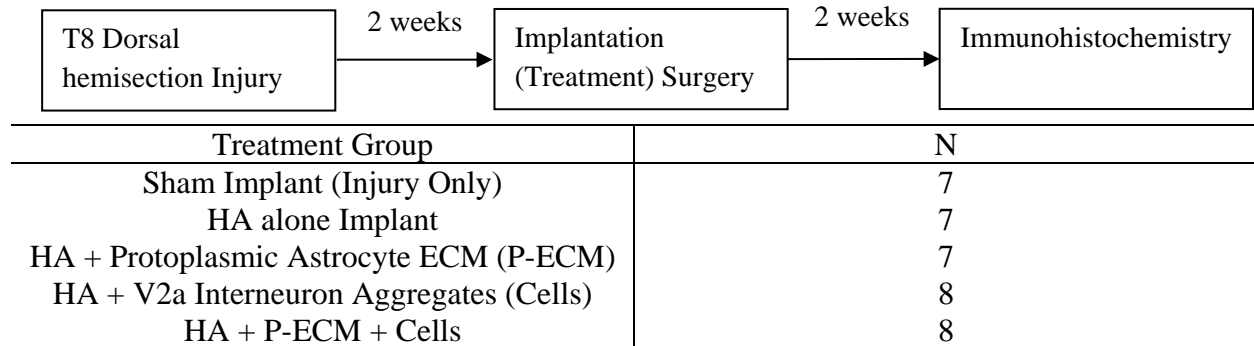
4.3.8 Immunohistochemistry

After sectioning, immunohistochemistry (IHC) was performed on 7 spinal cord sections, spaced 200 µm apart, for each animal in the study. For cord staining, OCT was washed from the slides with PBS and the sections were permeabilized with 0.1% Triton X-100 for 15 minutes. Following permeabilization, cord sections were washed 3x with PBS and blocked with 5% normal goat serum in PBS (NGS) for 1 hour. Primary antibodies were then applied overnight at 4

°C at the following dilutions in 2% NGS: Tuj-1 (BioLegend, San Diego, CA, Clone AA-10, 1:1000), GFAP (ImmunoStar, Hudson, WI, 1:100), chondroitin sulfate (CS56, Sigma, 1:250), CD68 (ED1, Bio-Rad Antibodies, Oxford, UK, 1:200), CD8α (Bio-Rad Antibodies, 1:1000), CD11b (Bio-Rad Antibodies, 1:1000), NeuN (EMD Millipore, Billerica, MA, 1:500), VGlut-2 (Millipore, 1:1000), NeuN (Millipore, 1:500). Following primary incubation, cords were washed 3x with PBS and were then incubated for 2 hours at room temperature in a 1:500 dilution of the appropriate AlexaFluor secondary antibody (Life Technologies) in 2% NGS. Finally, cords were washed 3 times with PBS and the sections mounted using ProLong Gold anti-fade reagent with DAPI (Life Technologies).

4.3.9 Immunohistochemistry Image Analysis

To quantify IHC staining, tile scan images were taken using a CMOS camera attached to a Leica DMi8 inverted fluorescent microscope with a 10x objective. Lesion areas were then traced using ImageJ and the traced lesion expanded by 500 µm to assess the host response to the implant. The resulting lesion area and lesion area + 500 µm images were quantified using a custom Matlab (Mathworks, Natick, MA) script as previously described (Wilems and Sakiyama-Elbert 2015). This script determines the intensity of each pixel and then determines whether the pixel is positive or negative for a given stain based on a user defined threshold. To facilitate comparison between animals and groups, all sections for a given group were stained, imaged, and analyzed at the same time. Additionally, data reported represents percent positive area for each stain which is defined as (positive pixels/all non-black pixels)*100. Using this approach helps to control for sectioning artifacts that result holes in the section. Quantification for the 500 µm surrounding the lesion alone was achieved by subtracting the positive and total pixel count in the lesion only image from the equivalent pixel counts in the lesion + 500 µm images. For

colocalization analysis, images were processed using CellProfiler (Broad Institute, Cambridge, MA) and the number of pixels positive for both the stain of interest (Tuj-1 or VGlut-2) and TdTomato was quantified.

4.3.10 Statistics

In vitro data was analyzed by two-way ANOVA with a Bonferroni post-hoc correction using a 95% confidence threshold. For *in vivo* studies, significance was determined using the non-parametric Kruskal-Wallis analysis of variance followed by Dunn's test to determine significance with 95% confidence. Power analysis was performed prior to starting the *in vivo* studies. Both studies were powered to show a 30% difference with 80% confidence.

4.4 Results

4.4.1 Protoplasmic ECM Incorporation Improves Motoneuron Growth on HA Hydrogels

Previous work has demonstrated that motoneurons exhibited longer neurite extension on decellularized mESC-derived protoplasmic astrocyte substrates than decellularized mESC-derived fibrous astrocytes substrates (R. E. Thompson et al. 2017). Since decellularization leaves only the ECM on the plate (Hudson, Liu, and Schmidt 2004), the ability of ECMs harvested from decellularized mESC-derived astrocyte substrates to improve motoneuron growth was explored. To allow these ECMs to form a growth substrate, ECM was combined with a previously described HA-furan PEG-dimaleimide hydrogel system. This HA system was chosen because of the gentle crosslinking reaction and its ability to be used *in vivo* (Nimmo, Owen, and Shoichet 2011). To preserve bioactivity, ECM was scraped from decellularized plates into 50 mM trehalose and then lyophilized. The resulting ECM powder was then dissolved in water with HA-furan in three different weight to weight ratios of ECM to HA (1:500, 1:100, 1:25 ECM:HA)

w/w ratio of ECM to HA
1:500   1:100   1:25

Protoplasmic

Fibrous

HA Control
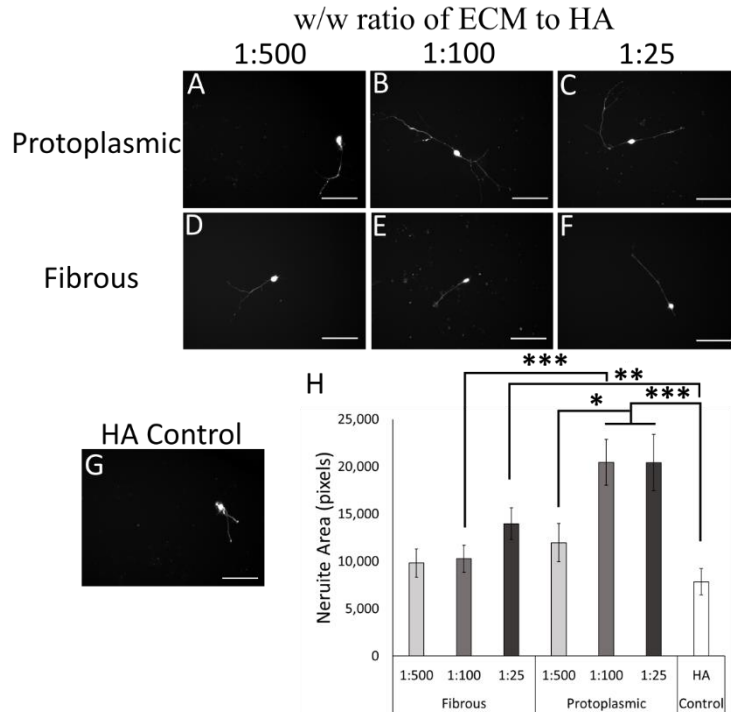
Figure 4.2: Protoplasmic ECM incorporation improves motoneuron growth after 48 hours in culture on HA hydrogels. Ratios given are weight of ECM to weight of HA. **A-G)** Representative images of motoneurons grown on different HA hydrogel substrate after 48 hours. A-C: HA hydrogels containing protoplasmic ECM; D-E: HA hydrogels containing fibrous ECM. Scale bars: 100 µm. **H)** Quantification of neurite area/nucleus of motoneurons after 48 hours in culture. Error bars = std error, n=25-45, *: p<0.05, **: p<0.01, ***: p<0.001.

prior to the addition of the PEG-dimaleimide crosslinker. A thin layer of gel was then allowed to form overnight in the culture plate prior to motoneuron seeding.

Motoneuron growth on ECM:HA hydrogels was assessed after 48 hours, and it was found that 1:25 Fibrous ECM (F-ECM) to HA, and 1:100 and 1:25 Protoplasmic ECM (P-ECM) to HA gels significantly improved motoneuron neurite extension when compared to HA gels with no added ECM (Figure 4.2B, C, F, H). There was also a trend demonstrating some dose dependency of the ECM with increasing ECM concentration improving neurite growth as evidenced by 1:100 P-ECM:HA showing significantly improved growth compared to 1:500 P-ECM:HA (Figure 4.2E). Finally, P-ECM demonstrated greater potency than F-ECM as illustrated by motoneurons extending significantly longer neurites on 1:100 P-ECM:HA gels than 1:100 F-ECM:HA gels (Figure 4.2B, E, H). These data indicate that ECM can be harvested from mESC-derived astrocyte cultures, and that the ECM maintains its ability to support neuronal growth. Based on these *in vitro* results, 1:100

ECM:HA ratio gels were used to determine the effect of astrocyte-derived ECM on SCI recovery *in vivo*.

4.4.2 Protoplasmic ECM can be Detected in HA Hydrogels in vitro and in vivo

Next, the ability of the HA hydrogels to retain ECM *in vivo* and *in vitro* was investigated using antibodies against collagen XIIα1. Collagen XIIα1 staining was used because previous proteomic data showed that collagen XIIα1 was the most prevalent protein within P-ECM that was significantly enriched in P-ECM over F-ECM, and it is too large to readily diffuse away (R. E. Thompson et al. 2017). Immunohistochemistry revealed that the collagen XIIα1 within the P-ECM could be detected in P-ECM:HA gels, but not in HA alone gels after 1 week *in vitro*, and that the incorporated collagen XIIα1 forms aggregates that are over 100 μm across within the gel (Figure 4.3A, B). Beyond 1 week *in vitro* the gels began to lose integrity.

Collagen XIIα1 staining was also used to determine if the P-ECM was present two weeks after implantation into a SCI lesion. Staining revealed collagen XIIα1 aggregates within the SCI lesion of animals implanted with P-ECM:HA gels that were similar in size to those observed in the *in vitro* staining (Figure 4.3B, D). These aggregates were not present in animals transplanted with HA alone gels, but more diffuse collagen XIIα1 staining was detected in the HA alone and P-ECM:HA gels suggesting that some native cells within the SCI lesion produce collagen XIIα1 (Figure 4.3C).

With collagen XIIα1 staining indicating the continued presence of implanted ECM for up to 2 weeks *in vivo*, the effect of F-ECM and P-ECM on histological recovery from SCI was explored to determine whether the observed *in vitro* effects of astrocyte ECMs translated into any *in vivo* effects. To address this question, a subacute implantation model in rats was used

where a T8 dorsal hemisection SCI was performed, followed two weeks later by an implantation

(treatment) surgery. The two-week delay between injury and treatment allows the glial scar and

lesion cavity to fully develop and stabilize in size. This limits the continued expansion of the lesion following implantation, which can impede the ability of native cells to penetrate the implant (Taylor and Sakiyama-Elbert 2006). Two weeks after implantation, recovery was assessed by measuring the response of immune cells, astrocytes, and neurons to the HA implants using immunohistochemistry.

Figure 4.3: A-B) Collagen XIIα1 staining in HA hydrogels either without ECM (A) or with P-ECM (B) after 1 week *in vitro*. **C-D)** Collagen XIIα1 (green) staining in animals transplanted with HA alone (C) or HA + P-ECM (D). Notice that native astrocytes do produce Collagen XIIα1 (C), but not in the same aggregate morphology seen in P-ECM gels (B, D). Scale bar: 100 µm. Arrowheads: Collagen XIIα1 aggregates from incorporated P-ECM.

4.4.3 Protoplasmic ECM Modulates Host Immune Response in Acellular Implants

The ECMs used for this study were harvested from mouse cells and transplanted into a

rat host, so it was important to ensure that there were no signs of implant rejection by the

immunocompetent host. The immune response to HA hydrogel implantation was assessed with

staining for CD11b (general myeloid cell marker), CD8a (cytotoxic T-cell marker), and ED-1

(marker of activated macrophages and microglia). Immune staining revealed no signs of

rejection of the xenogenic ECM based on the lack of any increase in immune cell staining in the

presence of ECM (Figure 4.4). In fact, the implantation of P-ECM:HA gels was found to

significantly reduce infiltration of myeloid cells (CD11b$^+$ area) into the lesion compared to all
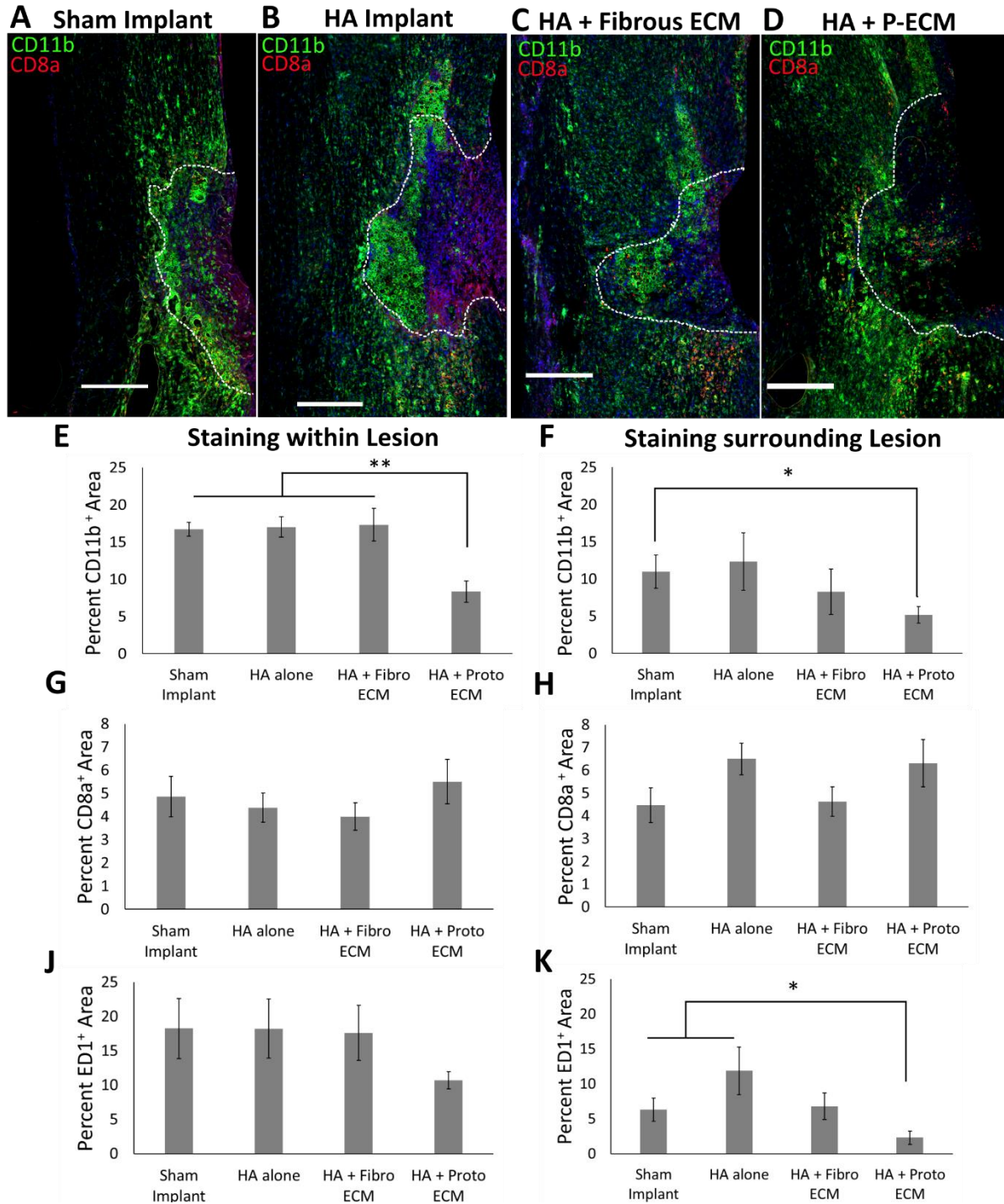
Figure 4.4: Protoplasmic ECM decreases immune cell infiltration into a SCI lesion. A-D) Representative images of CD8a (Cytotoxic T-cells, red) staining and the CD11b (myeloid lineage cells, green) staining 2 weeks after implantation (4 weeks after injury). Scale bars: 500 µm, dashed line denotes lesion boundary. **E,F)** Quantification of CD11b$^+$ area both within the SCI lesion (E) and in the 500 µm surrounding the SCI lesion (F). **G,H)** Quantification of CD8a$^+$ area both within the SCI lesion (G) and in the 500 µm surrounding the SCI lesion (H). **J,K)** Quantification of ED1$^+$ area (macrophages) both within the SCI lesion (J) and in the 500 µm surrounding the SCI lesion (K). *: p<0.05, **:p<0.01. n=7 HA + Fibro ECM, 8 for all other groups.

other groups (Figure 4.4A-E), and decrease CD11b staining around the lesion compared to the

sham implant group (Figure 4.4A, D, F). Staining for microglia and macrophages (ED-1$^+$ area)

was found to mirror the pattern observed in the CD11b staining with P-ECM incorporation

causing a significant decrease in the percent ED-1$^+$ area surrounding the lesion compared to both

the sham implant group and the HA hydrogel group (Figure 4.4J-K).

4.4.4 Protoplasmic ECM Incorporation Decreases the Presence of Inhibitory CSPGs and Size of the Glial Scar Following Acellular Implantation

The glial scar forms around the lesion core following SCI and is known to represent both

a physical and biochemical barrier to axonal regeneration following SCI. In addition, astrocyte

reactivity is known to be upregulated in the presence of some foreign materials (Y.-T. Kim et al.

2004). Thus, it is important to assess the astrocytic response to a material implant. To determine

the level of astrocyte reactivity, GFAP (a pan-reactive astrocyte marker) was used. The

production of inhibitory molecules within the cords was also determined with an antibody

against CS56, which detects CSPGs. GFAP staining revealed that P-ECM:HA gel implantation

decreased the size of the glial scar (based on percent GFAP$^+$ area in the 500 µm surrounding the

lesion) compared to both the sham implant group and the F-ECM:HA implant group (Figure

4.5A, C-D, F). CS56 staining also showed that P-ECM:HA gels decreased the presence of

inhibitory CSPGs within the lesion (Figure 4.5A, D, G). The presence of the HA itself was

sufficient to cause a decrease in the presence of inhibitory CSPGs in the glial scar (500 µm

surrounding the lesion); interestingly, this effect was lost in the F-ECM:HA gel group, but

maintained in the P-ECM:HA gel group (Figure 4.5A-D, H). Taken together these data show that

the type of astrocyte ECM within the implant affects the response of the host astrocytes to the

HA hydrogels with P-ECM decreasing the GFAP$^+$ area surrounding the lesion and F-ECM

potentially negating the reduction in CSPG staining surrounding the lesion seen in the HA alone

group.
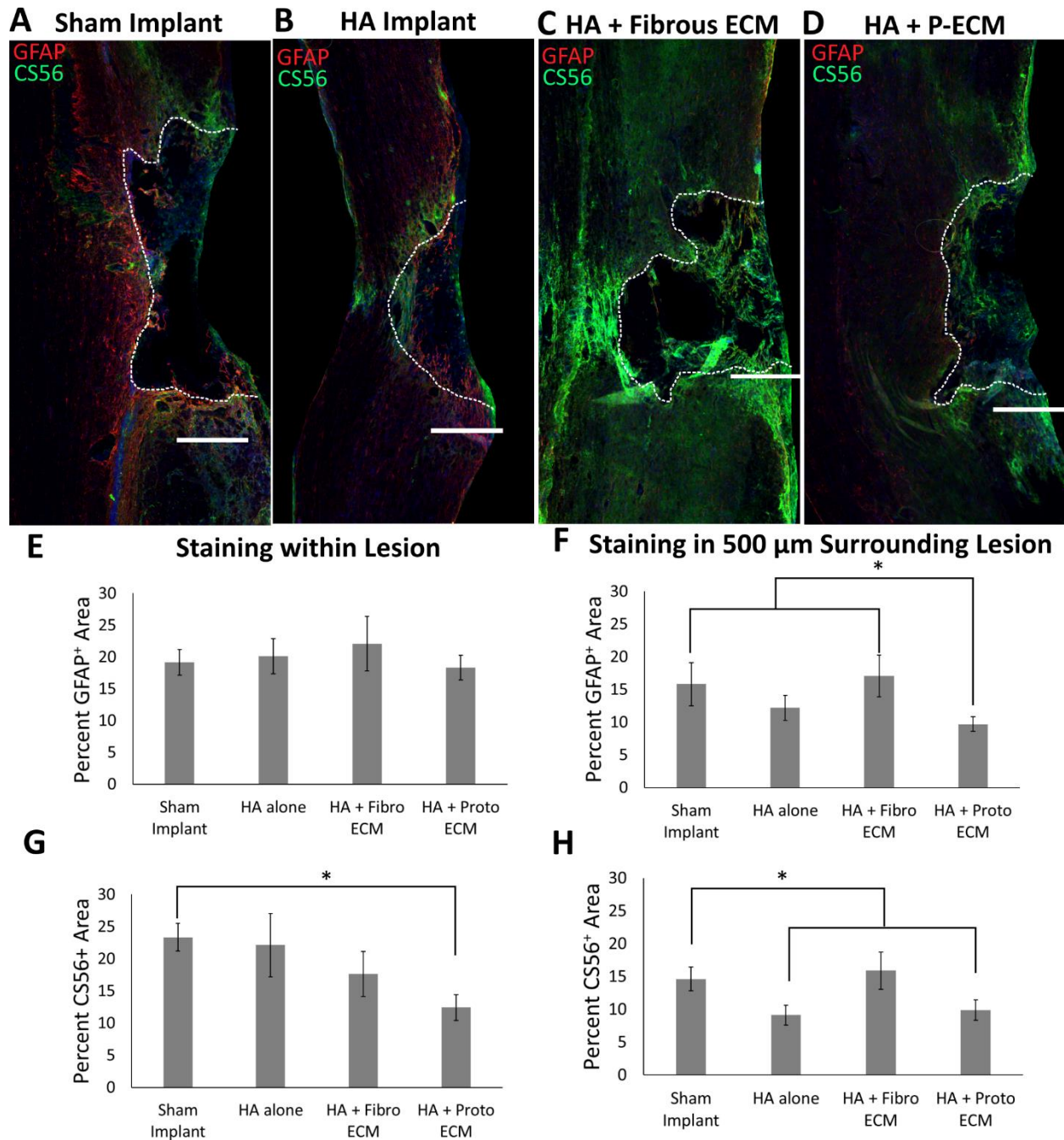
Figure 4.5: HA reduces CSPG staining and protoplasmic ECM incorporation decreases GFAP area. A-D) Representative images of CS56 (inhibitory CSPGs, green) staining and the GFAP (reactive astrocytes, red) staining 2 weeks after implantation (4 weeks after injury). Scale bars: 500 µm, dashed line denotes lesion boundary. **E,F)** Quantification of GFAP$^+$ area both within the SCI lesion (E) and in the 500 µm surrounding the SCI lesion (F). **G,H)** Quantification of CS56$^+$ area both within the SCI lesion (G) and in the 500 µm surrounding the SCI lesion (H). *: $p < 0.05$, **: $p < 0.01$. n=7 HA + Fibro ECM, 8 for all other groups.

4.4.5 Protoplasmic ECM Incorporation Increases Neurite Growth into a SCI Lesion Following Acellular Implantation

With encouraging results in terms of the immune and astrocyte reaction to P-ECM:HA gels, the next important question was whether these scaffolds had any impact on growth of axons into the SCI lesion. This is important to measure since the penetration of native axons into the transplanted material could aid in future reconnection of the signaling pathways within the spinal cord. Staining for β-tubulin III (Tuj-1) was used to assess the presence of neuronal processes within and around the SCI lesions. Based on percentage of the lesion/border area staining positive for β-tubulin III, it was found that P-ECM:HA gels increased axonal growth into the lesion compared to both the sham implant control and the F-ECM:HA gel group (Figure 4.6A-E). This increase in β-tubulin III indicates that the presence of P-ECM improves the ability of native neurons to extend into the SCI lesion and glial scar environment, consistent with the improvement seen in *in vitro* neuron growth in the presence of P-ECM (Figure 4.2) (R. E. Thompson et al. 2017).

Overall, P-ECM:HA hydrogel implantation appeared to improve histological outcomes following SCI injury, so the ability of these hydrogels to support the transplantation of a neuronal population was explored. For cellular transplantation within the HA gels to be possible, the HA crosslinking had to be modified to accelerate the gelation kinetics to enhance cell viability. Changing from HA-furan to HA-methylfuran (HA-mF) was recently described as a method that utilizes the same crosslinking chemistry and material properties, but allows for faster gelation (L. J. Smith et al., n.d.). By maintaining as much of the same material properties and similar chemistry, it seemed likely that the P-ECM:HA-mF gel implants would exhibit the same benefits that were observed in P-ECM:HA implants.
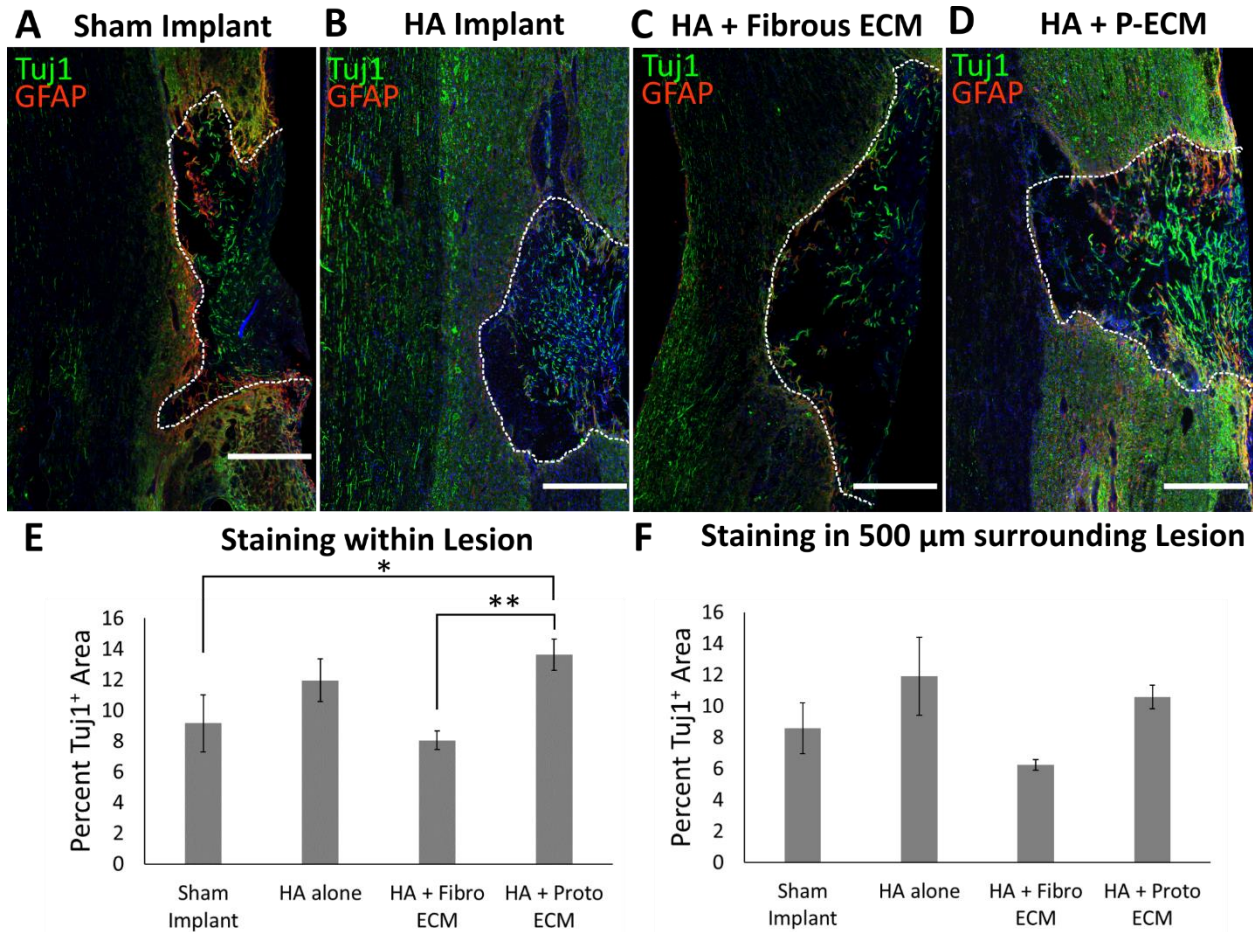
Figure 4.6: Protoplasmic ECM incorporation increases neural fiber staining within an SCI lesion. A-D) Representative images of β-tubulin III (neurons, green) staining and the GFAP (reactive astrocytes, red) staining 2 weeks after implantation (4 weeks after injury). Scale bars: 500 µm, dashed line denotes lesion boundary. **E,F)** Quantification of Tuj1$^+$ area both within the SCI lesion (E) and in the 500 µm surrounding the SCI lesion (F). *: $p<0.05$, **:$p<0.01$. n=7 HA + Fibro ECM, 8 for all other groups.

4.4.6 Protoplasmic ECM Maintains Immunomodulatory Effects in the Presence of Systemic Immune Suppression

Recently there has been increased interest in the ability of INs to support local rewiring and hence facilitate spontaneous recovery following SCI. Thus far IN transplantation has largely focused on inhibitory, GABAergic IN precursors that are isolated from the forebrain. These INs have been successfully transplanted into the spinal cord, and they have been shown to integrate and improve post-SCI pain and bladder function (Etlin et al. 2016; Fandel et al. 2016). Recently, a Chx10-PAC mESC line has been developed that allows for derivation of highly enriched V2a INs (Iyer et al. 2016). Since V2a INs have been suggested as an important type of neurons for

local rewiring and represent an excitatory population, mESC-derived V2a INs with constitutively active TdTomato were used in this study. To facilitate survival thru transplantation, V2a INs were aggregated with approximately 420 cells/NAs using an AggreWell™ plate before addition to the HA solution prior to gelation. Roughly 60 NAs were transplanted into each animal resulting in a total of ~25,000 cells per transplant. This cell transplantation study had 5 groups: sham implant (to allow for comparison to the acellular study), HA-mF alone, HA-mF + P-ECM, HA-mF + Cells and HA-mF + P-ECM + Cells (Table 4.2).
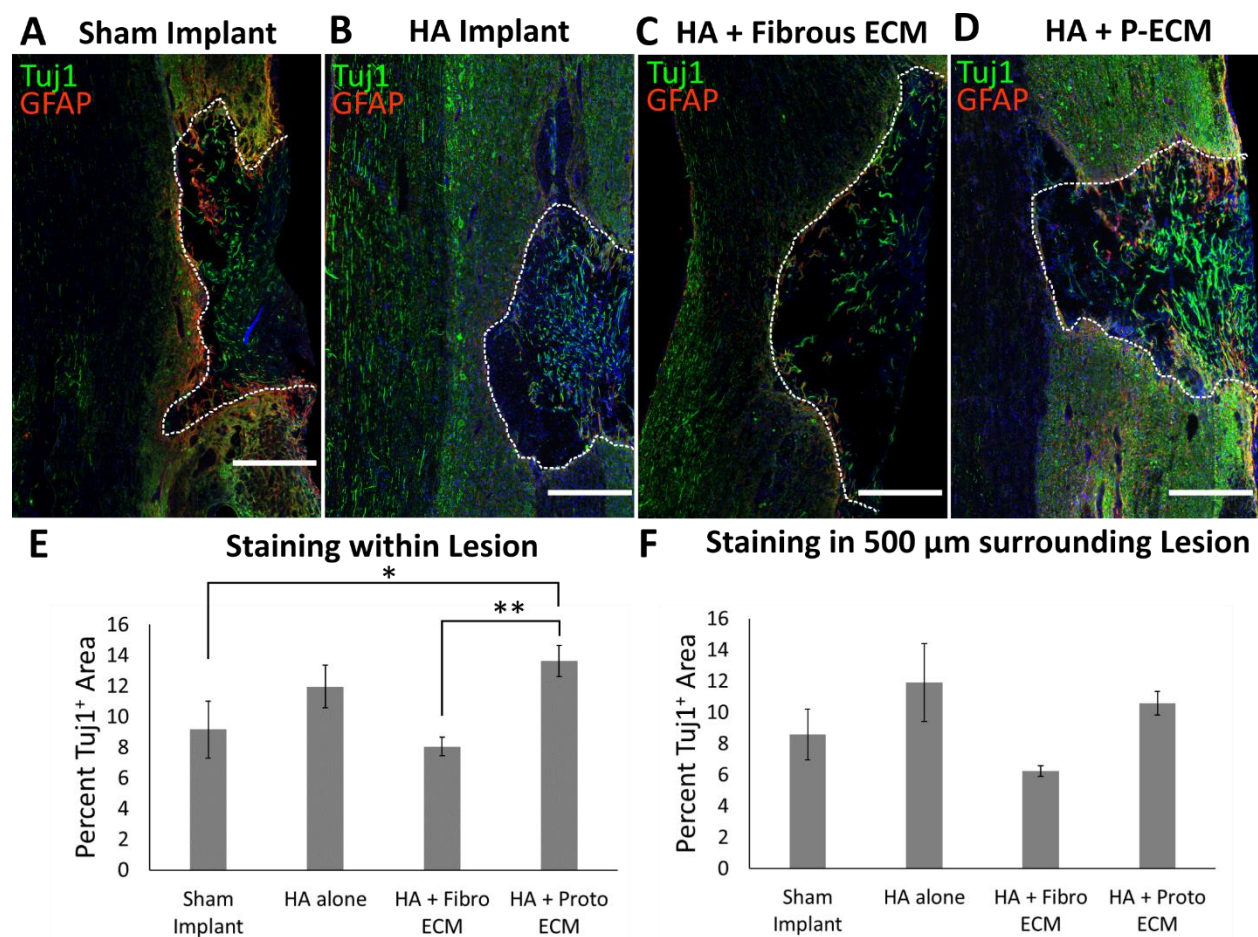
Figure 4.7: Protoplasmic ECM decreases macrophage staining, even in the presence of immunosuppression. A-E) Representative images of ED-1 staining (macrophages/microglia, green) 2 weeks after implantation (4 weeks after injury). Scale bars: 500 µm, dashed line denotes lesion boundary. **F,G)** Quantification of ED-1$^+$ area both within the SCI lesion (F) and in the 500 µm surrounding the SCI lesion (G). *: $p<0.05$. n=7 for Sham, HA, and HA + Proto ECM, 8 for HA + Cells and HA + Proto ECM + Cells.

To confirm that immune suppression was sufficient and to compare to the macrophage/microglia findings of the acellular study, ED-1 staining was performed on sections from the second *in vivo* study. Quantification of ED-1 staining revealed that, similar to what was observed in the acellular implantation study, P-ECM significantly decreased the percentage of the lesion area stained positive for ED1compared to sham and HA-mF alone (Figure 4.7F). The percent ED1$^+$ area was also found to be significantly lower in the 500 µm surrounding the lesion in P-ECM transplantation than the sham implant group (Figure 4.7F-G). Importantly there was no indication of a significant increase in ED-1 staining when the NAs were transplanted, indicating sufficient immune suppression (Figure 4.7A, D-E, F-G).

4.4.7 Incorporation of V2a INs Decreases GFAP Staining while HA-mF Decreases Inhibitory CSPG Staining

Staining for GFAP and CS56 in the cellular transplantation study revealed similar effects on the glial scar to those observed in the acellular implantation study. In particular, the presence of HA-mF hydrogels seemed to be sufficient to significantly decrease inhibitory CSPG staining within the 500 µm surrounding the lesion (Figure 4.8A-C, G). Similar to the acellular study, the percent GFAP$^+$ area was found to be significantly decreased in the presence of P-ECM compared to both sham and HA alone groups. (Figure 4.8J). The GFAP staining was also found to be altered in the presence of the V2a NAs with both cellular groups showing significantly less GFAP staining within and around the lesion than the HA alone group (Figure 4.8B, D-E, H-J). These observations indicate that HA-mF has the same effect on the scar astrocytes as observed in the HA furan and that P-ECM incorporation causes GFAP downregulation regardless of the HA used.
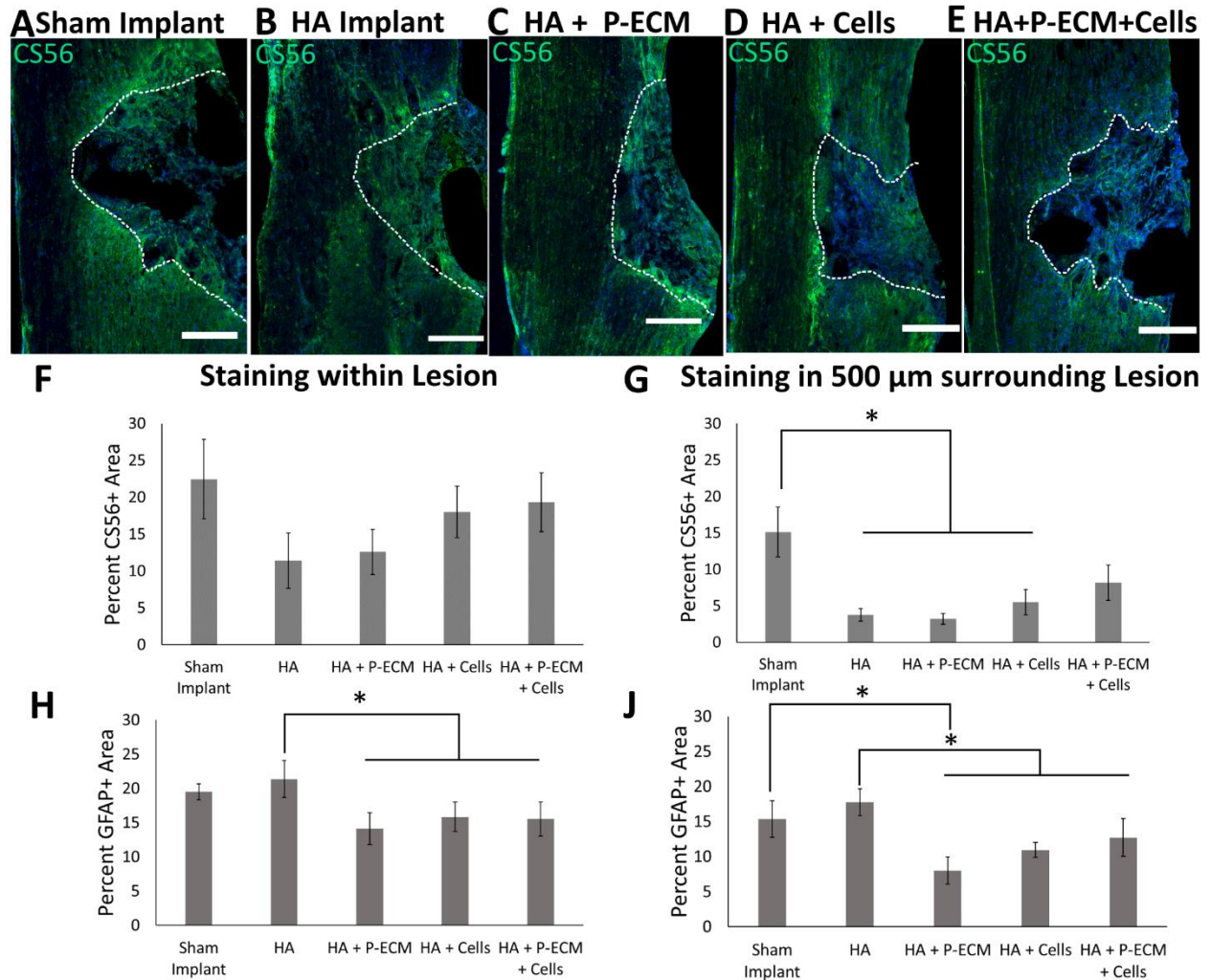
Figure 4.8: Hydrogel implantation modulates the response of the host astrocytes. A-E) Representative images of CS56 staining (inhibitory CSPGs, green) 2 weeks after implantation (4 weeks after injury). Scale bars: 500 µm, dashed line denotes lesion boundary. **F,G)** Quantification of CS56$^+$ area both within the SCI lesion (F) and in the 500 µm surrounding the SCI lesion (G). **H,J)** Quantification of GFAP$^+$ area both within the SCI lesion (H) and in the 500 µm surrounding the SCI lesion (J). *: $p<0.05$. n=7 for Sham, HA, and HA + Proto ECM, 8 for HA + Cells and HA + Proto ECM + Cells.

4.4.8 V2a IN Aggregates Survive Within HA-mF Hydrogels and P-ECM:HA Hydrogels and Increase Neuronal Process Staining Within and Surrounding the SCI Lesion

Since there was no sign of immune rejection of transplants, the presence of V2a INs within the lesion was assessed by quantifying TdTomato fluorescence. The percentage of the area within the SCI lesion found to be TdTomato$^+$ was significantly higher in the HA + Cells and the HA + P-ECM + Cells group than the associated acellular hydrogel groups (Figure 4.9B-F).

110
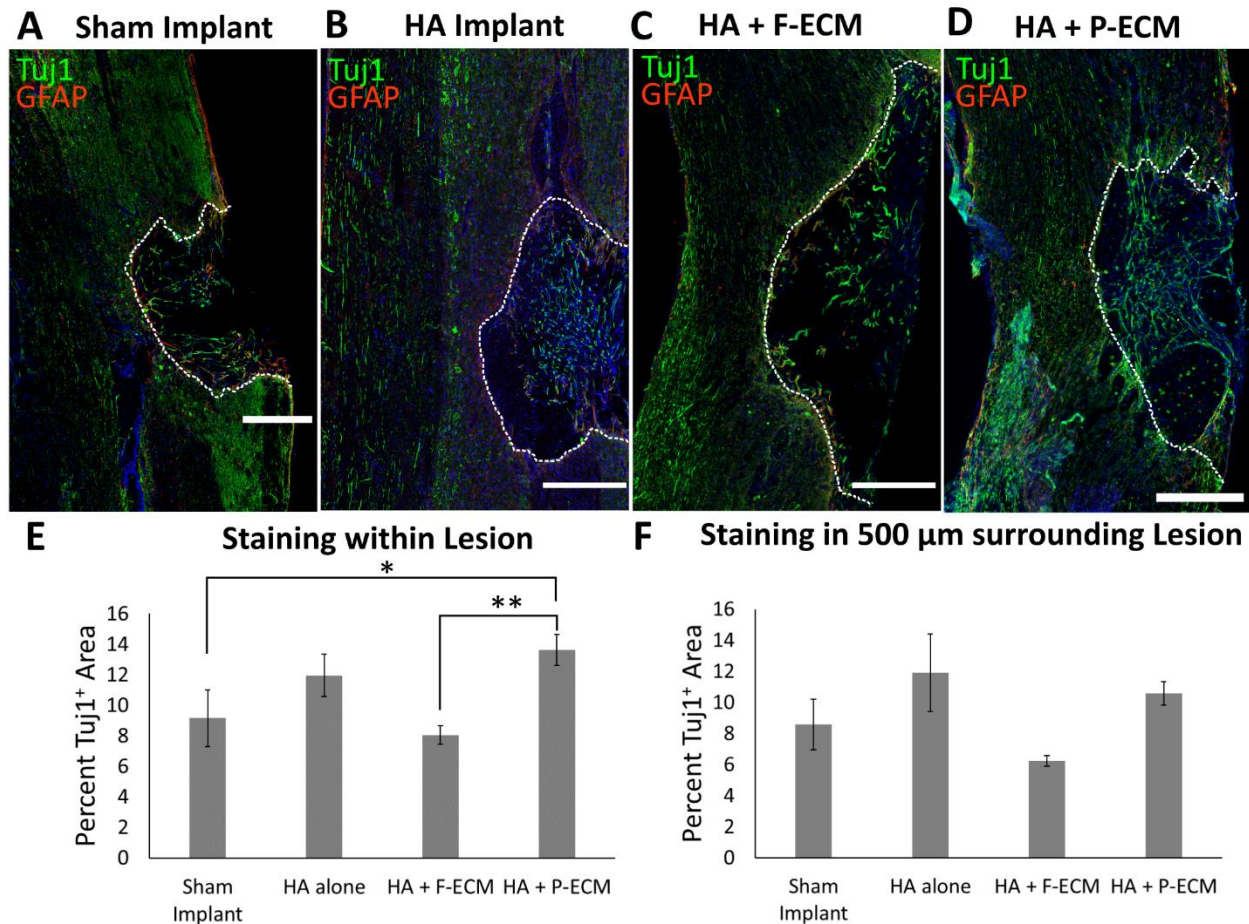
Figure 4.9: A-E) Representative images of β-tubulin III staining (neurons, green) and tdTomato (transplanted cells, red) 2 weeks after implantation (4 weeks after injury). Scale bars: 500 µm. **F,G)** Quantification of the percent TdTomato⁺ area both within the SCI lesion (F) and in the 500 µm surrounding the SCI lesion (G). **H,J)** Quantification of percent Tuj1⁺ area both within the SCI lesion (H) and in the 500 µm surrounding the SCI lesion (J). *: p<0.05. n=7 for Sham, HA, and HA + Proto ECM, 8 for HA + Cells and HA + Proto ECM + Cells.

However, this difference did not extend to the 500 µm surrounding the lesion (Figure 4.9G).

Together these observations suggest that the V2a NAs are surviving with the gel for up to 2 weeks following transplantation.

Based on the continued presence of V2a NAs within the SCI lesion, staining for β-tubulin III was performed to see if the presence of V2a NAs resulted in an increase of area staining positive for neuronal processes within and around the lesion. β-tubulin III staining revealed a similar pattern among the acellular groups as observed in the first *in vivo* study with HA + P-

ECM demonstrating significantly more neural fibers than either HA or sham within the SCI lesion (Figure 4.9H). The presence of cells also resulted in a significant increase of β-tubulin III within the lesion compared to both the sham implant and the HA alone implant groups (Figure 4.9H). β-tubulin III staining surrounding the lesion was also found to be significantly increased in HA + P-ECM, HA + Cells, and HA + P-ECM + Cells when compared to HA alone (Figure 4.9J). Furthermore, animals with HA + P-ECM + Cells transplants were found to have a significantly higher percentage of β-tubulin III$^+$ area around the lesion than sham transplant animals (Figure 4.9J).

4.4.9 Transplanted Cells Maintain V2a Identity, Extend Neural Processes within and around Lesion, and Migrate into Host Spinal Cord

To determine whether transplanted V2a interneurons maintained a glutamatergic, neuronal identity, colocalization between TdTomato fluorescence and staining for β-tubulin III, vesicular glutamate transporter 2 (VGlut-2), or neuronal nuclei (NeuN) was assessed. Visual inspection of cord sections revealed locations both within and around the lesion where these stains colocalized with TdTomato (Figure 4.10A-C). The presence this colocalization around the lesion suggests that the transplanted interneurons are able to migrate into the host spinal cord. The percent of area within and around the lesion that was positive for both β-tubulin III and TdTomato was quantified to determine the level of neuronal process extension from the transplanted cells both within the lesion and in the host. This analysis found that the cellular groups exhibited significantly more colocalization than the acellular groups, indicating that the transplanted V2a NAs extended neuronal processes (Figure 4.10D-E).

Similar quantification was performed on VGlut-2 staining and it was found that the HA + P-ECM + Cells group had significantly more colocalization of VGlut-2$^+$ and TdTomato$^+$ both
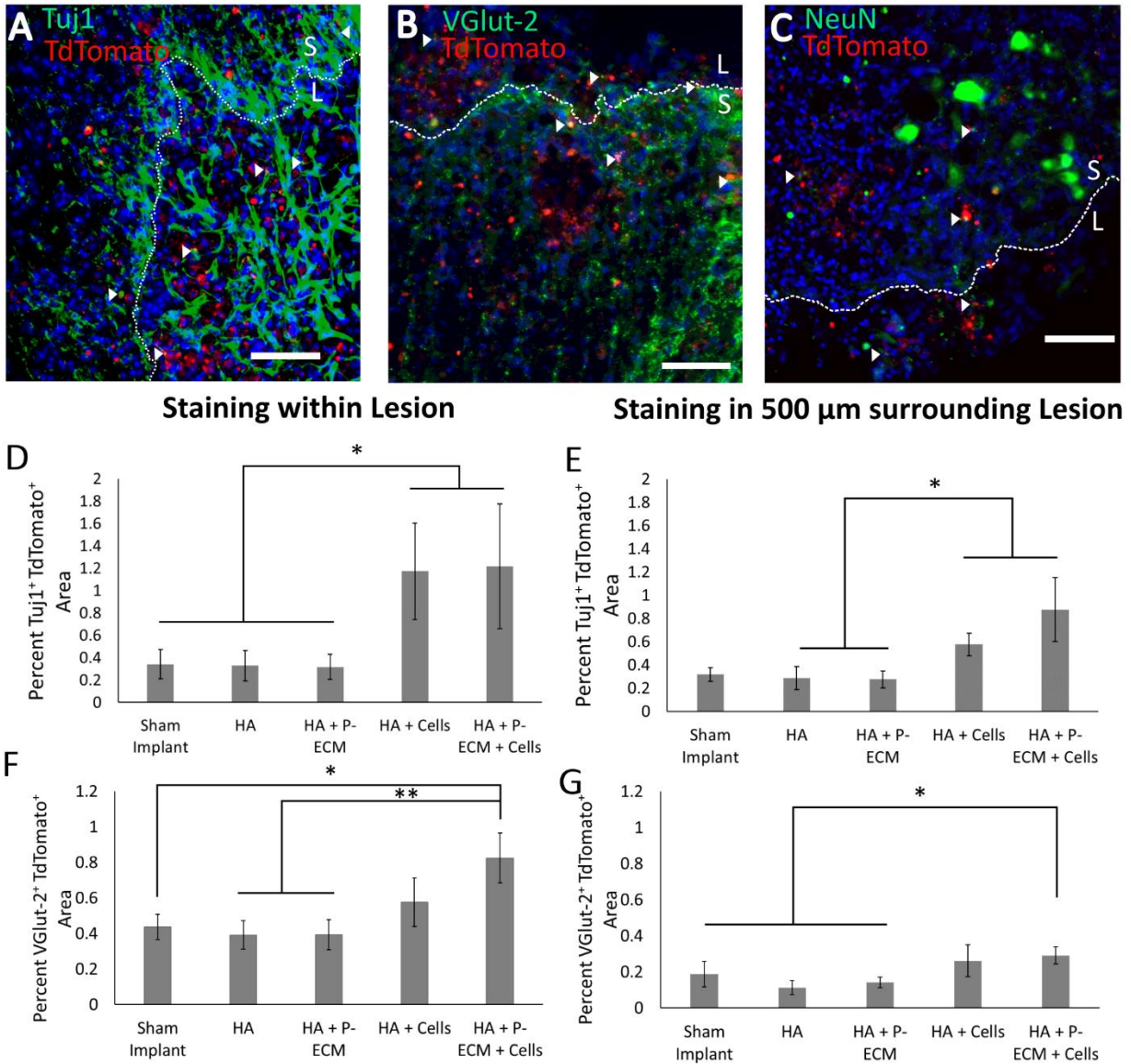
Figure 4.10: Transplanted V2a Interneurons maintain identity and enter the host spinal cord A-C) 20x magnification of the lesion boundary in animal transplanted with HA + P-ECM + Cells showing locations where β-tubulin III (A), VGLUT2 (B), or NeuN (C) staining colocalizes with TdTomato (arrowheads) both within the lesion (L) and in the glial scar (S). Scale bar: 100 µm. **D-E)** Percent of area within the lesion (D) and in the 500 µm surrounding the lesion (E) staining positive for both TdTomato and β-tubulin III. **F-G)** Percent of area within the lesion (F) and in the 500 µm surrounding the lesion (G) staining positive for both TdTomato and VGLUT-2. *: $p<0.05$, **:$p<0.01$. n=7 for Sham, HA, and HA + Proto ECM, 8 for HA + Cells and HA + Proto ECM + Cells.

within the lesion and in the 500 µm surrounding the lesion than any of the acellular groups

(Figure 4.10F-G). Together these observations suggest that the V2a NAs are surviving within the

HA hydrogels and that they continue to be glutamatergic. These data also suggest that some combination of the NAs extending neuronal processes and the host increasing axonal growth (perhaps due to the presence of the NAs) accounts for the observed increase in β-tubulin III$^+$ area both within and around the SCI lesion in the HA + Cells group compared to the HA alone group.

4.5 Discussion

4.5.1 HA Hydrogel Implantation Decreases Inhibitory CSPG Staining Within the Glial Scar and Protoplasmic Astrocyte ECM Incorporation Decreases Astrocyte Reactivity

Glial scar formation assessment with CS56 and GFAP staining revealed that the presence of either HA-furan or HA-mF hydrogels within the lesion area resulted in decreased staining of inhibitory proteoglycans in the 500 µm surrounding the lesion (Figures 4.5,4.8). Downregulation of CSPGs staining has been previous described in response to acute implantation of either a photo-crosslinked high molecular weight HA hydrogel or a poly-L-lysine (PLL) modified HA hydrogel (Khaing et al. 2011; Wen et al. 2016). This effect has been found the be dependent on the molecular weight of the HA with lower molecular HA (40 to 400 kDa) observed to cause an upregulation of CSPG expression and an increase in the size of glial scar (Pandey et al. 2013). In the present studies, HA hydrogel implantation is found to cause a similar downregulation of CSPG expression when delivered two weeks after injury, unlike the acute treatment used in previous studies. This effect of HA on CSPG expression has not been observed in implantation studies of fibrin (Wilems and Sakiyama-Elbert 2015), fetal spinal cord ECM (Lemons, Howland, and Anderson 1999), or methylcellulose hydrogels (Pakulska, Tator, and Shoichet 2017) following SCI. This suggests that the observed decrease in CSPG expression might be a specific benefit of HA hydrogels.

Despite the decrease in CSPG area, there was no observed downregulation of GFAP in the presence of HA hydrogels compared the sham implant animals (Figure 4.5, 4.8). GFAP immunoreactivity in response to material implantation has been found to be highly variable across with some materials, such as fibrin, leading to decreased GFAP$^+$ area (Johnson, Parker, and Sakiyama-Elbert 2009; Johnson et al. 2010), while others, such as poly(lactic-co-glycolic acid) (PLGA) and gelatin sponges, increased GFAP immunoreactivity (Du et al. 2014). Incorporation of P-ECM was found to reduce the percent GFAP$^+$ area in the 500 µm surrounding the lesion with both HA hydrogel formulations tested compared to sham implantation. The HA + P-ECM hydrogels were also found to demonstrate a similar decrease in CSPG staining as observed in the HA alone hydrogels (Figure 4.5, 4.8). This finding suggests that P-ECM presence may help to reduce the reactivity and/or hypertrophy of native astrocytes surrounding the lesion, while maintaining the benefits of HA on CSPG expression.

Interestingly, the beneficial effects of HA implantation on the glial scar was largely lost when a F-ECM:HA hydrogel was implanted. This change is evidenced by the significant increase in GFAP staining in the 500 µm surrounding the lesion in F-ECM:HA implanted animals compared to P-ECM:HA implanted groups, and the loss of the HA-associated CSPG reduction in the F-ECM:HA group (Figure 4.5). This suggests that F-ECM incorporation may result in some phenotype switch of native astrocytes toward a more inhibitory phenotype, which results in the observed increase in astrocyte reactivity and CSPG production. The concept of ECM components affecting astrocyte phenotype is not new, with astrocytes known to upregulate a "scar" phenotype in response the integrin binding to certain ECM components, such as collagen I (Hara et al. 2017; Tysseling-Mattiace et al. 2008). Studies of some of the major proteins found to be upregulated in P-ECM compared to F-ECM, namely fibronectin and

115

aggrecan (R. E. Thompson et al. 2017), have also been found to decrease GFAP and CSPG

expression by astrocytes *in vitro* (Hsiao, Tresco, and Hlady 2015). These studies provide a

potential basis for further experiments to identify the specific components within F-ECM and P-

ECM that cause these apparent changes in native astrocyte phenotype.

4.5.2 P-ECM Decreases Immune Cell Infiltration both in and around the SCI Lesion

Since the ECM transplants were xenogenic, it was important to ensure that they were not

being rejected by the host. Consistent with previous decellularized ECM implantation studies

(Hudson et al.), no increase in immune cell infiltration was observed in any of the ECM implant

groups despite an immunocompetent host in the acellular implant study (Figure 4.4). In fact, the

data indicated that P-ECM, but not F-ECM, resulted in a decrease in myeloid cell and

macrophage/microglia infiltration in the 500 µm surrounding the lesion compared to sham

implantation (Figure 4.4). Furthermore, HA:P-ECM implantation was found to significantly

reduce myeloid cell staining within the lesion compared to all other groups (Figure 4.4). This

observation suggests that P-ECM may exhibit an immunomodulatory role within the spinal cord.

ECM-dependent immune modulation has been previously described in the transplantation

of other ECM materials (Dziki et al. 2017), and has been observed in transplantation of either

decellularized urinary bladder or decellularized whole spinal cord ECM following SCI

(Tukmachev et al. 2016). One potential explanation for P-ECM, but not F-ECM, displaying

evidence of immunomodulation is the presence of significantly more fibronectin and laminin in

P-ECM. Fibronectin and laminin together have been found to cause tumor necrosis factor alpha

(TNF-α), a known pro-inflammatory cytokine, to bind to fibronectin and adopt a pro-adhesive

function (Hershkoviz, Goldkorn, and Lider 1995). This binding of TNF-α limits its diffusion and could help to control and localize the inflammatory response.

Another possible explanation is that P-ECM may alter the ratio of classically activated M1 macrophages, that cause tissue destruction, to "alternatively" activated M2 macrophages, which have been shown to be important to normal tissue repair throughout the body and CNS (Kigerl et al. 2009). In support of this idea, decreased macrophage infiltration and increased M2 macrophage presence has been described in response to implantation of increasing concentrations of decellularized urinary bladder ECM into a stroke cavity (Ghuman et al. 2016b). Based on these studies, it would be potentially enlightening to explore the macrophage activation state following P-ECM implantation to determine if P-ECM implantation is causing an increase in the presence of M2 macrophages. Overall, the immunomodulation effects observed in this study are a relatively unique advantage of ECM-based treatments, since many materials used for implantation are immunologically inert.

4.5.3 Protoplasmic, but not Fibrous, Astrocyte ECM Improves Neuron Growth on Acellular HA hydrogels both in vivo and in vitro

In vitro motoneuron growth assays on thin HA hydrogels found that both F-ECM and P-ECM increased average neurite extension. P-ECM exhibited more potency demonstrating an effect at a 1:100 weight ratio of ECM to HA, while no significant effect was observed with F-ECM until a 1:25 weight ratio (Figure 4.2). These *in vitro* findings were somewhat replicated in the *in vivo* implantation studies with 1:100 P-ECM:HA hydrogel implantation resulting in significantly more axon growth into the SCI lesion than when a 1:100 F-ECM:HA hydrogel or nothing was implanted (Figure 4.6). Both ECMs were used at 1:100 ratios for the *in vivo* studies to better facilitate comparison between them. P-ECM incorporation was also found to increase

axon growth in the HA-mF hydrogel system with acellular P-ECM:HA-mF hydrogels

demonstrating significantly more axon growth into the lesion compared to HA-mF alone

hydrogels and sham implant animals. Previous studies have shown implantation of either

decellularized fetal spinal cord or urinary bladder ECM following dorsal hemisection SCI

increases neuronal growth, supporting the idea that the **naïve** spinal cord ECM could have pro-

regenerative properties (Tukmachev et al. 2016).

In both *in vivo* studies, there is an observable inverse correlation in the acellular treatment

groups between the percent GFAP$^+$ area in the 500 μm surrounding the lesion and the percent β-

tubulin III$^+$ area within the lesion (Figures 4.5, 4.6, 4.8, 4.9). This suggests that the axonal

growth benefits observed in the presence of P-ECM may be related to a phenotypic switch of the

native astrocytes to a less reactive state. Further experimentation is required to determine the

precise nature of any astrocyte phenotype change and what specific factors within the implanted

ECMs might be responsible for these changes.

4.5.4 V2a INs Survive within HA Hydrogels, Migrate/Extend Processes into the Host, and Increase Neuronal Process Area both within and around the SCI Lesion regardless of P-ECM Presence

Quantification of the continued presence of the V2a IN NAs, using TdTomato

fluorescence, revealed that both HA-mF hydrogels and P-ECM:HA-mF supported cellular

transplantation (Figure 4.9). Staining for β-tubulin III revealed that the presence of V2a NAs led

to a significant increase in neuronal processes within and around the lesion area. This V2a IN-

associated increase in neuronal process staining could be the result of two different sources:

growth from the transplanted INs, and/or increased axon ingrowth from the host promoted by the

INs within the lesion. Quantification of the colocalization TdTomato and β-tubulin III suggests

that a combination of these two effects is occurring, since the TdTomato$^+$ neuronal processes

only explain some of the observed increase in neuronal processes (Figure 4.10D-E).

Colocalization analysis also revealed that some TdTomato$^+$ processes entered the host spinal

cord, indicating that these transplanted cells might be able to integrate with the host or at least

are able to move out the lesion site itself (Figure 4.10E). The ability of the transplanted cells to

migrate into the host is further supported by the presence of NeuN$^+$ TdTomato$^+$ nuclei in the

region surrounding the lesion (Figure 4.10C). Analysis of VGlut-2 staining showed that

VGLUT-2$^+$ TdTomato$^+$ pixels represented a significantly larger percent of the area within and

around the lesion in the HA + P-ECM + Cells group than observed in any acellular group (Figure

4.10F-G). This finding indicates that the transplanted V2as are maintaining their glutamatergic

identity following transplantation.

Overall, neuronal staining data demonstrated that either V2a IN NA transplantation or P-

ECM incorporation conferred a significant benefit on neuronal growth compared to HA alone,

but the combination of these factors did not significantly increase the area staining positive for

neuronal processes (Figure 4.9). Importantly, TdTomato colocalization with NeuN, VGlut-2, and

β-tubulin III indicates that the transplanted V2a interneurons maintain their identity as

glutamatergic neurons, migrate into the host, and extending neuronal processes both within the

lesion and into the surrounding cord (Figure 4.10). Future long-term recovery studies will be

required to determine if these transplanted V2a INs are able to functionally integrate into the host

spinal cord, and if the presence V2a INs and/or the increased neuronal area caused by P-ECM

incorporation translates into any behavioral improvements.

This work, as a whole, demonstrates that mESC-derived P-ECM, but not F-ECM,

incorporation into HA hydrogels results in significant improvements in histological markers of

recovery following SCI. Furthermore, ECM implantation was found to alter the behavior of

immune cells, astrocytes, and neurons within the context of the injured spinal cord, showing the multifactorial functionality of the HA:P-ECM material. The HA hydrogels were also found to support the transplantation of V2a INs into the SCI lesion and the presence of these cells was found to cause similar increases in neuronal process staining to those observed with P-ECM implantation. HA is the primary component of the native CNS ECM and HA alone implantation was found to decrease CSPG staining around the lesion, and support cellular transplantation. These observations indicate that HA may be preferable to other materials for CNS injury treatment. This work also shows that mESCs can be used as a scalable source of bioactive ECM as well as a source of V2a INs. The use of mESCs increases the potential clinical impact of this work, since the materials used do not require donor tissue to be generated. (R. E. Thompson et al. 2018)

Chapter 5: Summary of Findings and Future Directions

5.1 Summary of Findings

This work has strived to develop strategies to improve treatment for SCI by better defining the ability of different astrocyte populations to support neuron growth either *in vitro* and *in vivo* following SCI. We chose to focus on astrocytes in this project because recent studies have found that some astrocyte populations are required for recovery, and so it seems likely that not all astrocytes are primarily inhibitory as previously believed. With the goal of eventually translation of this project in mind, we focused on deriving the materials used in this work from mouse embryonic stem cells (mESCs). mESCs were chosen for this work because they can be more readily scaled up and involve fewer ethical concerns than primary cells. In addition, techniques that are developed in mESCs can, and have, been modified to allow similar cell populations to be derived from human induced pluripotent stem cells (iPSCs). This means that this work could eventually to be used to generate astrocyte population from human iPSCs, which would be an appropriate cell source for human transplantation.

The first aim of this project was to develop methodologies that could be used to differentiate specifically fibrous-like (white matter) astrocytes or protoplasmic-like (grey matter) astrocytes from mESCs. This protocol was developed based on previous work on mESC-derivation by Benveniste *et al*., iPSCs-derivation by Roybon *et al.,* and deriving specific astrocyte subtypes from primary glial progenitors by Davies *et al*. (R. J. Benveniste, Keller, and Germano 2005; Roybon et al. 2013; J. E. Davies et al. 2008). In Chapter 2, we showed that by combining aspects of these previously published works we could obtain cultures that contained

121

astrocytes that were predominantly fibrous or predominantly protoplasmic. Importantly, we found that these protocols resulted in protoplasmic populations that did not contain many astrocytes that exhibited fibrous hallmarks and vice versa. We then tested the abilities of these astrocytes to support the growth of motoneurons and interneurons. These experiments demonstrated that protoplasmic astrocytes were able to support significantly longer neurite extension than fibrous astrocytes from both neuron populations used.

Neuronal growth effect was particularly marked when the neurons were grown on decellularized astrocyte extracellular matrices (ECMs). Since ECM-based treatments have shown significant promise in other injuries with poor native regeneration, we focused on further characterization of the mESC-derived astrocytes ECMs. First, we identified all of the proteins found within our protoplasmic ECM (P-ECM) and fibrous ECM (F-ECM) using label-free proteomics. Then, with the help of Dr. Dougherty's lab, we compared the proteomics data to a dataset of the mRNA expression profile of astrocytes *in vivo*. This comparison revealed that our astrocyte ECMs were consistent with what an *in vivo* astrocyte produces. Finally, analysis of the ECM proteins revealed that P-ECM in general contained higher levels proteins known to be axon growth permissive than F-ECM, while F-ECM was found to be relatively enriched for proteins known to be inhibitory to axon growth. Knockdown of some of these proteins, with the highest levels of expression, revealed that the neuron growth benefits of protoplasmic ECM were somewhat reduced in laminin α5 or laminin β1 knockdown while F-ECM was able to support longer neurite extensions when spondin-1 was knocked down.

In Chapter 3 we discussed our efforts to develop a puromycin selectable astrocyte mESC line. A selectable cell line was important to develop since our astrocyte differentiation protocol does not result in pure astrocyte cultures, which could impede future experiments, and the

transplantation of unpurified ESC-derived cultures has been found to lead to teratoma formation, thus limiting to ability to transplant astrocytes using these techniques. This aspect of the project was based on previous work done in the lab by Dr. McCreedy and Dr. Iyer who developed the puromycin selectable motoneuron and V2a interneuron lines used in this work. We demonstrated that the puromycin-resistance gene (PAC) was inserted into the mESC genome within one of the *aqp4* loci. Furthermore, we found that the modified cell lines did exhibit an increase in PAC expression, coinciding with Aqp-4, over the course of astrocyte differentiation, but only in the protoplasmic cultures. This indicates that the developed aqp4-PAC cell line cannot be used for fibrous selection. Preliminary data does indicate that selection of aqp4-PAC-derived protoplasmic cultures does result in a significant increase in cells staining Aqp-4$^+$. Future work will be required to further confirm the purity of the selected protoplasmic cultures and develop a different selection strategy for fibrous astrocytes.

Due to the observed benefits of mESC-derived astrocyte ECM *in vitro*, in Chapter 4 of this work we explored the ability of these ECMs to affect recovery following SCI in rats. To develop the harvested mESC-derived astrocyte ECMS into a useable therapeutic, we combined the lyophilized ECM with a hyaluronic acid (HA) hydrogel system previously developed by Dr. Shoichet's group (Nimmo, Owen, and Shoichet 2011). Using a thin layer of hydrogel, we tested the effects of different ECM concentrations on the growth of motoneurons *in vitro*. This work revealed that a 1:100 weight ratio of ECM to HA was sufficient for the protoplasmic ECM to significantly improve neurite extension from the motoneurons *in vitro*. This observation led us to use this ratio for animal implant studies.

The initial animal study was performed with 4 groups: sham implant, HA alone, HA + F-ECM, and HA + P-ECM. This study revealed that the HA hydrogel reduced the presence of

inhibitory proteoglycans around the lesion and that addition of P-ECM reduced staining for reactive astrocyte as well. The observed beneficial effects on the glial scar environment were lost in the presence of F-ECM, indicating that F-ECM may cause an upregulation of a more inhibitory phenotype of the native astrocytes. HA + P-ECM implantation was also found to decrease immune cell infiltration into and around the SCI lesion and to significantly increase the penetration of axons into the SCI lesion. Based on these histological improvements, we performed a cellular transplantation study to explore the ability of these HA hydrogels to support transplantation of V2a interneurons as a pilot transplant population.

The V2a transplantation studies used a slightly modified HA hydrogel system, using HA-methylfuran (HA-mF), that was recently developed by Dr. Shoichet's group to have faster gelation kinetics and so allow for cellular encapsulation. Our V2a study had 5 groups: sham implant, HA alone, HA + P-ECM, HA + Cells, HA + P-ECM + Cells. This study found largely similar effects as observed in the first, acellular study with P-ECM incorporation demonstrating distinct benefits in histological markers of recovery compared to HA alone or sham implant. In addition, we found that either HA or HA + P-ECM supported the transplantation of V2a interneurons and that the presence of interneurons was found to significantly increase the staining for neuronal processes within the SCI lesion.

Overall, this work demonstrates that mESCs can be used to generate specific subtypes of astrocytes and that these astrocytes had differential capacities to support neuronal growth. We also found that these effects translated into an *in vivo* setting with P-ECM containing HA hydrogels improving histological outcomes in rats following a T8 dorsal hemisection SCI. Finally, HA hydrogels were shown to support transplantation of V2a interneurons. This work represents a novel approach to generating an ECM-based material and shows that the effect of

astrocyte ECM on histological outcomes SCI depends on astrocyte phenotype. Further work should focus on determining if the improved histological outcomes results in functional improves, and what proteins within the ECMs result in these observed histological changes.

5.2 Future Directions

5.2.1 Live Astrocyte Transplantation

Based on the results from our ECM transplantation, it would be interesting to explore the potential of live mESC-derived astrocyte transplantation to improve SCI outcomes. Toward this end, we are working toward the generation of a selectable astrocyte cell line uses an astrocyte specific gene, *aqp4*, to drive puromycin resistance expression. This cell line still needs to be further characterized to demonstrate that selection the residual stem cells from the culture so there is no risk of teratomas formation (Johnson et al. 2010), and that the astrocytes functionally mature based on calcium imaging. In addition, calcium imaging can be used to further validate that the mESC-derived astrocyte populations have functional properties consistent with *in vivo* populations. In particular, protoplasmic astrocytes should exhibit gap junction-dependent calcium waves (B. Haas et al. 2005), while fibrous astrocyte exhibit purinergic receptor-dependent calcium waves (Hamilton et al. 2008). Blocking these signaling pathways and performing calcium imaging in the cultures should elicit different responses in our mESC-derived astrocyte populations. Since calcium imaging is important for normal astrocyte-neuron interactions, this type of functional assay would be important to show to indicate that we have functionally mature astrocytes. Once selection has been accomplished, and validated, it would be interesting to transplant purified protoplasmic astrocytes in HA hydrogels and compare to results to the HA + P-ECM data reported in this work to see how much of the live cell transplant effect is captured by implanting the ECM alone.

5.2.2 Engineered ECMs

The proteomics data collected in this work shows the composition of both P-ECM and F-ECM. We did perform some validation experiments in this work that showed the importance of spondin-1 as an inhibitory component of the fibrous ECMs, and laminin α5 and laminin β1 as a permissive component of the protoplasmic ECM; however, further work is required to better define what elements in these ECMs cause the observed differences in neuronal growth and *in vivo* effects. Based on these future studies, and the data presented here, it would be potentially interesting to explore adding a small number of specific proteins to the HA hydrogels and determining if these hydrogels can replicate the effect of the full ECM implant. In addition to adding specific proteins, it could be also productive to add small peptides that contain the binding sequencing of the ECM proteins and cell surface proteins. This type of peptide implantation has been done in SCI treatment using integrin binding peptides with some success (Tysseling-Mattiace et al. 2008; Pan et al. 2014). I think that one particularly interesting peptide sequence to explore is the binding sequence of the neural cell adhesion molecule (NCAM) (Neiiendam et al. 2004). By incorporating this peptide sequence, it may be possible to capture some of the benefits observed when the neurons were grown on frozen astrocyte substrates because NCAM is a major astrocyte membrane component. In this way, the NCAM peptide could be used to increase the benefits of P-ECM implantation without adding any elements that require immunosuppression of the host. Overall the combination of pure proteins and binding peptide offers an exciting and controlled method to generate materials for the treatment of SCI.

5.2.3 Functional Recovery from SCI following P-ECM and/or V2a Interneuron Transplantation

We collected some encouraging data showing histological recovery in rats in response to transplant of either P-ECM or V2a Interneurons in a HA hydrogel. While the 2 week study

showing these results suggests that the materials developed in this work are worth pursuing further, it is important to test if any functional recovery occurs in the 8 weeks post transplantation of, in particular, the HA + Cells + P-ECM and HA + P-ECM gels. For the T8 dorsal hemisection model used in this work, functional recovery measurement is most appropriately accomplished with the Basso, Beattie and Bresnahan (BBB) open-field locomotor scale (Basso, Beattie, and Bresnahan 1995), horizontal ladder test, von Frey hair sensory test, and an incline plane test. This set of functional assays will allow for assessment of locomotor recovery, sensory recovery in the hind limbs, stability, and coordination. It would also be interesting to perform some tract tracing experiments following a longer recovery period to determine if the transplanted V2a interneurons are integrating into the host spinal cord. Overall, I believe that P-ECM represents an exciting, multifactorial treatment for SCI and I look forward to seeing what else can be done with these P-ECM:HA hydrogels.

References

Allodi, Ilary, Vasil Mecollari, Francisco González-Pérez, Ruben Eggers, Stefan Hoyng, Joost Verhaagen, Xavier Navarro, and Esther Udina. 2014. "Schwann Cells Transduced with a Lentiviral Vector Encoding Fgf-2 Promote Motor Neuron Regeneration Following Sciatic Nerve Injury." *Glia* 62 (10): 1736–46. doi:10.1002/glia.22712.

Altinova, Haktan, Sven Möllers, Tobias Führmann, Ronald Deumens, Ahmet Bozkurt, Ingo Heschel, Leon H.H. Olde Damink, Frank Schügner, Joachim Weis, and Gary A. Brook. 2014. "Functional Improvement Following Implantation of a Microstructured, Type-I Collagen Scaffold into Experimental Injuries of the Adult Rat Spinal Cord." *Brain Research* 1585 (October): 37–50. doi:10.1016/j.brainres.2014.08.041.

Anderson, Mark A., Joshua E. Burda, Yilong Ren, Yan Ao, Timothy M. O'Shea, Riki Kawaguchi, Giovanni Coppola, Baljit S. Khakh, Timothy J. Deming, and Michael V. Sofroniew. 2016. "Astrocyte Scar Formation Aids Central Nervous System Axon Regeneration." *Nature* 532 (7598): 195–200. doi:10.1038/nature17623.

Apostolova, Ivayla, Andrey Irintchev, and Melitta Schachner. 2006. "Tenascin-R Restricts Posttraumatic Remodeling of Motoneuron Innervation and Functional Recovery after Spinal Cord Injury in Adult Mice." *The Journal of Neuroscience : The Official Journal of the Society for Neuroscience* 26 (30): 7849–59. doi:10.1523/JNEUROSCI.1526-06.2006.

Badylak, Stephen F, Donald O Freytes, and Thomas W Gilbert. 2009. "Extracellular Matrix as a Biological Scaffold Material: Structure and Function." *Acta Biomaterialia* 5 (1): 1–13. doi:10.1016/j.actbio.2008.09.013.

Ballios, Brian G., Michael J. Cooke, Laura Donaldson, Brenda L.K. Coles, Cindi M. Morshead, Derek van der Kooy, and Molly S. Shoichet. 2015. "A Hyaluronan-Based Injectable Hydrogel Improves the Survival and Integration of Stem Cell Progeny Following Transplantation." *Stem Cell Reports* 4 (6). Elsevier: 1031–45. doi:10.1016/j.stemcr.2015.04.008.

Basso, D M, M S Beattie, and J C Bresnahan. 1995. "A Sensitive and Reliable Locomotor Rating Scale for Open Field Testing in Rats." *Journal of Neurotrauma* 12 (1): 1–21. http://www.ncbi.nlm.nih.gov/pubmed/7783230.

Benders, Kim E M, P René van Weeren, Stephen F Badylak, Daniël B F Saris, Wouter J A Dhert, and Jos Malda. 2013. "Extracellular Matrix Scaffolds for Cartilage and Bone Regeneration." *Trends in Biotechnology* 31 (3): 169–76. doi:10.1016/j.tibtech.2012.12.004.

Benveniste, E N, S M Sparacio, J G Norris, H E Grenett, and G M Fuller. 1990. "Induction and Regulation of Interleukin-6 Gene Expression in Rat Astrocytes." *Journal of Neuroimmunology* 30 (2–3): 201–12. http://www.ncbi.nlm.nih.gov/pubmed/2121800.

Benveniste, Ronald J, Gordon Keller, and Isabelle Germano. 2005. "Embryonic Stem Cell-Derived Astrocytes Expressing Drug-Inducible Transgenes: Differentiation and Transplantion into the Mouse Brain." *Journal of Neurosurgery* 103: 115–23.

doi:10.3171/jns.2005.103.1.0115.

Bignami, A, M Hosley, and D Dahl. 1993. "Hyaluronic Acid and Hyaluronic Acid-Binding Proteins in Brain Extracellular Matrix." *Anatomy and Embryology* 188 (5): 419–33. http://www.ncbi.nlm.nih.gov/pubmed/7508695.

Biotherapeutics, Asterias. 2017. "Dose Escalation Study of AST-OPC1 in Spinal Cord Injury - Full Text View - ClinicalTrials.Gov." https://clinicaltrials.gov/ct2/show/NCT02302157.

Biran, Roy, Mark D Noble, and Patrick A Tresco. 2003. "Directed Nerve Outgrowth Is Enhanced by Engineered Glial Substrates." *Experimental Neurology* 184 (1): 141–52. doi:10.1016/S0014-4886(03)00253-X.

Boakye, Maxwell, Barbara C Leigh, and Andrea C Skelly. 2012. "Quality of Life in Persons with Spinal Cord Injury: Comparisons with Other Populations." *Journal of Neurosurgery. Spine* 17 (1 Suppl): 29–37. doi:10.3171/2012.6.AOSPINE1252.

Bradbury, Elizabeth J, Lawrence D F Moon, Reena J Popat, Von R King, Gavin S Bennett, Preena N Patel, James W Fawcett, and Stephen B McMahon. 2002. "Chondroitinase ABC Promotes Functional Recovery after Spinal Cord Injury." *Nature* 416 (6881): 636–40. doi:10.1038/416636a.

Brook, G.A., D. Plate, R. Franzen, D. Martin, G. Moonen, J. Schoenen, A.B. Schmitt, J. Noth, and W. Nacimiento. 1998. "Spontaneous Longitudinally Orientated Axonal Regeneration Is Associated with the Schwann Cell Framework within the Lesion Site Following Spinal Cord Compression Injury of the Rat." *Journal of Neuroscience Research* 53 (1). John Wiley & Sons, Inc.: 51–65. doi:10.1002/(SICI)1097-4547(19980701)53:1<51::AID-JNR6>3.0.CO;2-I.

Brown, Chelsea R, Jessica C Butts, Dylan A McCreedy, and Shelly E Sakiyama-Elbert. 2014. "Generation of V2a Interneurons from Mouse Embryonic Stem Cells." *Stem Cells and Development* 23 (15). Mary Ann Liebert, Inc. 140 Huguenot Street, 3rd Floor New Rochelle, NY 10801 USA: 1765–76. doi:10.1089/scd.2013.0628.

Brunne, Bianka, Shanting Zhao, Amin Derouiche, Joachim Herz, Petra May, Michael Frotscher, and Hans H Bock. 2010. "Origin, Maturation, and Astroglial Transformation of Secondary Radial Glial Cells in the Developing Dentate Gyrus." *Glia* 58 (13). NIH Public Access: 1553–69. doi:10.1002/glia.21029.

Bsibsi, Malika, Rivka Ravid, Djordje Gveric, and Johannes M van Noort. 2002. "Broad Expression of Toll-like Receptors in the Human Central Nervous System." *Journal of Neuropathology and Experimental Neurology* 61 (11): 1013–21. http://www.ncbi.nlm.nih.gov/pubmed/12430718.

Bui, Tuan V, Nicolas Stifani, Turgay Akay, and Robert M Brownstone. 2016. "Spinal Microcircuits Comprising DI3 Interneurons Are Necessary for Motor Functional Recovery Following Spinal Cord Transection." *ELife* 5 (December). doi:10.7554/eLife.21715.

Bunge, Mary Bartlett. 2016. "Efficacy of Schwann Cell Transplantation for Spinal Cord Repair

Is Improved with Combinatorial Strategies." *The Journal of Physiology* 594 (13): 3533–38. doi:10.1113/JP271531.

Burstyn-Cohen, Tal, Vered Tzarfaty, Ayala Frumkin, Yael Feinstein, Esther Stoeckli, and Avihu Klar. 1999. "F-Spondin Is Required for Accurate Pathfinding of Commissural Axons at the Floor Plate." *Neuron* 23 (2): 233–46. doi:10.1016/S0896-6273(00)80776-X.

Bush, T G, T C Savidge, T C Freeman, H J Cox, E A Campbell, L Mucke, M H Johnson, and M V Sofroniew. 1998. "Fulminant Jejuno-Ileitis Following Ablation of Enteric Glia in Adult Transgenic Mice." *Cell* 93 (2): 189–201. http://www.ncbi.nlm.nih.gov/pubmed/9568712.

Byrnes, Kimberly R., Stanley T. Fricke, and Alan I. Faden. 2010. "Neuropathological Differences between Rats and Mice after Spinal Cord Injury." *Journal of Magnetic Resonance Imaging* 32 (4): 836–46. doi:10.1002/jmri.22323.

Cahoy, John D, Ben Emery, Amit Kaushal, Lynette C Foo, Jennifer L Zamanian, Karen S Christopherson, Yi Xing, et al. 2008. "A Transcriptome Database for Astrocytes, Neurons, and Oligodendrocytes: A New Resource for Understanding Brain Development and Function." *The Journal of Neuroscience : The Official Journal of the Society for Neuroscience* 28 (1): 264–78. doi:10.1523/JNEUROSCI.4178-07.2008.

Cao, Q., Q. He, Y. Wang, X. Cheng, R. M. Howard, Y. Zhang, W. H. DeVries, et al. 2010. "Transplantation of Ciliary Neurotrophic Factor-Expressing Adult Oligodendrocyte Precursor Cells Promotes Remyelination and Functional Recovery after SpinalCord Injury." *Journal of Neuroscience* 30 (8). NIH Public Access: 2989–3001. doi:10.1523/JNEUROSCI.3174-09.2010.

Caroni, P, and M E Schwab. 1988. "Antibody against Myelin-Associated Inhibitor of Neurite Growth Neutralizes Nonpermissive Substrate Properties of CNS White Matter." *Neuron* 1 (1): 85–96. http://www.ncbi.nlm.nih.gov/pubmed/3272156.

Cassiani-Ingoni, Riccardo, Turhan Coksaygan, Haipeng Xue, Susan A Reichert-Scrivner, Heinz Wiendl, Mahendra S Rao, and Tim Magnus. 2006. "Cytoplasmic Translocation of Olig2 in Adult Glial Progenitors Marks the Generation of Reactive Astrocytes Following Autoimmune Inflammation." *Experimental Neurology* 201 (2): 349–58. doi:10.1016/j.expneurol.2006.04.030.

Chedly, Jamila, Sylvia Soares, Alexandra Montembault, Ysander von Boxberg, Michèle Veron-Ravaille, Christine Mouffle, Marie-Noelle Benassy, Jacques Taxi, Laurent David, and Fatiha Nothias. 2017. "Physical Chitosan Microhydrogels as Scaffolds for Spinal Cord Injury Restoration and Axon Regeneration." *Biomaterials* 138 (September): 91–107. doi:10.1016/j.biomaterials.2017.05.024.

Chen, Zi-Wei, Karoline Fuchs, Werner Sieghart, R Reid Townsend, and Alex S Evers. 2012. "Deep Amino Acid Sequencing of Native Brain GABAA Receptors Using High-Resolution Mass Spectrometry." *Molecular & Cellular Proteomics : MCP* 11 (1): M111.011445. http://www.ncbi.nlm.nih.gov/pubmed/22338125.

Chu, Tianci, Hengxing Zhou, Fuyuan Li, Tianyi Wang, Lu Lu, and Shiqing Feng. 2014.

"Astrocyte Transplantation for Spinal Cord Injury: Current Status and Perspective." *Brain Research Bulletin* 107: 18–30. doi:10.1016/j.brainresbull.2014.05.003.

Church, Jamie S., Lindsay M. Milich, Jessica K. Lerch, Phillip G. Popovich, and Dana M. McTigue. 2017. "E6020, a Synthetic TLR4 Agonist, Accelerates Myelin Debris Clearance, Schwann Cell Infiltration, and Remyelination in the Rat Spinal Cord." *Glia* 65 (6): 883–99. doi:10.1002/glia.23132.

Cloutier, Frank, Tomas Kalincik, Jenny Lauschke, Gervase Tuxworth, Brenton Cavanagh, Adrian Meedeniya, Alan Mackay-Sim, Pascal Carrive, and Phil Waite. 2016. "Olfactory Ensheathing Cells but Not Fibroblasts Reduce the Duration of Autonomic Dysreflexia in Spinal Cord Injured Rats." *Autonomic Neuroscience* 201 (December): 17–23. doi:10.1016/j.autneu.2016.08.015.

Codeluppi, Simone, Teresa Fernandez-Zafra, Katalin Sandor, Jacob Kjell, Qingsong Liu, Mathew Abrams, Lars Olson, Nathanael S Gray, Camilla I Svensson, and Per Uhlén. 2014. "Interleukin-6 Secretion by Astrocytes Is Dynamically Regulated by PI3K-MTOR-Calcium Signaling." *PloS One* 9 (3). Public Library of Science: e92649. doi:10.1371/journal.pone.0092649.

Cong, L., F. A. Ran, D. Cox, S. Lin, R. Barretto, N. Habib, P. D. Hsu, et al. 2013. "Multiplex Genome Engineering Using CRISPR/Cas Systems." *Science* 339 (6121): 819–23. doi:10.1126/science.1231143.

Corey, Joseph M., David Y. Lin, Katherine B. Mycek, Qiaoran Chen, Stanley Samuel, Eva L. Feldman, and David C. Martin. 2007. "Aligned Electrospun Nanofibers Specify the Direction of Dorsal Root Ganglia Neurite Growth." *Journal of Biomedical Materials Research Part A* 83A (3). Wiley Subscription Services, Inc., A Wiley Company: 636–45. doi:10.1002/jbm.a.31285.

Courtine, Gregoire, Bingbing Song, Roland R Roy, Hui Zhong, Julia E Herrmann, Yan Ao, Jingwei Qi, V Reggie Edgerton, and Michael V Sofroniew. 2008. "Recovery of Supraspinal Control of Stepping via Indirect Propriospinal Relay Connections after Spinal Cord Injury." *Nature Medicine* 14 (1): 69–74. doi:10.1038/nm1682.

Crapo, Peter M., Christopher J. Medberry, Janet E. Reing, Stephen Tottey, Yolandi van der Merwe, Kristen E. Jones, and Stephen F. Badylak. 2012. "Biologic Scaffolds Composed of Central Nervous System Extracellular Matrix." *Biomaterials* 33 (13). NIH Public Access: 3539–47. doi:10.1016/j.biomaterials.2012.01.044.

Cregg, Jared M, Marc A DePaul, Angela R Filous, Bradley T Lang, Amanda Tran, and Jerry Silver. 2014. "Functional Regeneration beyond the Glial Scar." *Experimental Neurology* 253 (March): 197–207. doi:10.1016/j.expneurol.2013.12.024.

Crone, S. A., J.-C. Viemari, S. Droho, A. Mrejeru, J.-M. Ramirez, and K. Sharma. 2012. "Irregular Breathing in Mice Following Genetic Ablation of V2a Neurons." *Journal of Neuroscience* 32 (23): 7895–7906. doi:10.1523/JNEUROSCI.0445-12.2012.

Crone, S. A., G. Zhong, R. Harris-Warrick, and K. Sharma. 2009. "In Mice Lacking V2a

Interneurons, Gait Depends on Speed of Locomotion." *Journal of Neuroscience* 29 (21): 7098–7109. doi:10.1523/JNEUROSCI.1206-09.2009.

Crone, Steven A., Katharina A. Quinlan, Laskaro Zagoraiou, Steven Droho, Carlos Ernesto Restrepo, Line Lundfald, Toshiaki Endo, et al. 2008. "Genetic Ablation of V2a Ipsilateral Interneurons Disrupts Left-Right Locomotor Coordination in Mammalian Spinal Cord." *Neuron* 60 (1): 70–83. doi:10.1016/j.neuron.2008.08.009.

Davies, Jeannette E, Carol Huang, Christoph Proschel, Mark Noble, Margot Mayer-Proschel, and Stephen J A Davies. 2006. "Astrocytes Derived from Glial-Restricted Precursors Promote Spinal Cord Repair." *Journal of Biology* 5 (3): 7.

Davies, Jeannette E, Christoph Pröschel, Ningzhe Zhang, Mark Noble, Margot Mayer-Pröschel, and Stephen J A Davies. 2008. "Transplanted Astrocytes Derived from BMP- or CNTF-Treated Glial-Restricted Precursors Have Opposite Effects on Recovery and Allodynia after Spinal Cord Injury." *Journal of Biology* 7 (7): 24. doi:10.1186/jbiol85.

Davies, Stephen J A, Chung-Hsuan Shih, Mark Noble, Margot Mayer-Proschel, Jeannette E Davies, and Christoph Proschel. 2011. "Transplantation of Specific Human Astrocytes Promotes Functional Recovery after Spinal Cord Injury." *PloS One* 6 (3): e17328. doi:10.1371/journal.pone.0017328.

Deloulme, Jean Christophe, Eric Raponi, Benoît Jean Gentil, Nathalie Bertacchi, Alexander Marks, Gérard Labourdette, and Jacques Baudier. 2004. "Nuclear Expression of S100B in Oligodendrocyte Progenitor Cells Correlates with Differentiation toward the Oligodendroglial Lineage and Modulates Oligodendrocytes Maturation." *Molecular and Cellular Neurosciences* 27 (4): 453–65. doi:10.1016/j.mcn.2004.07.008.

Donoghue, Peter S, Rebecca Lamond, Stephanie D Boomkamp, Tao Sun, Nikolaj Gadegaard, Mathis O Riehle, and Susan C Barnett. 2013. "The Development of a E-Polycaprolactone Scaffold for Central Nervous System Repair." *Tissue Engineering Part A* 19 (3–4): 497–507. doi:10.1089/ten.tea.2012.0382.

Dougherty, Joseph D, Eric F Schmidt, Miho Nakajima, and Nathaniel Heintz. 2010. "Analytical Approaches to RNA Profiling Data for the Identification of Genes Enriched in Specific Cells." *Nucleic Acids Research* 38 (13): 4218–30. doi:10.1093/nar/gkq130.

Dougherty, K. J., and O. Kiehn. 2010. "Firing and Cellular Properties of V2a Interneurons in the Rodent Spinal Cord." *Journal of Neuroscience* 30 (1): 24–37. doi:10.1523/JNEUROSCI.4821-09.2010.

Doyle, Joseph P., Joseph D. Dougherty, Myriam Heiman, Eric F. Schmidt, Tanya R. Stevens, Guojun Ma, Sujata Bupp, et al. 2008. "Application of a Translational Profiling Approach for the Comparative Analysis of CNS Cell Types." *Cell* 135 (4): 749–62. doi:10.1016/j.cell.2008.10.029.

Du, Bao-ling, Chen-guang Zeng, Wei Zhang, Da-ping Quan, Eng-ang Ling, and Yuan-shan Zeng. 2014. "A Comparative Study of Gelatin Sponge Scaffolds and PLGA Scaffolds Transplanted to Completely Transected Spinal Cord of Rat." *Journal of Biomedical*

Materials Research Part A 102 (6): 1715–25. doi:10.1002/jbm.a.34835.

Dziki, Jenna L., Luai Huleihel, Michelle E. Scarritt, and Stephen F. Badylak. 2017. "Extracellular Matrix Bioscaffolds as Immunomodulatory Biomaterials." *Tissue Engineering Part A*, May, ten.tea.2016.0538. doi:10.1089/ten.tea.2016.0538.

East, Emma, Daniela Blum de Oliveira, Jon P. Golding, and James B. Phillips. 2010. "Alignment of Astrocytes Increases Neuronal Growth in Three-Dimensional Collagen Gels and Is Maintained Following Plastic Compression to Form a Spinal Cord Repair Conduit." *Tissue Engineering Part A* 16 (10): 3173–84. doi:10.1089/ten.tea.2010.0017.

Eaton, Mary J, Stacey Quintero Wolfe, Miguel Martinez, Massiel Hernandez, Cassandra Furst, Jian Huang, Beata R Frydel, and Orlando Gómez-Marín. 2007. "Subarachnoid Transplant of a Human Neuronal Cell Line Attenuates Chronic Allodynia and Hyperalgesia after Excitotoxic Spinal Cord Injury in the Rat." *The Journal of Pain : Official Journal of the American Pain Society* 8 (1): 33–50. doi:10.1016/j.jpain.2006.05.013.

Erceg, Slaven, Mohammad Ronaghi, Marc Oria, Mireia García Roselló, Maria Amparo Pérez Aragó, Maria Gomez Lopez, Ivana Radojevic, et al. 2010. "Transplanted Oligodendrocytes and Motoneuron Progenitors Generated from Human Embryonic Stem Cells Promote Locomotor Recovery after Spinal Cord Transection." *Stem Cells (Dayton, Ohio)* 28 (9): 1541–49. doi:10.1002/stem.489.

Etlin, Alex, Joao M. Bráz, Julia A. Kuhn, Xidao Wang, Katherine A. Hamel, Ida J. Llewellyn-Smith, and Allan I. Basbaum. 2016. "Functional Synaptic Integration of Forebrain GABAergic Precursors into the Adult Spinal Cord." *The Journal of Neuroscience* 36 (46): 11634–45. doi:10.1523/JNEUROSCI.2301-16.2016.

Fam, Sami R., Conor J. Gallagher, and Michael W. Salter. 2000. "P2Y1 Purinoceptor-Mediated Ca2+ Signaling and Ca2+ Wave Propagation in Dorsal Spinal Cord Astrocytes." *Journal of Neuroscience* 20 (8). http://www.jneurosci.org/content/20/8/2800.long.

Fandel, Thomas M., Alpa Trivedi, Cory R. Nicholas, Haoqian Zhang, Jiadong Chen, Aida F. Martinez, Linda J. Noble-Haeusslein, and Arnold R. Kriegstein. 2016. "Transplanted Human Stem Cell-Derived Interneuron Precursors Mitigate Mouse Bladder Dysfunction and Central Neuropathic Pain after Spinal Cord Injury." *Cell Stem Cell* 19 (4): 544–57. doi:10.1016/j.stem.2016.08.020.

Faulkner, Jill, and Hans S. Keirstead. 2005. "Human Embryonic Stem Cell-Derived Oligodendrocyte Progenitors for the Treatment of Spinal Cord Injury." *Transplant Immunology* 15 (2): 131–42. doi:10.1016/j.trim.2005.09.007.

Faulkner, Jill R, Julia E Herrmann, Michael J Woo, Keith E Tansey, Ngan B Doan, and Michael V Sofroniew. 2004. "Reactive Astrocytes Protect Tissue and Preserve Function after Spinal Cord Injury." *The Journal of Neuroscience : The Official Journal of the Society for Neuroscience* 24 (9): 2143–55. doi:10.1523/JNEUROSCI.3547-03.2004.

Führmann, T., R.Y. Tam, B. Ballarin, B. Coles, I. Elliott Donaghue, D. van der Kooy, A. Nagy, C.H. Tator, C.M. Morshead, and M.S. Shoichet. 2016. "Injectable Hydrogel Promotes Early

Survival of Induced Pluripotent Stem Cell-Derived Oligodendrocytes and Attenuates Longterm Teratoma Formation in a Spinal Cord Injury Model." *Biomaterials* 83 (March): 23–36. doi:10.1016/j.biomaterials.2015.12.032.

Führmann, T, J Obermeyer, C H Tator, and M S Shoichet. 2015. "Click-Crosslinked Injectable Hyaluronic Acid Hydrogel Is Safe and Biocompatible in the Intrathecal Space for Ultimate Use in Regenerative Strategies of the Injured Spinal Cord." *Methods (San Diego, Calif.)* 84 (August): 60–69. doi:10.1016/j.ymeth.2015.03.023.

Gaffey, Ann C., Minna H. Chen, Chantel M. Venkataraman, Alen Trubelja, Christopher B. Rodell, Patrick V. Dinh, George Hung, et al. 2015. "Injectable Shear-Thinning Hydrogels Used to Deliver Endothelial Progenitor Cells, Enhance Cell Engraftment, and Improve Ischemic Myocardium." *The Journal of Thoracic and Cardiovascular Surgery* 150 (5): 1268–77. doi:10.1016/j.jtcvs.2015.07.035.

Gensert, JoAnn M, and James E Goldman. 1997. "Endogenous Progenitors Remyelinate Demyelinated Axons in the Adult CNS." *Neuron* 19 (1): 197–203. doi:10.1016/S0896-6273(00)80359-1.

Ghuman, Harmanvir, Andre R. Massensini, Julia Donnelly, Sung-Min Kim, Christopher J. Medberry, Stephen F. Badylak, and Michel Modo. 2016a. "ECM Hydrogel for the Treatment of Stroke: Characterization of the Host Cell Infiltrate." *Biomaterials* 91 (June): 166–81. doi:10.1016/j.biomaterials.2016.03.014.

———. 2016b. "ECM Hydrogel for the Treatment of Stroke: Characterization of the Host Cell Infiltrate." *Biomaterials* 91 (June): 166–81. doi:10.1016/j.biomaterials.2016.03.014.

Goldshmit, Y., F. Frisca, J. Kaslin, A.R. Pinto, J.-K.K.Y. Tang, A. Pébay, R. Pinkas-Kramarski, and P.D. Currie. 2015. "Decreased Anti-Regenerative Effects after Spinal Cord Injury in Spry4−/− Mice." *Neuroscience* 287 (February): 104–12. doi:10.1016/j.neuroscience.2014.12.020.

Goldshmit, Yona, Frisca Frisca, Alexander R Pinto, Alice Pébay, Jean-Kitty K Y Tang, Ashley L Siegel, Jan Kaslin, and Peter D Currie. 2014. "Fgf2 Improves Functional Recovery-Decreasing Gliosis and Increasing Radial Glia and Neural Progenitor Cells after Spinal Cord Injury." *Brain and Behavior* 4 (2): 187–200. doi:10.1002/brb3.172.

Goldshmit, Yona, Tamar E. Sztal, Patricia R. Jusuf, Thomas E. Hall, Mai Nguyen-Chi, and Peter D. Currie. 2012. "Fgf-Dependent Glial Cell Bridges Facilitate Spinal Cord Regeneration in Zebrafish." *The Journal of Neuroscience : The Official Journal of the Society for Neuroscience* 32 (22). Society for Neuroscience: 7477–92. doi:10.1523/JNEUROSCI.0758-12.2012.

Goursaud, Stéphanie, Elena N Kozlova, Jean-Marie Maloteaux, and Emmanuel Hermans. 2009. "Cultured Astrocytes Derived from Corpus Callosum or Cortical Grey Matter Show Distinct Glutamate Handling Properties." *Journal of Neurochemistry* 108 (6): 1442–52. doi:10.1111/j.1471-4159.2009.05889.x.

Gupta, Dimpy, Charles H. Tator, and Molly S. Shoichet. 2006. "Fast-Gelling Injectable Blend of

Hyaluronan and Methylcellulose for Intrathecal, Localized Delivery to the Injured Spinal Cord." *Biomaterials* 27 (11): 2370–79. doi:10.1016/j.biomaterials.2005.11.015.

Haas, B., Carola G. Schipke, Oliver Peters, Goran Söhl, Klaus Willecke, and Helmut Kettenmann. 2005. "Activity-Dependent ATP-Waves in the Mouse Neocortex Are Independent from Astrocytic Calcium Waves." *Cerebral Cortex* 16 (2). Oxford University Press: 237–46. doi:10.1093/cercor/bhi101.

Haas, Christopher, Birgit Neuhuber, Takaya Yamagami, Mahendra Rao, and Itzhak Fischer. 2012. "Phenotypic Analysis of Astrocytes Derived from Glial Restricted Precursors and Their Impact on Axon Regeneration." *Experimental Neurology* 233 (2). NIH Public Access: 717–32. doi:10.1016/j.expneurol.2011.11.002.

Hachem, S., A. Aguirre, V. Vives, A. Marks, V. Gallo, and C. Legraverend. 2005. "Spatial and Temporal Expression of S100B in Cells of Oligodendrocyte Lineage." *Glia* 51 (2): 81–97. doi:10.1002/glia.20184.

Haggerty, Agnes E, Megan M Marlow, and Martin Oudega. 2017. "Extracellular Matrix Components as Therapeutics for Spinal Cord Injury." *Neuroscience Letters* 652: 50–55. doi:10.1016/j.neulet.2016.09.053.

Hakim, Jeffrey S, Melika Esmaeili Rad, Peter J Grahn, Bingkun K Chen, Andrew M Knight, Ann M Schmeichel, Nasro A Isaq, Mahrokh Dadsetan, Michael J Yaszemski, and Anthony J Windebank. 2015. "Positively Charged Oligo[Poly(Ethylene Glycol) Fumarate] Scaffold Implantation Results in a Permissive Lesion Environment after Spinal Cord Injury in Rat." *Tissue Engineering. Part A* 21 (13–14): 2099–2114. doi:10.1089/ten.TEA.2015.0019.

Hamilton, Nicola, Steven Vayro, Frank Kirchhoff, Alexej Verkhratsky, Jon Robbins, Dariuz C. Gorecki, and Arthur M. Butt. 2008. "Mechanisms of ATP- and Glutamate-Mediated Calcium Signaling in White Matter Astrocytes." *Glia* 56 (7). Wiley Subscription Services, Inc., A Wiley Company: 734–49. doi:10.1002/glia.20649.

Hapach, Lauren A, Jacob A VanderBurgh, Joseph P Miller, and Cynthia A Reinhart-King. 2015. "Manipulation of in Vitro Collagen Matrix Architecture for Scaffolds of Improved Physiological Relevance." *Physical Biology* 12 (6): 061002. doi:10.1088/1478-3975/12/6/061002.

Hara, Masamitsu, Kazu Kobayakawa, Yasuyuki Ohkawa, Hiromi Kumamaru, Kazuya Yokota, Takeyuki Saito, Ken Kijima, et al. 2017. "Interaction of Reactive Astrocytes with Type I Collagen Induces Astrocytic Scar Formation through the Integrin–N-Cadherin Pathway after Spinal Cord Injury." *Nature Medicine* 23 (7): 818–28. doi:10.1038/nm.4354.

Hatch, B B, C M Wood-Wentz, T M Therneau, M G Walker, J M Payne, and R K Reeves. 2017. "Factors Predictive of Survival and Estimated Years of Life Lost in the Decade Following Nontraumatic and Traumatic Spinal Cord Injury." *Spinal Cord*, February. doi:10.1038/sc.2016.182.

Herrmann, Julia E, Tetsuya Imura, Bingbing Song, Jingwei Qi, Yan Ao, Thu K Nguyen, Rose A Korsak, Kiyoshi Takeda, Shizuo Akira, and Michael V Sofroniew. 2008. "STAT3 Is a

Critical Regulator of Astrogliosis and Scar Formation after Spinal Cord Injury." *The Journal of Neuroscience : The Official Journal of the Society for Neuroscience* 28 (28). NIH Public Access: 7231–43. doi:10.1523/JNEUROSCI.1709-08.2008.

Hershkoviz, R, I Goldkorn, and O Lider. 1995. "Tumour Necrosis Factor-Alpha Interacts with Laminin and Functions as a pro-Adhesive Cytokine." *Immunology* 85 (1): 125–30. http://www.ncbi.nlm.nih.gov/pubmed/7635514.

Hoban, Deirdre B., Ben Newland, Teresa C. Moloney, Linda Howard, Abhay Pandit, and Eilís Dowd. 2013. "The Reduction in Immunogenicity of Neurotrophin Overexpressing Stem Cells after Intra-Striatal Transplantation by Encapsulation in an in Situ Gelling Collagen Hydrogel." *Biomaterials* 34 (37): 9420–29. doi:10.1016/j.biomaterials.2013.08.073.

Holland, E C. 2001. "Gliomagenesis: Genetic Alterations and Mouse Models." *Nature Reviews. Genetics* 2 (2): 120–29. doi:10.1038/35052535.

Horn, Eric M, Michael Beaumont, Xiao Zheng Shu, Adrian Harvey, Glenn D Prestwich, Kris M Horn, Alan R Gibson, Mark C Preul, and Alyssa Panitch. 2007. "Influence of Cross-Linked Hyaluronic Acid Hydrogels on Neurite Outgrowth and Recovery from Spinal Cord Injury." *Journal of Neurosurgery. Spine* 6 (2): 133–40. doi:10.3171/spi.2007.6.2.133.

Hsiao, Tony W., Patrick A. Tresco, and Vladimir Hlady. 2015. "Astrocytes Alignment and Reactivity on Collagen Hydrogels Patterned with ECM Proteins." *Biomaterials* 39 (January): 124–30. doi:10.1016/j.biomaterials.2014.10.062.

Hudson, Terry W, Stephen Y Liu, and Christine E Schmidt. 2004. "Engineering an Improved Acellular Nerve Graft via Optimized Chemical Processing." *Tissue Engineering* 10: 1346–58. doi:10.1089/ten.2004.10.1346.

Hudson, Terry W, Scott Zawko, Curt Deister, Scott Lundy, Char Y Hu, Kate Lee, and Christine E Schmidt. "Optimized Acellular Nerve Graft Is Immunologically Tolerated and Supports Regeneration." *Tissue Engineering* 10 (11–12): 1641–51. doi:10.1089/ten.2004.10.1641.

Isaacs, Jonathan. 2013. "Major Peripheral Nerve Injuries." *Hand Clinics* 29 (3): 371–82. doi:10.1016/j.hcl.2013.04.006.

Iyer, Nisha R, James E Huettner, Jessica C Butts, Chelsea R Brown, and Shelly E Sakiyama-Elbert. 2016. "Generation of Highly Enriched V2a Interneurons from Mouse Embryonic Stem Cells." *Experimental Neurology* 277 (March): 305–16. doi:10.1016/j.expneurol.2016.01.011.

Iyer, Nisha R, Thomas S Wilems, and Shelly E Sakiyama-Elbert. 2016. "Stem Cells for Spinal Cord Injury: Strategies to Inform Differentiation and Transplantation." *Biotechnology and Bioengineering*, August. doi:10.1002/bit.26074.

Jackson, Cheryl A., Jeffery Messinger, Jean D. Peduzzi, David C. Ansardi, and Casey D. Morrow. 2005. "Enhanced Functional Recovery from Spinal Cord Injury Following Intrathecal or Intramuscular Administration of Poliovirus Replicons Encoding IL-10." *Virology* 336 (2): 173–83. doi:10.1016/j.virol.2005.03.025.

Jin, Xuemei, and Toshihide Yamashita. 2016. "Microglia in Central Nervous System Repair after Injury." *Journal of Biochemistry* 159 (5): 491–96. doi:10.1093/jb/mvw009.

Jin, Y, J Bouyer, J S Shumsky, C Haas, and I Fischer. 2016. "Transplantation of Neural Progenitor Cells in Chronic Spinal Cord Injury." *Neuroscience* 320 (April): 69–82. doi:10.1016/j.neuroscience.2016.01.066.

Jin, Ying, Karna Sura, and Itzhak Fischer. 2012. "Differential Effects of Distinct Central Nervous System Regions on Cell Migration and Axonal Extension of Neural Precursor Transplants." *Journal of Neuroscience Research* 90 (11): 2065–73. doi:10.1002/jnr.23099.

Johnson, Philip J., Stanley R. Parker, and Shelly E. Sakiyama-Elbert. 2010. "Fibrin-Based Tissue Engineering Scaffolds Enhance Neural Fiber Sprouting and Delay the Accumulation of Reactive Astrocytes at the Lesion in a Subacute Model of Spinal Cord Injury." *Journal of Biomedical Materials Research Part A* 92A (1): 152–63. doi:10.1002/jbm.a.32343.

Johnson, Philip J, Stanley R Parker, and Shelly E Sakiyama-Elbert. 2009. "Controlled Release of Neurotrophin-3 from Fibrin-Based Tissue Engineering Scaffolds Enhances Neural Fiber Sprouting Following Subacute Spinal Cord Injury." *Biotechnology and Bioengineering* 104 (6): 1207–14. doi:10.1002/bit.22476.

Johnson, Philip J, Alexander Tatara, Dylan A McCreedy, Alicia Shiu, and Shelly E Sakiyama-Elbert. 2010. "Tissue-Engineered Fibrin Scaffolds Containing Neural Progenitors Enhance Functional Recovery in a Subacute Model of SCI." *Soft Matter* 6 (20): 5127–37. doi:10.1039/c0sm00173b.

Kaneko, Ai, Akira Matsushita, and Yoshiyuki Sankai. 2015. "A 3D Nanofibrous Hydrogel and Collagen Sponge Scaffold Promotes Locomotor Functional Recovery, Spinal Repair, and Neuronal Regeneration after Complete Transection of the Spinal Cord in Adult Rats." *Biomedical Materials (Bristol, England)* 10 (1): 015008. doi:10.1088/1748-6041/10/1/015008.

Kawabata, Soya, Morito Takano, Yuko Numasawa-Kuroiwa, Go Itakura, Yoshiomi Kobayashi, Yuichiro Nishiyama, Keiko Sugai, et al. 2016. "Grafted Human IPS Cell-Derived Oligodendrocyte Precursor Cells Contribute to Robust Remyelination of Demyelinated Axons after Spinal Cord Injury." *Stem Cell Reports* 6 (1): 1–8. doi:10.1016/j.stemcr.2015.11.013.

Keirstead, H S, and W F Blakemore. 1997. "Identification of Post-Mitotic Oligodendrocytes Incapable of Remyelination within the Demyelinated Adult Spinal Cord." *Journal of Neuropathology and Experimental Neurology* 56 (11): 1191–1201. http://www.ncbi.nlm.nih.gov/pubmed/9370229.

Keller, Andrew, Alexey I Nesvizhskii, Eugene Kolker, and Ruedi Aebersold. 2002. "Empirical Statistical Model to Estimate the Accuracy of Peptide Identifications Made by MS/MS and Database Search." *Analytical Chemistry* 74 (20): 5383–92. http://www.ncbi.nlm.nih.gov/pubmed/12403597.

Khaing, Zin Z, Brian D Milman, Jennifer E Vanscoy, Stephanie K Seidlits, Raymond J Grill, and

Christine E Schmidt. 2011. "High Molecular Weight Hyaluronic Acid Limits Astrocyte Activation and Scar Formation after Spinal Cord Injury." *Journal of Neural Engineering* 8 (4): 046033. doi:10.1088/1741-2560/8/4/046033.

Khankan, Rana R, Khris G Griffis, James R Haggerty-Skeans, Hui Zhong, Roland R Roy, V Reggie Edgerton, and Patricia E Phelps. 2016. "Olfactory Ensheathing Cell Transplantation after a Complete Spinal Cord Transection Mediates Neuroprotective and Immunomodulatory Mechanisms to Facilitate Regeneration." *The Journal of Neuroscience : The Official Journal of the Society for Neuroscience* 36 (23): 6269–86. doi:10.1523/JNEUROSCI.0085-16.2016.

Kigerl, K. A., J. C. Gensel, D. P. Ankeny, J. K. Alexander, D. J. Donnelly, and P. G. Popovich. 2009. "Identification of Two Distinct Macrophage Subsets with Divergent Effects Causing Either Neurotoxicity or Regeneration in the Injured Mouse Spinal Cord." *Journal of Neuroscience* 29 (43): 13435–44. doi:10.1523/JNEUROSCI.3257-09.2009.

Kim, Moonhang, So Ra Park, and Byung Hyune Choi. 2014. "Biomaterial Scaffolds Used for the Regeneration of Spinal Cord Injury (SCI)." *Histology and Histopathology* 29 (11): 1395–1408. http://www.ncbi.nlm.nih.gov/pubmed/24831814.

Kim, Young-Tae, Robert W Hitchcock, Michael J Bridge, and Patrick A Tresco. 2004. "Chronic Response of Adult Rat Brain Tissue to Implants Anchored to the Skull." *Biomaterials* 25 (12): 2229–37. http://www.ncbi.nlm.nih.gov/pubmed/14741588.

Kleiderman, Susanne, João V. Sá, Ana P. Teixeira, Catarina Brito, Simon Gutbier, Lars G. Evje, Mussie G. Hadera, et al. 2016. "Functional and Phenotypic Differences of Pure Populations of Stem Cell-Derived Astrocytes and Neuronal Precursor Cells." *Glia* 64 (5): 695–715. doi:10.1002/glia.22954.

Kushchayev, Sergiy V, Morgan B Giers, Doris Hom Eng, Nikolay L Martirosyan, Jennifer M Eschbacher, Martin M Mortazavi, Nicholas Theodore, Alyssa Panitch, and Mark C Preul. 2016. "Hyaluronic Acid Scaffold Has a Neuroprotective Effect in Hemisection Spinal Cord Injury." *Journal of Neurosurgery. Spine* 25 (1): 114–24. doi:10.3171/2015.9.SPINE15628.

Lemons, Michele L., Dena R. Howland, and Douglas K. Anderson. 1999. "Chondroitin Sulfate Proteoglycan Immunoreactivity Increases Following Spinal Cord Injury and Transplantation." *Experimental Neurology* 160 (1): 51–65. doi:10.1006/exnr.1999.7184.

Leung, Y K J, M Pankhurst, S A Dunlop, S Ray, J Dittmann, E D Eaton, P Palumaa, et al. 2009. "Metallothionein Induces a Regenerative Reactive Astrocyte Phenotype via JAK/STAT and RhoA Signalling Pathways." *Experimental Neurology* 221: 98–106. doi:10.1016/j.expneurol.2009.10.006.

Levine, Joel M, Richard Reynolds, and James W Fawcett. 2001. "The Oligodendrocyte Precursor Cell in Health and Disease." *Trends in Neurosciences* 24 (1): 39–47. doi:10.1016/S0166-2236(00)01691-X.

Li, Ke, Elham Javed, Daniel Scura, Tamara J Hala, Suneil Seetharam, Aditi Falnikar, Jean-Philippe Richard, et al. 2015. "Human IPS Cell-Derived Astrocyte Transplants Preserve

Respiratory Function after Spinal Cord Injury." *Experimental Neurology* 271 (September). NIH Public Access: 479–92. doi:10.1016/j.expneurol.2015.07.020.

Li, Xiaoran, Zhifeng Xiao, Jin Han, Lei Chen, Hanshan Xiao, Fukai Ma, Xianglin Hou, et al. 2013. "Promotion of Neuronal Differentiation of Neural Progenitor Cells by Using EGFR Antibody Functionalized Collagen Scaffolds for Spinal Cord Injury Repair." *Biomaterials* 34 (21): 5107–16. doi:10.1016/j.biomaterials.2013.03.062.

Liddelow, Shane A., and Ben A. Barres. 2017. "Reactive Astrocytes: Production, Function, and Therapeutic Potential." *Immunity* 46 (6): 957–67. doi:10.1016/j.immuni.2017.06.006.

Liesi, Päivi, Thomas Kirkwood, and Antti Vaheri. 1986. "Fibronectin Is Expressed by Astrocytes Cultured from Embryonic and Early Postnatal Rat Brain." *Experimental Cell Research* 163 (1): 175–85. doi:10.1016/0014-4827(86)90570-7.

Liu, Ting, John D Houle, Jinye Xu, Barbara P Chan, and Sing Yian Chew. 2012. "Nanofibrous Collagen Nerve Conduits for Spinal Cord Repair." *Tissue Engineering. Part A* 18 (9–10). Mary Ann Liebert, Inc.: 1057–66. doi:10.1089/ten.TEA.2011.0430.

Liu, Zhongwu, Yi Li, Yisheng Cui, Cynthia Roberts, Mei Lu, Ulrika Wilhelmsson, Milos Pekny, and Michael Chopp. 2014. "Beneficial Effects of Gfap/Vimentin Reactive Astrocytes for Axonal Remodeling and Motor Behavioral Recovery in Mice after Stroke." *Glia* 62 (12): 2022–33. doi:10.1002/glia.22723.

Lukovic, Dunja, Lourdes Valdés-Sanchez, Irene Sanchez-Vera, Victoria Moreno-Manzano, Miodrag Stojkovic, Shomi S. Bhattacharya, and Slaven Erceg. 2014. "Brief Report: Astrogliosis Promotes Functional Recovery of Completely Transected Spinal Cord Following Transplantation of HESC-Derived Oligodendrocyte and Motoneuron Progenitors." *Stem Cells* 32: 594–99. doi:10.1002/stem.1562.

Macaya, Daniel J., Kazuhide Hayakawa, Ken Arai, and Myron Spector. 2013. "Astrocyte Infiltration into Injectable Collagen-Based Hydrogels Containing FGF-2 to Treat Spinal Cord Injury." *Biomaterials* 34 (14): 3591–3602. doi:10.1016/j.biomaterials.2012.12.050.

Martino, Mikaël M, and Jeffrey A Hubbell. 2010. "The 12th-14th Type III Repeats of Fibronectin Function as a Highly Promiscuous Growth Factor-Binding Domain." *FASEB Journal : Official Publication of the Federation of American Societies for Experimental Biology* 24 (12): 4711–21. doi:10.1096/fj.09-151282.

Matthews, M A, M F St Onge, C L Faciane, and J B Gelderd. 2016. "Spinal Cord Transection: A Quantitative Analysis of Elements of the Connective Tissue Matrix Formed within the Site of Lesion Following Administration of Piromen, Cytoxan or Trypsin." *Neuropathology and Applied Neurobiology* 5 (3): 161–80. Accessed November 15. http://www.ncbi.nlm.nih.gov/pubmed/471188.

Mayeur, Anne, Célia Duclos, Axel Honoré, Maxime Gauberti, Laurent Drouot, Jean-Claude do Rego, Nicolas Bon-Mardion, et al. 2013. "Potential of Olfactory Ensheathing Cells from Different Sources for Spinal Cord Repair." *PloS One* 8 (4): e62860. doi:10.1371/journal.pone.0062860.

McCreedy, D A, T S Wilems, H Xu, J C Butts, C R Brown, A W Smith, and S E Sakiyama-Elbert. 2014. "Survival, Differentiation, and Migration of High-Purity Mouse Embryonic Stem Cell-Derived Progenitor Motor Neurons in Fibrin Scaffolds after Sub-Acute Spinal Cord Injury." *Biomaterials Science* 2 (11): 1672–82. doi:10.1039/c4bm00106k.

Mccreedy, Dylan a., Chelsea R. Brown, Jessica C. Butts, Hao Xu, James E. Huettner, and Shelly E. Sakiyama-Elbert. 2014. "A New Method for Generating High Purity Motoneurons from Mouse Embryonic Stem Cells." *Biotechnology and Bioengineering*. doi:10.1002/bit.25260.

McCreedy, Dylan a., Cara R. Rieger, David I. Gottlieb, and Shelly E. Sakiyama-Elbert. 2012. "Transgenic Enrichment of Mouse Embryonic Stem Cell-Derived Progenitor Motor Neurons." *Stem Cell Research* 8 (3). Elsevier B.V.: 368–78. doi:10.1016/j.scr.2011.12.003.

Medalha, Carla Christina, Ying Jin, Takaya Yamagami, Christopher Haas, and Itzhak Fischer. 2014. "Transplanting Neural Progenitors into a Complete Transection Model of Spinal Cord Injury." *Journal of Neuroscience Research* 92 (5): 607–18. doi:10.1002/jnr.23340.

Medberry, Christopher J, Peter M Crapo, Bernard F Siu, Christopher A Carruthers, Matthew T Wolf, Shailesh P Nagarkar, Vineet Agrawal, et al. 2013. "Hydrogels Derived from Central Nervous System Extracellular Matrix." *Biomaterials* 34 (4). NIH Public Access: 1033–40. doi:10.1016/j.biomaterials.2012.10.062.

Min, Seul Ki, Sang Myung Jung, Jung Hyeon Ju, Yeo Seon Kwon, Gwang Heum Yoon, and Hwa Sung Shin. 2015. "Regulation of Astrocyte Activity via Control over Stiffness of Cellulose Acetate Electrospun Nanofiber." *In Vitro Cellular & Developmental Biology - Animal* 51 (9). Springer US: 933–40. doi:10.1007/s11626-015-9925-8.

Mirmalek-Sani, Sayed-Hadi, David C Sullivan, Cynthia Zimmerman, Thomas D Shupe, and Bryon E Petersen. 2013. "Immunogenicity of Decellularized Porcine Liver for Bioengineered Hepatic Tissue." *The American Journal of Pathology* 183 (2): 558–65. doi:10.1016/j.ajpath.2013.05.002.

Moe, Svein Erik, Jan Gunnar Sorbo, Rikke Sogaard, Thomas Zeuthen, Ole Petter Ottersen, and Torgeir Holen. 2008. "New Isoforms of Rat Aquaporin-4." *Genomics* 91 (4): 367–77. doi:10.1016/j.ygeno.2007.12.003.

Moore, Amy M, Matthew MacEwan, Katherine B Santosa, Kristofer E Chenard, Wilson Z Ray, Daniel A Hunter, Susan E Mackinnon, and Philip J Johnson. 2011. "Acellular Nerve Allografts in Peripheral Nerve Regeneration: A Comparative Study." *Muscle & Nerve* 44 (2): 221–34. doi:10.1002/mus.22033.

Myers, Scott A, Andrew N Bankston, Darlene A Burke, Sujata Saraswat Ohri, and Scott R Whittemore. 2016. "Does the Preclinical Evidence for Functional Remyelination Following Myelinating Cell Engraftment into the Injured Spinal Cord Support Progression to Clinical Trials?" *Experimental Neurology*, April. doi:10.1016/j.expneurol.2016.04.009.

Nagelhus, E A, M L Veruki, R Torp, F M Haug, J H Laake, S Nielsen, P Agre, and O P Ottersen. 1998. "Aquaporin-4 Water Channel Protein in the Rat Retina and Optic Nerve: Polarized Expression in Müller Cells and Fibrous Astrocytes." *The Journal of Neuroscience : The*

Official Journal of the Society for Neuroscience 18 (7): 2506–19. http://www.ncbi.nlm.nih.gov/pubmed/9502811.

Nakamura, Masaya, Seiji Okada, Yoshiaki Toyama, and Hideyuki Okano. 2005. "Role of IL-6 in Spinal Cord Injury in a Mouse Model." *Clinical Reviews in Allergy & Immunology* 28 (3): 197–204. doi:10.1385/CRIAI:28:3:197.

Nakamura, Ryosuke, Fumio Nakamura, and Shigeharu Fukunaga. 2015. "Diverse Functions of Perlecan in Central Nervous System Cells in Vitro." *Animal Science Journal = Nihon Chikusan Gakkaihō* 86 (10): 904–11. doi:10.1111/asj.12376.

Neiiendam, Johanne Louise, Lene Boding Kohler, Claus Christensen, Shizhong Li, Martin Volmer Pedersen, Dorte Kornerup Ditlevsen, Martin Kirkegaard Kornum, Vladislav V. Kiselyov, Vladimir Berezin, and Elisabeth Bock. 2004. "An NCAM-Derived FGF-Receptor Agonist, the FGL-Peptide, Induces Neurite Outgrowth and Neuronal Survival in Primary Rat Neurons." *Journal of Neurochemistry* 91 (4). Blackwell Science Ltd: 920–35. doi:10.1111/j.1471-4159.2004.02779.x.

Nesvizhskii, Alexey I, Andrew Keller, Eugene Kolker, and Ruedi Aebersold. 2003. "A Statistical Model for Identifying Proteins by Tandem Mass Spectrometry." *Analytical Chemistry* 75 (17): 4646–58. http://www.ncbi.nlm.nih.gov/pubmed/14632076.

Nimmo, Chelsea M, Shawn C Owen, and Molly S Shoichet. 2011. "Diels-Alder Click Cross-Linked Hyaluronic Acid Hydrogels for Tissue Engineering." *Biomacromolecules* 12 (3): 824–30. doi:10.1021/bm101446k.

Novak, Margaret L, and Timothy J Koh. 2013. "Macrophage Phenotypes during Tissue Repair." *Journal of Leukocyte Biology* 93 (6): 875–81. doi:10.1189/jlb.1012512.

Oberheim, Nancy Ann, Steven A Goldman, and Maiken Nedergaard. 2012. "Heterogeneity of Astrocytic Form and Function." *Methods in Molecular Biology (Clifton, N.J.)* 814. NIH Public Access: 23–45. doi:10.1007/978-1-61779-452-0_3.

Of, Auses. 2013. "Spinal Cord Injury Facts and Figures at a Glance." *The Journal of Spinal Cord Medicine* 37 (February): 479–80. doi:10.1179/1079026814Z.000000000322.

Ohtake, Yosuke, and Shuxin Li. 2014. "Molecular Mechanisms of Scar-Sourced Axon Growth Inhibitors." *Brain Research*, September. doi:10.1016/j.brainres.2014.08.064.

Oohira, A, F Matsui, and R Katoh-Semba. 1991. "Inhibitory Effects of Brain Chondroitin Sulfate Proteoglycans on Neurite Outgrowth from PC12D Cells." *The Journal of Neuroscience : The Official Journal of the Society for Neuroscience* 11 (3): 822–27. http://www.ncbi.nlm.nih.gov/pubmed/2002362.

Pakulska, Malgosia M., Charles H. Tator, and Molly S. Shoichet. 2017. "Local Delivery of Chondroitinase ABC with or without Stromal Cell-Derived Factor 1α Promotes Functional Repair in the Injured Rat Spinal Cord." *Biomaterials* 134 (July): 13–21. doi:10.1016/j.biomaterials.2017.04.016.

Pakulska, Malgosia M, Brian G Ballios, and Molly S Shoichet. 2012. "Injectable Hydrogels for Central Nervous System Therapy." *Biomedical Materials (Bristol, England)* 7 (2): 024101. doi:10.1088/1748-6041/7/2/024101.

Pan, Liuliu, Hilary A North, Vibhu Sahni, Su Ji Jeong, Tammy L Mcguire, Eric J Berns, Samuel I Stupp, and John A Kessler. 2014. "B1-Integrin and Integrin Linked Kinase Regulate Astrocytic Differentiation of Neural Stem Cells." *PloS One* 9 (8). Public Library of Science: e104335. doi:10.1371/journal.pone.0104335.

Pandey, Madhu S., Bruce A. Baggenstoss, Jennifer Washburn, Edward N. Harris, and Paul H. Weigel. 2013. "The Hyaluronan Receptor for Endocytosis (HARE) Activates NF-KB-Mediated Gene Expression in Response to 40–400-KDa, but Not Smaller or Larger, Hyaluronans." *Journal of Biological Chemistry* 288 (20): 14068–79. doi:10.1074/jbc.M112.442889.

Pawar, Kiran, Peter Prang, Rainer Müller, Massimiliano Caioni, Ulrich Bogdahn, Werner Kunz, and Norbert Weidner. 2015. "Intrinsic and Extrinsic Determinants of Central Nervous System Axon Outgrowth into Alginate-Based Anisotropic Hydrogels." *Acta Biomaterialia* 27 (November): 131–39. doi:10.1016/j.actbio.2015.08.032.

Pekny, M, C B Johansson, C Eliasson, J Stakeberg, A Wallén, T Perlmann, U Lendahl, C Betsholtz, C H Berthold, and J Frisén. 1999. "Abnormal Reaction to Central Nervous System Injury in Mice Lacking Glial Fibrillary Acidic Protein and Vime." *The Journal of Cell Biology* 145 (3): 503–14. http://www.pubmedcentral.nih.gov/articlerender.fcgi?artid=2185074&tool=pmcentrez&rendertype=abstract.

Petter-Puchner, Alexander H., Wolfgang Froetscher, Reinhild Krametter-Froetscher, Dragan Lorinson, Heinz Redl, and Martijn van Griensven. 2007. "The Long-Term Neurocompatibility of Human Fibrin Sealant and Equine Collagen as Biomatrices in Experimental Spinal Cord Injury." *Experimental and Toxicologic Pathology* 58 (4): 237–45. doi:10.1016/j.etp.2006.07.004.

Pfeifer, Katharina, Maurice Vroemen, Armin Blesch, and Norbert Weidner. 2004. "Adult Neural Progenitor Cells Provide a Permissive Guiding Substrate for Corticospinal Axon Growth Following Spinal Cord Injury." *The European Journal of Neuroscience* 20 (7): 1695–1704. doi:10.1111/j.1460-9568.2004.03657.x.

Priest, Catherine A, Nathan C Manley, Jerrod Denham, Edward D Wirth, and Jane S Lebkowski. 2015. "Preclinical Safety of Human Embryonic Stem Cell-Derived Oligodendrocyte Progenitors Supporting Clinical Trials in Spinal Cord Injury." *Regenerative Medicine* 10 (8): 939–58. doi:10.2217/rme.15.57.

Qu, Jing, Dan Wang, Huihui Wang, Yunhai Dong, Feng Zhang, Baoqi Zuo, and Huanxiang Zhang. 2013. "Electrospun Silk Fibroin Nanofibers in Different Diameters Support Neurite Outgrowth and Promote Astrocyte Migration." *Journal of Biomedical Materials Research. Part A* 101 (9): 2667–78. doi:10.1002/jbm.a.34551.

Rao, M S, M Noble, and M Mayer-Pröschel. 1998. "A Tripotential Glial Precursor Cell Is

Present in the Developing Spinal Cord." *Proceedings of the National Academy of Sciences of the United States of America* 95 (7). National Academy of Sciences: 3996–4001. /pmc/articles/PMC19951/?report=abstract.

Raponi, Eric, Fabien Agenes, Christian Delphin, Nicole Assard, Jacques Baudier, Catherine Legraverend, and Jean-Christophe Deloulme. 2007. "S100B Expression Defines a State in Which GFAP-Expressing Cells Lose Their Neural Stem Cell Potential and Acquire a More Mature Developmental Stage." *Glia* 55 (2). Inserm: 165–77. doi:10.1002/glia.20445.

Raposo, Catarina, Nadine Graubardt, Merav Cohen, Chen Eitan, Anat London, Tamara Berkutzki, and Michal Schwartz. 2014. "CNS Repair Requires Both Effector and Regulatory T Cells with Distinct Temporal and Spatial Profiles." *The Journal of Neuroscience : The Official Journal of the Society for Neuroscience* 34 (31): 10141–55. doi:10.1523/JNEUROSCI.0076-14.2014.

Reddy, Adarsh S., David O'Brien, Nilambari Pisat, Claire T. Weichselbaum, Kristina Sakers, Miriam Lisci, Jasbir S. Dalal, and Joseph D. Dougherty. 2016. "A Comprehensive Analysis of Cell Type–Specific Nuclear RNA From Neurons and Glia of the Brain." *Biological Psychiatry*, February. doi:10.1016/j.biopsych.2016.02.021.

Ren, Hao, Min Han, Jing Zhou, Ze-Feng Zheng, Ping Lu, Jun-Juan Wang, Jia-Qiu Wang, Qi-Jiang Mao, Jian-Qing Gao, and Hong Wei Ouyang. 2014. "Repair of Spinal Cord Injury by Inhibition of Astrocyte Growth and Inflammatory Factor Synthesis through Local Delivery of Flavopiridol in PLGA Nanoparticles." *Biomaterials* 35 (24): 6585–94. doi:10.1016/j.biomaterials.2014.04.042.

Rosciszewski, Gerardo, Vanesa Cadena, Veronica Murta, Jeronimo Lukin, Alejandro Villarreal, Thierry Roger, and Alberto Javier Ramos. 2017. "Toll-Like Receptor 4 (TLR4) and Triggering Receptor Expressed on Myeloid Cells-2 (TREM-2) Activation Balance Astrocyte Polarization into a Proinflammatory Phenotype." *Molecular Neurobiology*, May. doi:10.1007/s12035-017-0618-z.

Roybon, Laurent, NunoJ Lamas, Alejandro Garcia-Diaz, EunJu Yang, Rita Sattler, Vernice Jackson-Lewis, YoonA Kim, et al. 2013. "Human Stem Cell-Derived Spinal Cord Astrocytes with Defined Mature or Reactive Phenotypes." *Cell Reports* 4 (5). The Authors: 1035–48. doi:10.1016/j.celrep.2013.06.021.

Russell, Lauren N., and Kyle J. Lampe. 2016. "Engineering Biomaterials to Influence Oligodendroglial Growth, Maturation, and Myelin Production." *Cells Tissues Organs* 202 (1–2): 85–101. doi:10.1159/000446645.

Sakiyama-Elbert, S E, and J A Hubbell. 2000. "Controlled Release of Nerve Growth Factor from a Heparin-Containing Fibrin-Based Cell Ingrowth Matrix." *Journal of Controlled Release : Official Journal of the Controlled Release Society* 69 (1): 149–58. http://www.ncbi.nlm.nih.gov/pubmed/11018553.

Sakiyama, S E, J C Schense, and J A Hubbell. 1999. "Incorporation of Heparin-Binding Peptides into Fibrin Gels Enhances Neurite Extension: An Example of Designer Matrices in Tissue Engineering." *FASEB Journal : Official Publication of the Federation of American*

Societies for Experimental Biology 13 (15): 2214–24.
http://www.ncbi.nlm.nih.gov/pubmed/10593869.

Schaub, Nicholas J., Christopher D. Johnson, Blair Cooper, and Ryan J. Gilbert. 2016.
"Electrospun Fibers for Spinal Cord Injury Research and Regeneration." *Journal of Neurotrauma* 33 (15). Mary Ann Liebert, Inc. 140 Huguenot Street, 3rd Floor New Rochelle, NY 10801 USA : 1405–15. doi:10.1089/neu.2015.4165.

Schaub, Nicholas J, and Ryan J Gilbert. 2011. "Controlled Release of 6-Aminonicotinamide from Aligned, Electrospun Fibers Alters Astrocyte Metabolism and Dorsal Root Ganglia Neurite Outgrowth." *Journal of Neural Engineering* 8 (4): 046026. doi:10.1088/1741-2560/8/4/046026.

Schense, J C, J Bloch, P Aebischer, and J A Hubbell. 2000. "Enzymatic Incorporation of Bioactive Peptides into Fibrin Matrices Enhances Neurite Extension." *Nature Biotechnology* 18 (4): 415–19. doi:10.1038/74473.

Seidlits, Stephanie K., Zin Z. Khaing, Rebecca R. Petersen, Jonathan D. Nickels, Jennifer E. Vanscoy, Jason B. Shear, and Christine E. Schmidt. 2010. "The Effects of Hyaluronic Acid Hydrogels with Tunable Mechanical Properties on Neural Progenitor Cell Differentiation." *Biomaterials* 31 (14): 3930–40. doi:10.1016/j.biomaterials.2010.01.125.

Seif-Naraghi, Sonya B, Jennifer M Singelyn, Michael A Salvatore, Kent G Osborn, Jean J Wang, Unatti Sampat, Oi Ling Kwan, et al. 2013. "Safety and Efficacy of an Injectable Extracellular Matrix Hydrogel for Treating Myocardial Infarction." *Science Translational Medicine* 5 (173): 173ra25. doi:10.1126/scitranslmed.3005503.

Sharif-Alhoseini, M, M Khormali, M Rezaei, M Safdarian, A Hajighadery, M M Khalatbari, M Safdarian, et al. 2017. "Animal Models of Spinal Cord Injury: A Systematic Review." *Spinal Cord*, January. doi:10.1038/sc.2016.187.

Sharp, Kelli G, Amanda R Dickson, Steve A Marchenko, Kelly M Yee, Pauline N Emery, Ivo Laidmåe, Raivo Uibo, Evelyn S Sawyer, Oswald Steward, and Lisa A Flanagan. 2012. "Salmon Fibrin Treatment of Spinal Cord Injury Promotes Functional Recovery and Density of Serotonergic Innervation." *Experimental Neurology* 235 (1). NIH Public Access: 345–56. doi:10.1016/j.expneurol.2012.02.016.

Shih, C.-H., M. Lacagnina, K. Leuer-Bisciotti, and C. Proschel. 2014. "Astroglial-Derived Periostin Promotes Axonal Regeneration after Spinal Cord Injury." *Journal of Neuroscience* 34 (7): 2438–43. doi:10.1523/JNEUROSCI.2947-13.2014.

Shinozaki, Munehisa, Akio Iwanami, Kanehiro Fujiyoshi, Shouichi Tashiro, Kazuya Kitamura, Shinsuke Shibata, Hiroshi Fujita, Masaya Nakamura, and Hideyuki Okano. 2016. "Combined Treatment with Chondroitinase ABC and Treadmill Rehabilitation for Chronic Severe Spinal Cord Injury in Adult Rats." *Neuroscience Research*. doi:10.1016/j.neures.2016.07.005.

Shu, Xiao Zheng, Yanchun Liu, Yi Luo, Meredith C. Roberts, and Glenn D. Prestwich. 2002. "Disulfide Cross-Linked Hyaluronan Hydrogels." *Biomacromolecules* 3 (6). American

Chemical Society : 1304–11. doi:10.1021/bm025603c.

Siddiq, Mustafa M., Sari S. Hannila, Jason B. Carmel, John B. Bryson, Jianwei Hou, Elena Nikulina, Matthew R. Willis, et al. 2015. "Metallothionein-I/II Promotes Axonal Regeneration in the Central Nervous System." *Journal of Biological Chemistry* 290 (26): 16343–56. doi:10.1074/jbc.M114.630574.

Silva, Gabriel A, Catherine Czeisler, Krista L Niece, Elia Beniash, Daniel A Harrington, John A Kessler, and Samuel I Stupp. 2004. "Selective Differentiation of Neural Progenitor Cells by High-Epitope Density Nanofibers." *Science (New York, N.Y.)* 303 (5662): 1352–55. doi:10.1126/science.1093783.

Silva, Joana, Ana R. Bento, Daniela Barros, Tiago L. Laundos, Susana R. Sousa, Pedro Quelhas, Mónica M. Sousa, Ana P. Pêgo, and Isabel F. Amaral. 2017. "Fibrin Functionalization with Synthetic Adhesive Ligands Interacting with A6β1 Integrin Receptor Enhance Neurite Outgrowth of Embryonic Stem Cell-Derived Neural Stem/Progenitors." *Acta Biomaterialia* 59 (September): 243–56. doi:10.1016/j.actbio.2017.07.013.

Simonen, Marjo, Vera Pedersen, Oliver Weinmann, Lisa Schnell, Armin Buss, Birgit Ledermann, Franziska Christ, Gilles Sansig, Herman van der Putten, and Martin E Schwab. 2003. "Systemic Deletion of the Myelin-Associated Outgrowth Inhibitor Nogo-A Improves Regenerative and Plastic Responses after Spinal Cord Injury." *Neuron* 38 (2): 201–11. http://www.ncbi.nlm.nih.gov/pubmed/12718855.

Singelyn, Jennifer M, Priya Sundaramurthy, Todd D Johnson, Pamela J Schup-Magoffin, Diane P Hu, Denver M Faulk, Jean Wang, et al. 2012. "Catheter-Deliverable Hydrogel Derived from Decellularized Ventricular Extracellular Matrix Increases Endogenous Cardiomyocytes and Preserves Cardiac Function Post-Myocardial Infarction." *Journal of the American College of Cardiology* 59 (8): 751–63. doi:10.1016/j.jacc.2011.10.888.

Smith, G M, and R H Miller. 1991. "Immature Type-1 Astrocytes Suppress Glial Scar Formation, Are Motile and Interact with Blood Vessels." *Brain Research* 543 (1): 111–22. http://www.ncbi.nlm.nih.gov/pubmed/2054666.

Smith, G M, and J Silver. 1988. "Transplantation of Immature and Mature Astrocytes and Their Effect on Scar Formation in the Lesioned Central Nervous System." *Progress in Brain Research* 78: 353–61. http://www.ncbi.nlm.nih.gov/pubmed/3247435.

Smith, Laura J, S. Maryamdokht Taimoory, Roger Y. Tam, Alexander E. G. Baker, Niema Binth Mohammad, John F Trant, and Molly Shoichet. n.d. "Diels-Alder Click-Crosslinked Hydrogels with Increased Reactivity Enable 3D Cell Encapsulation." *Biomacromolecules*.

Snider, Silvia, Andrea Cavalli, Francesca Colombo, Alberto Luigi Gallotti, Angelo Quattrini, Luca Salvatore, Marta Madaghiele, Maria Rosa Terreni, Alessandro Sannino, and Pietro Mortini. 2017. "A Novel Composite Type I Collagen Scaffold with Micropatterned Porosity Regulates the Entrance of Phagocytes in a Severe Model of Spinal Cord Injury." *Journal of Biomedical Materials Research Part B: Applied Biomaterials* 105 (5): 1040–53. doi:10.1002/jbm.b.33645.

Stewart, G R, and A L Pearlman. 1987. "Fibronectin-like Immunoreactivity in the Developing Cerebral Cortex." *The Journal of Neuroscience : The Official Journal of the Society for Neuroscience* 7 (10): 3325–33. http://www.ncbi.nlm.nih.gov/pubmed/3668630.

Sun, Daniel, and Tatjana C. Jakobs. 2012. "Structural Remodeling of Astrocytes in the Injured CNS." *The Neuroscientist* 18 (6): 567–88. doi:10.1177/1073858411423441.

Sun, Daniel, Ming Lye-Barthel, Richard H Masland, and Tatjana C Jakobs. 2010. "Structural Remodeling of Fibrous Astrocytes after Axonal Injury." *The Journal of Neuroscience : The Official Journal of the Society for Neuroscience* 30 (42). NIH Public Access: 14008–19. doi:10.1523/JNEUROSCI.3605-10.2010.

Suzuki, Hidenori, Tsukasa Kanchiku, Yasuaki Imajo, Yuichiro Yoshida, Norihiro Nishida, Toshikazu Gondo, Satoru Yoshii, and Toshihiko Taguchi. 2015. "Artificial Collagen-Filament Scaffold Promotes Axon Regeneration and Long Tract Reconstruction in a Rat Model of Spinal Cord Transection." *Medical Molecular Morphology* 48 (4): 214–24. doi:10.1007/s00795-015-0104-5.

Tabakow, Pawel, Wlodzimierz Jarmundowicz, Bogdan Czapiga, Wojciech Fortuna, Ryszard Miedzybrodzki, Marcin Czyz, Juliusz Huber, et al. 2013. "Transplantation of Autologous Olfactory Ensheathing Cells in Complete Human Spinal Cord Injury." *Cell Transplantation*, April. doi:10.3727/096368913X663532.

Taylor, Sara J., and Shelly E. Sakiyama-Elbert. 2006. "Effect of Controlled Delivery of Neurotrophin-3 from Fibrin on Spinal Cord Injury in a Long Term Model." *Journal of Controlled Release* 116 (2): 204–10. doi:10.1016/j.jconrel.2006.07.005.

Taylor, Sara J, Ephron S Rosenzweig, John W McDonald, and Shelly E Sakiyama-Elbert. 2006. "Delivery of Neurotrophin-3 from Fibrin Enhances Neuronal Fiber Sprouting after Spinal Cord Injury." *Journal of Controlled Release : Official Journal of the Controlled Release Society* 113 (3): 226–35. doi:10.1016/j.jconrel.2006.05.005.

Terraf, Panieh, Shideh Montasser Kouhsari, Jafar Ai, and Hamideh Babaloo. 2017. "Tissue-Engineered Regeneration of Hemisected Spinal Cord Using Human Endometrial Stem Cells, Poly ε-Caprolactone Scaffolds, and Crocin as a Neuroprotective Agent." *Molecular Neurobiology* 54 (7): 5657–67. doi:10.1007/s12035-016-0089-7.

Tetzlaff, Wolfram, Elena B. Okon, Soheila Karimi-Abdolrezaee, Caitlin E. Hill, Joseph S. Sparling, Jason R. Plemel, Ward T. Plunet, et al. 2011. "A Systematic Review of Cellular Transplantation Therapies for Spinal Cord Injury." *Journal of Neurotrauma* 28 (8). Mary Ann Liebert, Inc.: 1611–82. doi:10.1089/neu.2009.1177.

Thomas, Aline M, Stephanie K Seidlits, Ashley G Goodman, Todor V Kukushliev, Donna M Hassani, Brian J Cummings, Aileen J Anderson, and Lonnie D Shea. 2014. "Sonic Hedgehog and Neurotrophin-3 Increase Oligodendrocyte Numbers and Myelination after Spinal Cord Injury." *Integrative Biology : Quantitative Biosciences from Nano to Macro* 6 (7). NIH Public Access: 694–705. doi:10.1039/c4ib00009a.

Thompson, Russell E., Jennifer Pardieck, Laura Smith, Peter Kenny, Lindsay Crawford, Molly

Shoichet, and Shelly Sakiyama-Elbert. 2018. "Effect of Hyaluronic Acid Hydrogels Containing Astrocyte-Derived Extracellular Matrix and/or V2a Interneurons on Histologic Outcomes Following Spinal Cord Injury." *Biomaterials* 162 (April): 208–23. doi:10.1016/j.biomaterials.2018.02.013.

Thompson, Russell E, Allison Lake, Peter Kenny, Michael Saunders, Kristina Sakers, Nisha Iyer, Joseph D Dougherty, and Shelly E Sakiyama-Elbert. 2017. "Different Mixed Astrocyte Populations Derived from Embryonic Stem Cells Have Variable Neuronal Growth Support Capacities." *Stem Cells and Development*, August, scd.2017.0121. doi:10.1089/scd.2017.0121.

Thompson, Russell, and Shelly Sakiyama-Elbert. 2018. "Using Biomaterials to Promote Pro-Regenerative Glial Phenotypes after Nervous System Injuries." *Biomedical Materials* 13 (2): 024104. doi:10.1088/1748-605X/aa9e23.

Tien, An-Chi, Hui-Hsin Tsai, Anna V Molofsky, Martin McMahon, Lynette C Foo, Aparna Kaul, Joseph D Dougherty, et al. 2012. "Regulated Temporal-Spatial Astrocyte Precursor Cell Proliferation Involves BRAF Signalling in Mammalian Spinal Cord." *Development (Cambridge, England)* 139 (14): 2477–87. doi:10.1242/dev.077214.

Tiryaki, Volkan Müjdat, Virginia M Ayres, Ijaz Ahmed, and David I Shreiber. 2015. "Differentiation of Reactive-like Astrocytes Cultured on Nanofibrillar and Comparative Culture Surfaces." *Nanomedicine* 10 (4). Future Medicine Ltd London, UK : 529–45. doi:10.2217/nnm.14.33.

Tiryaki, Volkan Mujdat, Virginia M Ayres, Adeel A Khan, Ijaz Ahmed, David I Shreiber, and Sally Meiners. 2012. "Nanofibrillar Scaffolds Induce Preferential Activation of Rho GTPases in Cerebral Cortical Astrocytes." *International Journal of Nanomedicine* 7. Dove Press: 3891–3905. doi:10.2147/IJN.S32681.

Toft, Andrew, Mercedes Tome, Susan C Barnett, and John S Riddell. 2013. "A Comparative Study of Glial and Non-Neural Cell Properties for Transplant-Mediated Repair of the Injured Spinal Cord." *Glia* 61 (4): 513–28. doi:10.1002/glia.22452.

Tom, Veronica J, Catherine M Doller, Alfred T Malouf, and Jerry Silver. 2004. "Astrocyte-Associated Fibronectin Is Critical for Axonal Regeneration in Adult White Matter." *The Journal of Neuroscience : The Official Journal of the Society for Neuroscience* 24 (42): 9282–90. doi:10.1523/JNEUROSCI.2120-04.2004.

Tukmachev, Dmitry, Serhiy Forostyak, Zuzana Koci, Kristyna Zaviskova, Irena Vackova, Karel Vyborny, Ioanna Sandvig, et al. 2016. "Injectable Extracellular Matrix Hydrogels as Scaffolds for Spinal Cord Injury Repair." *Tissue Engineering. Part A* 22 (3–4). Mary Ann Liebert, Inc.: 306–17. doi:10.1089/ten.TEA.2015.0422.

Tysseling-Mattiace, Vicki M, Vibhu Sahni, Krista L Niece, Derin Birch, Catherine Czeisler, Michael G Fehlings, Samuel I Stupp, and John A Kessler. 2008. "Self-Assembling Nanofibers Inhibit Glial Scar Formation and Promote Axon Elongation after Spinal Cord Injury." *The Journal of Neuroscience : The Official Journal of the Society for Neuroscience* 28 (14). NIH Public Access: 3814–23. doi:10.1523/JNEUROSCI.0143-08.2008.

Urbanski, Mateusz M, Lyle Kingsbury, Daniel Moussouros, Imran Kassim, Saraf Mehjabeen, Navid Paknejad, and Carmen V Melendez-Vasquez. 2016. "Myelinating Glia Differentiation Is Regulated by Extracellular Matrix Elasticity." *Scientific Reports* 6 (September). Nature Publishing Group: 33751. doi:10.1038/srep33751.

Vadivelu, Sudhakar, Todd J Stewart, Yun Qu, Kevin Horn, Su Liu, Qun Li, Jerry Silver, and John W McDonald. 2015. "NG2+ Progenitors Derived From Embryonic Stem Cells Penetrate Glial Scar and Promote Axonal Outgrowth Into White Matter After Spinal Cord Injury." *Stem Cells Translational Medicine*, February. doi:10.5966/sctm.2014-0107.

Vanhoutte, Nicolas, Isabelle de Hemptinne, Céline Vermeiren, Jean-Marie Maloteaux, and Emmanuel Hermans. 2004. "In Vitro Differentiated Neural Stem Cells Express Functional Glial Glutamate Transporters." *Neuroscience Letters* 370 (2–3): 230–35. doi:10.1016/j.neulet.2004.08.039.

Veres, Adrian, Bridget S. Gosis, Qiurong Ding, Ryan Collins, Ashok Ragavendran, Harrison Brand, Serkan Erdin, Chad A. Cowan, Michael E. Talkowski, and Kiran Musunuru. 2014. "Low Incidence of Off-Target Mutations in Individual CRISPR-Cas9 and TALEN Targeted Human Stem Cell Clones Detected by Whole-Genome Sequencing." *Cell Stem Cell* 15 (1): 27–30. doi:10.1016/j.stem.2014.04.020.

Villacampa, Nàdia, Beatriz Almolda, Antonietta Vilella, Iain L. Campbell, Berta González, and Bernardo Castellano. 2015. "Astrocyte-Targeted Production of IL-10 Induces Changes in Microglial Reactivity and Reduces Motor Neuron Death after Facial Nerve Axotomy." *Glia* 63 (7): 1166–84. doi:10.1002/glia.22807.

Wang, Haibo, Ambika Tewari, Steven Einheber, James L Salzer, and Carmen V Melendez-Vasquez. 2008. "Myosin II Has Distinct Functions in PNS and CNS Myelin Sheath Formation." *The Journal of Cell Biology* 182 (6). The Rockefeller University Press: 1171–84. doi:10.1083/jcb.200802091.

Wang, Yuanfei, Yakov Lapitsky, Catherine E Kang, and Molly S Shoichet. 2009. "Accelerated Release of a Sparingly Soluble Drug from an Injectable Hyaluronan-Methylcellulose Hydrogel." *Journal of Controlled Release : Official Journal of the Controlled Release Society* 140 (3): 218–23. doi:10.1016/j.jconrel.2009.05.025.

Wen, Yujun, Shukui Yu, Yanhong Wu, Rongkai Ju, Hao Wang, Yujun Liu, Ying Wang, and Qunyuan Xu. 2016. "Spinal Cord Injury Repair by Implantation of Structured Hyaluronic Acid Scaffold with PLGA Microspheres in the Rat." *Cell and Tissue Research* 364 (1). Springer Berlin Heidelberg: 17–28. doi:10.1007/s00441-015-2298-1.

Wichterle, Hynek, Hynek Wichterle, Ivo Lieberam, Ivo Lieberam, Jeffery a Porter, Jeffery a Porter, Thomas M Jessell, and Thomas M Jessell. 2002. "Directed Differentiation of Embryonic Stem Cells into Motor Neurons." *Cell* 110: 385–97. doi:10.1016/S0092-8674(02)00835-8.

Wilcox, Jared T, Kajana Satkunendrarajah, Jeffrey A Zuccato, Farshad Nassiri, and Michael G Fehlings. 2014. "Neural Precursor Cell Transplantation Enhances Functional Recovery and Reduces Astrogliosis in Bilateral Compressive/Contusive Cervical Spinal Cord Injury."

Stem Cells Translational Medicine 3 (10): 1148–59. doi:10.5966/sctm.2014-0029.

Wilems, Thomas S, Jennifer Pardieck, Nisha Iyer, and Shelly E Sakiyama-Elbert. 2015. "Combination Therapy of Stem Cell Derived Neural Progenitors and Drug Delivery of Anti-Inhibitory Molecules for Spinal Cord Injury." *Acta Biomaterialia* 28 (December): 23–32. doi:10.1016/j.actbio.2015.09.018.

Wilems, Thomas S, and Shelly E Sakiyama-Elbert. 2015. "Sustained Dual Drug Delivery of Anti-Inhibitory Molecules for Treatment of Spinal Cord Injury." *Journal of Controlled Release : Official Journal of the Controlled Release Society* 213 (June): 103–11. doi:10.1016/j.jconrel.2015.06.031.

Wilhelmsson, U., E. A. Bushong, D. L. Price, B. L. Smarr, V. Phung, M. Terada, M. H. Ellisman, and M. Pekny. 2006. "Redefining the Concept of Reactive Astrocytes as Cells That Remain within Their Unique Domains upon Reaction to Injury." *Proceedings of the National Academy of Sciences* 103 (46). National Academy of Sciences: 17513–18. doi:10.1073/pnas.0602841103.

Willenberg, Bradley Jay, Tong Zheng, Fan-Wei Meng, Juan Carlos Meneses, Candace Rossignol, Christopher D. Batich, Naohiro Terada, Dennis A. Steindler, and Michael D. Weiss. 2011. "Gelatinized Copper–Capillary Alginate Gel Functions as an Injectable Tissue Scaffolding System for Stem Cell Transplants." *Journal of Biomaterials Science, Polymer Edition* 22 (12): 1621–37. doi:10.1163/092050610X519453.

Wu, Sen, Guoxin Ying, Qiang Wu, and Mario R Capecchi. 2008. "A Protocol for Constructing Gene Targeting Vectors: Generating Knockout Mice for the Cadherin Family and Beyond." *Nature Protocols* 3 (6): 1056–76. http://www.ncbi.nlm.nih.gov/pubmed/18546598.

Xu, Hao, Nisha Iyer, James E Huettner, and Shelly E Sakiyama-Elbert. 2015. "A Puromycin Selectable Cell Line for the Enrichment of Mouse Embryonic Stem Cell-Derived V3 Interneurons." *Stem Cell Research & Therapy* 6 (January): 220. doi:10.1186/s13287-015-0213-z.

Yang, Lei, Yingbin Ge, Jian Tang, Jinxia Yuan, Dawei Ge, Hongtao Chen, Hongxiu Zhang, and Xiaojian Cao. 2015. "Schwann Cells Transplantation Improves Locomotor Recovery in Rat Models with Spinal Cord Injury: A Systematic Review and Meta-Analysis." *Cellular Physiology and Biochemistry : International Journal of Experimental Cellular Physiology, Biochemistry, and Pharmacology* 37 (6): 2171–82. doi:10.1159/000438574.

Zamanian, Jennifer L, Lijun Xu, Lynette C Foo, Navid Nouri, Lu Zhou, Rona G Giffard, and Ben A Barres. 2012. "Genomic Analysis of Reactive Astrogliosis." *The Journal of Neuroscience : The Official Journal of the Society for Neuroscience* 32 (18): 6391–6410. doi:10.1523/JNEUROSCI.6221-11.2012.

Zhang, Shanshan, Mark A Anderson, Yan Ao, Baljit S Khakh, Jessica Fan, Timothy J Deming, and Michael V Sofroniew. 2014. "Tunable Diblock Copolypeptide Hydrogel Depots for Local Delivery of Hydrophobic Molecules in Healthy and Injured Central Nervous System." *Biomaterials* 35 (6). NIH Public Access: 1989–2000. doi:10.1016/j.biomaterials.2013.11.005.

Zhang, Shanshan, Joshua E. Burda, Mark A. Anderson, Ziru Zhao, Yan Ao, Yin Cheng, Yi Sun, Timothy J. Deming, and Michael V. Sofroniew. 2015. "Thermoresponsive Copolypeptide Hydrogel Vehicles for Central Nervous System Cell Delivery." *ACS Biomaterials Science & Engineering* 1 (8): 705–17. doi:10.1021/acsbiomaterials.5b00153.

Zholudeva, Lyandysha V., Jordyn S. Karliner, Kimberly J. Dougherty, and Michael A. Lane. 2017. "Anatomical Recruitment of Spinal V2a Interneurons into Phrenic Motor Circuitry after High Cervical Spinal Cord Injury." *Journal of Neurotrauma*, June, neu.2017.5045. doi:10.1089/neu.2017.5045.

Zuidema, Jonathan M, María C Hyzinski-García, Kristien Van Vlasselaer, Nicholas W Zaccor, George E Plopper, Alexander A Mongin, and Ryan J Gilbert. 2014. "Enhanced GLT-1 Mediated Glutamate Uptake and Migration of Primary Astrocytes Directed by Fibronectin-Coated Electrospun Poly-L-Lactic Acid Fibers." *Biomaterials* 35 (5). NIH Public Access: 1439–49. doi:10.1016/j.biomaterials.2013.10.079.

Zukor, Katherine, Stephane Belin, Chen Wang, Nadia Keelan, Xuhua Wang, and Zhigang He. 2013. "Short Hairpin RNA against PTEN Enhances Regenerative Growth of Corticospinal Tract Axons after Spinal Cord Injury." *The Journal of Neuroscience : The Official Journal of the Society for Neuroscience* 33 (39): 15350–61. doi:10.1523/JNEUROSCI.2510-13.2013.

<u>Vita</u>

Russell Edward Thompson

<u>EDUCATION</u>
Washington University in St Louis, Saint Louis, MO
PhD, Biomedical Engineering   May 2019
MD   May 2019

Harvey Mudd College, Claremont, CA
B.S, Chemistry/Biology   May 2012

<u>RESEARCH EXPERIENCE</u>
Washington University in St Louis, Biomedical Engineering   2014-present
Doctoral Student, Mentor: Shelly Sakiyama-Elbert
Thesis: Elucidating the Roles of Astrocyte-derived Factors in Recovery and Regeneration Following Spinal Cord Injury
- Developed methods to derive spinal white matter (fibrous) or grey matter (protoplasmic) astrocytes from mouse embryonic stem cells
- Generated a puromycin selectable cell line using CRISPR/Cas9 that allows for the generation of purified astrocyte cultures.
- Developed a hyaluronic acid:astrocyte extracellular matrix scaffold that improves histological markers of recovery in rats following spinal cord injury and supports neuronal transplantation

The Ohio State University Spinal Cord Injury Research Training Program   Spring 2016
- Trained in multiple models of rat spinal cord injury and in behavioral assessments

Washington University in St Louis, Genetics   Summer 2013
*Rotation Student***,** Mentor: Jeffery Milbrandt
- Worked on design of a high-throughput, automated screening method to determine what genes are involved in axon regeneration/degredation by human induced pluripotent stem cell-derived neurons with the long-term goal of testing these pathways in cells derived from patients with peripheral neuropathies.

Harvey Mudd College, Engineering   2009-2012
Undergraduate Research Assistant, Mentor: Elizabeth Orwin
- Determined the effect of different collagen substrates on the phenotype of subcultured corneal keratocytes, specifically focusing on the effect of three-dimensional growth environments
- Designed a casting system to generate tunable, three-dimensional collagen gels for the manipulation of corneal keratocyte phenotype.

Lawrence Berkeley National Labs, Life Sciences   Summers 2006-2008

High School Summer Intern, *Mentor: Miaw-Sheue Tsai*
- Explored the effects of different *E. coli* strains on the efficiency of mammalian protein folding and expression.
- Developed a tricistronic vector for the expression of the human rad9-hus1-rad1 DNA repair complex in *E. coli*.

AWARDS/ORGANIZATIONS
- AAP/ASCI/APSA Joint Meeting Travel Award   2017
- Student Member, American Physician Scientist Association   2017-present
- Student Member, Society for Biomaterials   2017-present
- Student Member, Biomedical Engineering Society   2016-present
- Student Member, American Medical Student Association   2012-present
- Harvey Mudd "*Mindlin Prize for Innovative Ideas in Science*"   2012
    - Awarded to the best senior thesis project
- High Honors and Departmental Honors in Chemistry and Biology, Harvey Mudd   2012
- Phi Lambda Upsilon (Honorary Chemical Society)   2012
- Beckman Scholarship: Awarded to 4 students every 3 years   2010-2011
- Harvey Mudd College Dean's List (7 semesters)   2009-2012
- Engman Fellowship: Awarded to 2 students per year   2009
- High School Student Research Participation Program   2007-2008

PUBLICATIONS IN PRINT
1. **Thompson RE**, Pardieck J, Smith L, Kenny P, Crawford L, Shoichet M, Sakiyama-Elbert S. Effect of hyaluronic acid hydrogels containing astrocyte-derived extracellular matrix and/or V2a interneurons on histologic outcomes following spinal cord injury. Biomaterials. 2018 Apr;162:208-223. doi: 10.1016/j.biomaterials.2018.02.013.
2. **Thompson R**, Sakiyama-Elbert S. Using biomaterials to promote pro-regenerative glial phenotypes after nervous system injuries. Biomed Mater. 2018 Feb 8;13(2):024104. doi: 10.1088/1748-605X/aa9e23
3. **Thompson RE**, Lake A, Kenny P, Saunders, M, Sakers K, Iyer NR, Dougherty JD, and Sakiyama-Elbert, SE. 2017 "Different Mixed Astrocyte Populations Derived from Embryonic Stem Cells have Variable Neuronal Growth Support Capacities" *Stem Cells Dev.* Aug 29.
4. **Thompson RE,** Boraas LC, Sowder M, Bechtel MK, and EJ Orwin. 2013 "Three-dimensional cell culture environment promotes partial recovery of the native corneal keratocyte phenotype from a subcultured population" *Tissue Eng Part A*. 19(13-14): 1564-72.

PUBLICATIONS IN PREPARATION

1. Vardhan S, **Thompson RE,** Kenny P, and SE Sakiyama-Elbert. "Generation of Enriched Astrocyte Cultures from a Selectable Mouse Embryonic Stem Cell Line." *In preparation*.
2. McDevitt S, Todd C, Butts JC, Iyer N, White, N, **Thompson RE**, and SE Sakiyama-Elbert. "V2a Interneuron Differentiation from Mouse and Human Pluripotent Stem Cells." *In preparation.*

CONFERENCE PRESENTATIONS

Oral presentations

1. **Thompson, RE,** Pardieck J, Smith, L, Shoichet, M, and Sakiyama-Elbert, SE **"**Hyaluronic Acid-Astrocyte Extracellular Matrix Hydrogels Improve Histological Outcomes following Spinal Cord." Society for Biomaterials Meeting, April 2018.
2. **Thompson, RE**, Pardieck, J, Smith, L, Shoichet, M, and Sakiyama-Elbert, SE "Implantation of an Astrocyte Extracellular Matrix containing Hydrogel Improves Neural Fiber Growth into a Spinal Cord Lesion" Biomedical Engineering Society Meeting, October 2017.
3. **Thompson, RE¸** Crawford, L, Pardieck, J, and Sakiyama-Elbert, SE. "Astrocyte Extracellular Matrix Incorporation Improves Neurite Growth on Hyaluronic Acid Hydrogels" Society for Biomaterials Meeting, April 2017.
4. **Thompson, RE**, Sakiyama-Elbert, SE "Ability of Astrocyte Extracellular Matrix to Support Axon Growth depends on Astrocyte Phenotype" Biomedical Engineering Society Meeting, October 2016.
5. **Thompson, RE,** Sakiyama-Elbert, SE "Protoplasmic Astrocyte-derived Extracellular Matrix Supports *in vitro* Motor Neuron Growth" Washington University Medical Scientist Training Program Retreat, April 2016.

Poster Presentations

1. **Thompson, RE,** Pardieck J, Smith, L, Shoichet, M, and Sakiyama-Elbert, SE "Hyaluronic Acid-Astrocyte Extracellular Matrix Hydrogels Improve Histological Outcomes following Spinal Cord." AAP/ASCI/APSA Joint Meeting, April 2018.
2. **Thompson, RE**, Pardieck, J, Crawford, L, and Sakiyama-Elbert, SE "Astrocyte-derived Extracellular Matrices have Different Growth Support Capacities depending on Astrocyte Subtype" AAP/ASCI/APSA Joint Meeting, April 2017.
3. **Thompson RE**, Boraas LC and EJ Orwin. "Comparison of the Relative Effects of Culture Conditions and Cytokines on Subcultured Keratocyte Phenotype" TERMIS World Congress, September 2012.
4. **Thompson RE**, Boraas LC and EJ Orwin. "Effect of Three Dimensional Culture and Interleukin 1 Receptor Antagonist on alpha-Smooth Muscle Actin Expression by Rabbit Corneal Fibroblasts" TERMIS North America Meeting, December 2010.